
L. E. BOWMAN
PH.D.

PH.D

1991

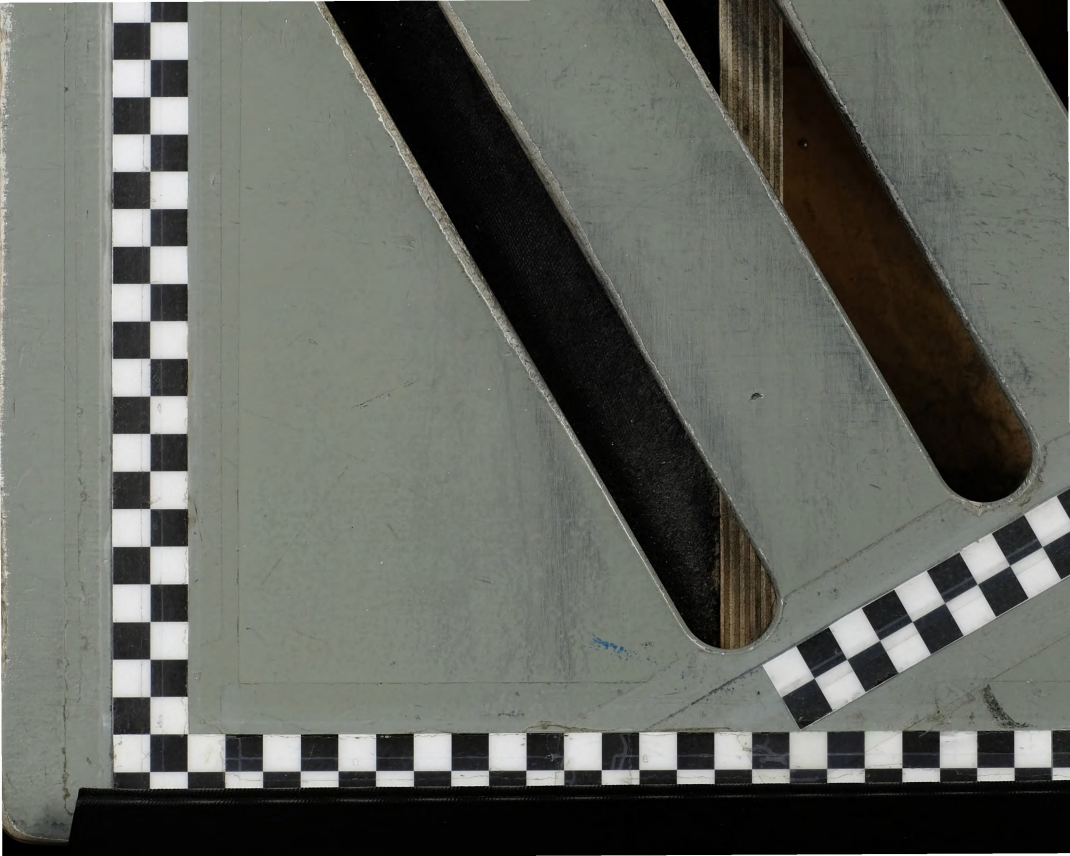

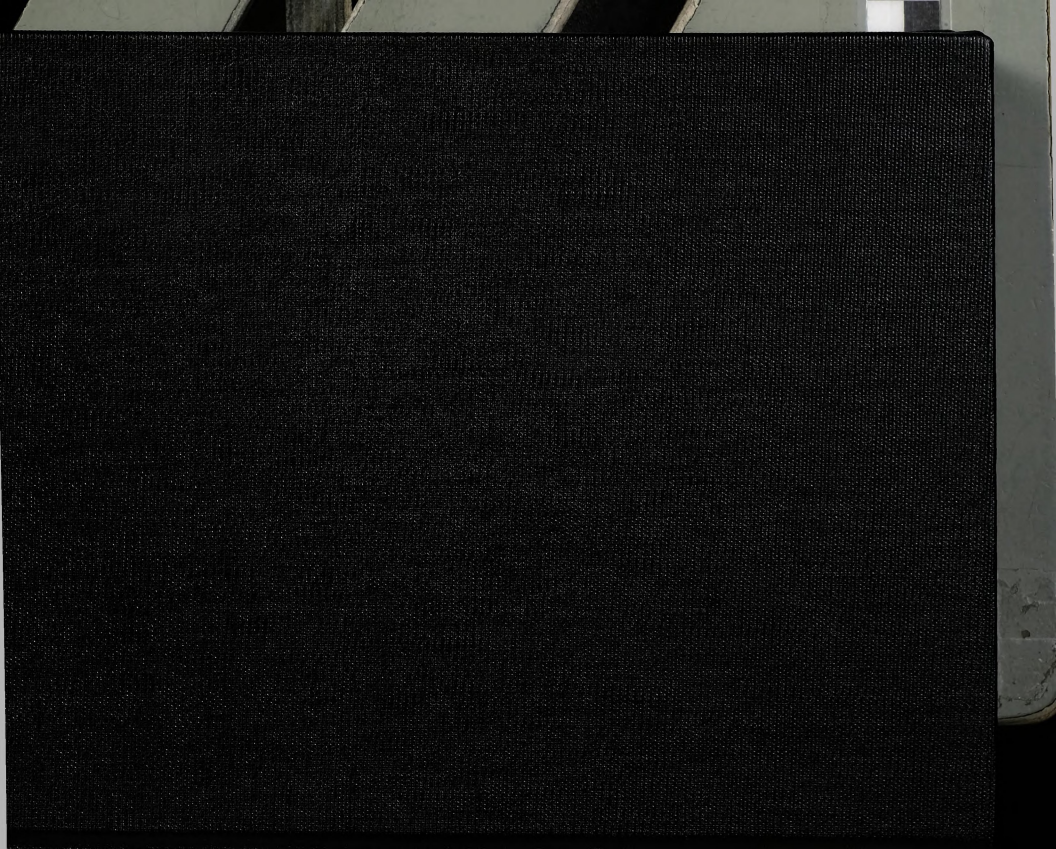

This is to certify that the

dissertation entitled

IMPROVING THE CONFIDENCE OF
MOLECULAR FLUORESCENCE MEASUREMENTS

presented by

LAWRENCE EUGENE BOWMAN

has been accepted towards fulfillment
of the requirements for

Ph.D. degree in Chemistry

S K. Crouch GFB.
Major professor

Date April 10, 1991

IMPROVING THE CONFIDENCE OF MOLECULAR FLUORESCENCE MEASUREMENTS

By

Lawrence Eugene Bowman

A DISSERTATION

Submitted to
Michigan State University
in partial fulfillment of the requirements
for the degree of

DOCTOR OF PHILOSOPHY

Department of Chemistry

1991

ABSTRACT

IMPROVING THE CONFIDENCE OF MOLECULAR FLUORESCENCE MEASUREMENTS

By

Lawrence Eugene Bowman

Two molecular fluorescence spectrometers have been developed that correct molecular fluorescence measurements for processes that reduce the steady-state fluorescence intensity. One of the constructed spectrometers corrects for one of the most common sources of reduced fluorescence intensity, collisional quenching. This spectrometer determines the ratio of the observed intensity to the excited-state lifetime in real time. The spectrometer constructed in this work uses a frequency domain technique to determine the excited-state lifetime in real time. It is somewhat limited in the range of excited-state lifetimes that can be determine.

In addition to the frequency domain instrument, a single-photon timing (SPT) apparatus was constructed and used to make independent measurements of excited-state lifetimes. The constructed SPT instrument is very versatile. It can record fluorescence decays as short as 25 ps or as long as a few hundred ns. From excited-state lifetimes determined with SPT, accurate correction for collisional quenching is demonstrated in a chemical system where the intensity is reduced by a factor of 30 relative to the intensity in the absence of quenching.

In the second, corrected spectrometer, correction for sample absorption, accomplished using a previously reported cell-shift method, is included in addition to correction for collisional quenching. When the fluorescence intensity corrected for sample absorption is ratioed to the excited-state lifetime, one obtains a quantity that is proportional to the concentration of the fluorophore that is corrected for the reduction caused by both collisional quenching and sample absorption. The constructed spectrometer that uses this combined correction approach has been termed a highly corrected molecular fluorescence spectrometer. Measurements based on this dual-correction scheme have demonstrated near immunity to collisional quenching and sample absorption over a limited range of quencher concentration and sample absorption.

TABLE OF CONTENTS

LIST OF TABLES

TABL

TABL

TABL

TABL

TABL

LIST OF FIGURES

CHAPTER

Molecular

of a variety of c

selectivity and ex

fluorescence assa

product of the de

chemical process

thus introducing

directly proportio

The fluor

expressed as:

where E_L is the

excitation source

instrumental cons

assumes that the

wavelengths. If

one assumes that

set also affect th

mechanisms that

the fluorescence i

sample such that

CHAPTER 1: INTRODUCTION TO CORRECTED FLUORESCENCE MEASUREMENTS

Molecular fluorescence spectroscopy is a popular technique for the quantitation of a variety of classes of compounds. This popularity is primarily due to the high selectivity and excellent detection limits of the method. The only requirement for a fluorescence assay is that the analyte fluoresces or can be derivatized such that the product of the derivatization reaction is fluorescent. However, several physical and chemical processes can affect the measured fluorescence intensity of a given sample, thus introducing error in the assumption that the measured fluorescence intensity is directly proportional to the concentration of the fluorophore.

The fluorescence intensity one measures with a typical fluorometer can be expressed as:

$$E_L = \Phi\phi kc \qquad (1\text{-}1)$$

where E_L is the measured fluorescence intensity, Φ is the radiant power of the excitation source, ϕ is the quantum yield of the fluorophore, k is a collection of instrumental constants, and c is the concentration of the fluorophore. This expression assumes that the solution absorbance is negligible at the excitation and emission wavelengths. If one directly compares fluorescence intensities from multiple solutions, one assumes that processes influencing the fluorescence intensity of one solution in the set also affect the other solutions to the same degree. Such processes can act via mechanisms that depopulate the excited state of the fluorophore causing a reduction in the fluorescence intensity, or they may involve extremes in physical parameters of the sample such that assumptions made in deriving the expression are no longer valid.

If an ele

fluorescence occu

vibrational energ

commonly referre

intensity and the

Molecular oxyger

effective quenche

If the abs

exciting radiation

intensity will be l

filter effect, and

light prior to and

fewer molecules

This region of th

caused by such a

effect is due to a

viewed and in th

boundary nearest

intensity relative t

due to a high anal

absorption is used

The review

fluorescence meas

quenching and one

If an electronically excited fluorophore collides with another body before fluorescence occurs, the energy stored in the excited fluorophore can be released as vibrational energy in a process known as collisional quenching. This process is commonly referred to simply as quenching, and it reduces the observed fluorescence intensity and the excited-state lifetime. Many species can quench fluorescence. Molecular oxygen and halide ions are among the most widely known and the most effective quenchers.

If the absorbance of the solution is such that a large fraction of either the exciting radiation or the emitted fluorescence is absorbed, the measured fluorescence intensity will be less than that predicted by equation (1-1). This is known as the inner-filter effect, and consists two types of sample absorption. Absorption of the source light prior to and within the volume of the sample viewed results in the excitation of fewer molecules of the fluorophore than for a solution having a lower absorbance. This region of the solution is known as the pre-filter region, and hence a deviation caused by such absorption is known as the pre-filter effect. Similarly, the post-filter effect is due to absorption of the fluorescent radiation by the sample in the volume viewed and in the region of solution between the volume viewed and the solution boundary nearest the point of observation. It too reduces the measured fluorescence intensity relative to a lower absorbance solution. Significant solution absorption can be due to a high analyte concentration or to concomitant absorbing species. The term self absorption is used to describe absorption due exclusively to the analyte.

The review of the scientific literature on correcting for these sources of error in fluorescence measurements is presented in two parts: one devoted to correction for quenching and one devoted to correction for sample absorption.

The theor
quenching was fi
report numerous
reported. In
measurements, v
developed to mini

Quenchir
considerable time
and solvents have
perhaps the most
thaw cycles [5].
been reported by
dry ice to the sam
measurement is n
evacuation with st
[11], and chemic
continuous remova
apparatus uses a
create a gradient i
the solution and th

REVIEW

Correction for Quenching

The theoretical basis for the reduction in fluorescence intensity due to collisional quenching was first described in the classic work of Stern and Volmer [1]. Since that report numerous chemical systems that exhibit collisional quenching have been reported. In an effort to improve the accuracy of molecular fluorescence measurements, various chemical and instrumentation based approaches have been developed to minimize the effects of quenching.

CHEMICALLY-BASED APPROACHES

Quenching of fluorescence by molecular oxygen has been known for a considerable time [2], and many schemes to remove oxygen from analytical samples and solvents have been reported. Purging of samples with nitrogen [3] or argon [4] is perhaps the most common method, but it is not as rigorous as repeated freeze-pump-thaw cycles [5]. Recently, an incredibly simple and thorough means of degassing has been reported by Matsuzawa et. al. [6] in which one simply adds a small piece of clean dry ice to the sample, and allows it to sublime completely, just before the fluorescence measurement is made. More exotic methods such as purging while refluxing [7], evacuation with stirring [8], purging followed by evacuation [9,10], ultrasonification [11], and chemical scavenging [12,13] have been reported. A system for the continuous removal of oxygen from a flowing stream has also been reported [14]. This apparatus uses a semi-permeable membrane and an oxygen scavenging solution to create a gradient in the oxygen concentration. The dissolved oxygen diffuses through the solution and the membrane to the scavenging solution where it is reduced to water.

A similar schem

[15].

Another a

shields the fluorc

them from the m

"organized medi

complexes such

envelop the fluor

the advantage tha

are more difficult

Several re

in the literature.

issue of the journa

As one m

chemical sensors.

in fluorescence i

quenching that re

type for *in vivo* u

Wolfbeis, Posch,

oxygen and haloth

A similar scheme has been used in an automated system for sample deoxygenation [15].

Another approach for reducing quenching involves adding a compound that shields the fluorophore from would-be quenchers to the sample, rather than removing them from the matrix. This is one of the objectives of fluorescence spectroscopy in "organized media", a topic of great interest in the recent literature. Inclusion complexes such as micelles and cyclodextrins can partially surround or completely envelop the fluorophore and protect it from collisional quenching. This approach has the advantage that it can reduce quenching from oxygen, and from other quenchers that are more difficult to expel from the sample.

Several reviews of organized media in fluorescence spectroscopy have appeared in the literature. The most recent of these was in the semi-annual fundamental review issue of the journal *Analytical Chemistry* [16].

As one might expect, quenching has been used to advantage; especially in chemical sensors. Such sensors determine the quencher concentration by the decrease in fluorescence intensity of a fluorescent dye. This decrease is of course due to quenching that results from collisions with the quencher. An oxygen sensor of this type for *in vivo* use has been reported by Peterson, Fitzgerald, and Buckhold [17]. Wolfbeis, Posch, and Kroneis [18] reported a similar sensor for the determination of oxygen and halothane, a common anesthetic.

Attempts

measurement rat

instrumentation-b

disturbed and less

necessarily pertur

case of *in situ* me

The first i

was reported by

that both the flu

collisional quench

ratio of the fluore

the concentration

quenching species

The fluores

where k is a pro

parameters such as

ϕ is the quantum

fluorophore. The

lifetime, τ, to the

INSTRUMENTATION-BASED APPROACHES

Attempts to reduce the effects of quenching by improving the basis of the measurement rather than manipulating the matrix has been the focus of a few instrumentation-based approaches. These have the advantage that the sample is not disturbed and less effort is expended in sample preparation. Chemically-based methods necessarily perturb the sample, but this may not be desirable or even possible as in the case of *in situ* measurements.

The first instrumentation-based approach to correct for the effect of quenching was reported by Hieftje and Haugen [19]. Their method takes advantage of the fact that both the fluorescence intensity and the excited-state lifetime are reduced by collisional quenching, and involves ratioing these quantities. They showed that the ratio of the fluorescence intensity to the excited-state lifetime is directly proportional to the concentration of the fluorophore and independent of the concentration of collisional quenching species. The following derivation was presented in their paper:

The fluorescence intensity, F, can be expressed as:

$$F = k\phi c \tag{1-2}$$

where k is a proportionality constant that takes into account several instrumental parameters such as the radiant power of the source, the area of the source viewed etc., ϕ is the quantum efficiency of the fluorophore, and c is the concentration of the fluorophore. The quantum efficiency can be expressed as the ratio of the observed lifetime, τ, to the lifetime in the absence of quenching, τ_0 (i.e. the natural lifetime):

$$\phi = \frac{\tau}{\tau_0} \tag{1-3}$$

Substituting this e

If K is defined as

equation (1-4) bec

Hence the ratio o

and is not affecte

quantum efficienc

In the orig

quenching in two

chloride and the q

were determined

determined with

Haugen were also

limited success.

time-correlated si

synchronously pu

anode pulse rate

processed fluoresc

Although each q

intensity, they botl

counting technique

required for the n

Substituting this expression for the quantum efficiency into equation (2), one obtains:

$$F = k\frac{\tau}{\tau_0} c \qquad (1\text{-}4)$$

If K is defined as the ratio of the constants k and τ_0,

$$K = \frac{k}{\tau_0} \qquad (1\text{-}5)$$

equation (1-4) becomes after rearrangement:

$$\frac{F}{\tau} = Kc \qquad (1\text{-}6)$$

Hence the ratio of F/τ is directly proportional to the concentration of the fluorophore and is not affected by collisional quenching or any other process that decreases the quantum efficiency.

In the original work [19], the Hieftje-Haugen approach was used to correct for quenching in two chemical systems. These were the quenching of quinine sulfate by chloride and the quenching of 1-pyrene butyric acid by iodide. Fluorescence intensities were determined with a conventional fluorometer and excited-state lifetimes were determined with a time-correlated single-photon counting apparatus. Hieftje and Haugen were also able to determine these quantities on a single instrument, albeit with limited success. For this endeavor, they replaced the discharge lamp source of the time-correlated single-photon counting apparatus with a more amplitude stable synchronously pumped, cavity-dumped, frequency-doubled dye laser. The average anode pulse rate integrated over a ten second time period and the integral of the processed fluorescence decay were both used as a measure of the fluorescence intensity. Although each quantity yielded reasonable precision as measures of fluorescence intensity, they both suffer from limitations inherent in the time-correlated single-photon counting technique. If the count rate of the system is increased to reduce the time required for the measurement of intensity, a distortion in the shape of the recorded

decay results. T
determined by in
the intensity to th
the measurement

Alfano, F
correcting for the
rate, gated photon
the integrated area
The temporal dec
emission informat
single fluorescence
with an electrical
exciting light. A
photodiode and the
were generated in
reference and samp
obtained by plottin
position. As in t
excited-state decay
approach a real-tim

Demas, Jone
quenching in fluores
detection via a dual
method, the light
lifetime. The mod

decay results. This greatly reduces the accuracy in the lifetime and in the intensity determined by integrating the decay. Although Hieftje and Haugen showed the ratio of the intensity to the lifetime is independent of quenching, they were not able to perform the measurement of that ratio in real time.

Alfano, Fong, and Lytle [20] implemented the Hieftje-Haugen approach to correcting for the effects of quenching with an instrument designed for high repetition rate, gated photon counting. Similar to Hieftje and Haugen's work, Alfano et al. used the integrated area of the fluorescence decay as a measure of the fluorescence intensity. The temporal decay of the excited state was recorded by mixing the time-dependent emission information with a temporally scanned reference. The signal generated by single fluorescence photons impinging on a fast microchannel plate detector was mixed with an electrical pulse generated by a fast photodiode that sampled the pulses of exciting light. A trombone line and different lengths of coaxial cable between the photodiode and the mixer provided the temporal scanning mechanism. Electrical pulses were generated in the mixer and subsequently counted by a rate meter when the reference and sample pulses were coincident at the mixer. The fluorescence decay was obtained by plotting counts per unit time from the ratemeter versus the trombone line position. As in the paper by Hieftje and Haugen, Alfano et al. had to curve fit the excited-state decay data to obtain the fluorescence lifetime, and hence could not approach a real-time measurement of the ratio of intensity to observed lifetime.

Demas, Jones, and Keller [21] reported two methods for reducing the effects of quenching in fluorescence measurements. A modulated light source and phase sensitive detection via a dual-channel lock-in amplifier were used in both methods. In the first method, the light source was modulated faster than the period of the excited-state lifetime. The modulation frequency was set sufficiently high that the fluorescence

detected at that

intensity by a si

technique of Hie

the phase shift b

the dual-channel

modulation inten

relating these qua

Here S is the obs

unquenched samp

modulation freque

of the uranyl ion

Although

measurement [21]

μs), and not repre

modulation bandw

lifetimes of ten t

available, it is ve

The second metho

for the analyte flu

angle must also be

detected at that frequency occurred before collisional quenching could reduce the intensity by a significant extent. The second method is similar to the time-domain technique of Hieftje and Haugen [19]. In "method 2", the modulated amplitude and the phase shift between excitation and emission were simultaneously determined with the dual-channel lock-in amplifier, and were used to calculate the unquenched modulation intensity at a modulation frequency of zero. The following expression relating these quantities was given, but its derivation was not:

$$S = \frac{S_o}{\left[\left(\frac{1}{\phi}\right)^2 + (\omega\tau_o)^2\right]^{\frac{1}{2}}} \qquad (1\text{-}7)$$

Here S is the observed modulated amplitude and S_o is the modulated amplitude for an unquenched sample at a modulation frequency of zero. The quantum yield, radial modulation frequency, and natural lifetime are ϕ, ω and τ_o respectively. Fluorescence of the uranyl ion quenched by chloride was studied by both methods.

Although both methods worked well and demonstrated the principle of the measurement [21], the system studied was that of a long-lived fluorophore (τ = 170 μs), and not representative of common fluorophores. The first method would require a modulation bandwidth of gigahertz for fluorophores having more typical un-quenched lifetimes of ten to 20 nanoseconds. Although instrumentation of this bandwidth is available, it is very expensive and not directly compatible with the reported system. The second method requires that the natural lifetime must also be determined or known for the analyte fluorophore in the matrix at hand. The instrumental zero-time phase angle must also be known. The method is also somewhat computationally complex.

There is

spectroscopy at

[22], Christmann

to be completed

in them constitu

corrected fluores

Yappert,

polychromatic lu

based on a dual

record fluoresce

contained in a st

the work of Parke

where the soluti

bandpasses, and

assumed in previo

these wavelength

methyl red system

chemiluminescenc

Correction for Sample Absorption

There is a long history of research in absorption corrected fluorescence spectroscopy at Michigan State University. It includes the dissertations of Holland [22], Christmann [23], Ratzlaff [24], Adamsons [25,26], and Doherty [27] (and the yet to be completed work of Victor [28]). These dissertations and the references contained in them constitute an excellent review. This section reviews work in absorption corrected fluorescence published since the most recent of those dissertations [27].

Yappert, Schuyler, and Ingle reported a scheme for the correction of polychromatic luminescence signals for the inner-filter effect [29]. Their work was based on a dual multichannel, fiber optic based instrument that can simultaneously record fluorescence, absorption and chemiluminescence spectra from a sample contained in a standard four cm by one cm^2 cuvette [30]. In essence, they extended the work of Parker and Barnes [3] and Holland and coworkers [31] to include situations where the solution absorbance is not constant over the excitation and emission bandpasses, and where optical fibers are used to collect the fluorescence. It was assumed in previous correction procedures that the solution absorbance is constant over these wavelength intervals. Their correction scheme was tested with a quinine sulfate - methyl red system and subsequently used to study the lucigenin - hydrogen peroxide chemiluminescence system [32].

1. Stern, O.; V
2. Kautsky, H.
3. Parker, C.A
4. Lund, W.;
5. Whery, E.L
Dekker: Ne
6. Matsuzawa,
7. Bratin, K.;
8. Battino, R.;
9. Norris, B.J.
10. Fox, M.A.;
11. Dell'Ova, V
12. Rollie, M.E.
13. MacCrehan,
14. Reim, R. *An*
15. Rollie, M.E.
16. McGown, L.
17. Peterson, J.I
18. Wolfbeis, O.
19. Hieftje, G.M
20. Alfano, A.J.;
21. Demas, J.N.;

CHAPTER 1 REFERENCES

1. Stern, O.; Volmer, M. *Z. Phys.* **1919**, *20*, 183.
2. Kautsky, H. *Trans. Faraday Soc.* **1939**, *35*, 216.
3. Parker, C.A.; Barnes, W.J. *Analyst*, **1957**, *82*, 606.
4. Lund, W.; Opheim, L.-N. *Anal. Chim. Acta.* **1975**, *79*, 35.
5. Whery, E.L. in *Fluorescence Theory, Instrumentaton, and Practice*, Marcel Dekker: New York, 1967, p.92. G.G. Guilbault, Ed.
6. Matsuzawa, S.; Wakisaka, A.; Tamura, M. *Anal. Chem.* **1990**, 62, 2645.
7. Bratin, K.; Kisinger, P.T.; Brunlett, C.S. *J. Liq. Chromatogr.* **1981**, *4*, 1777.
8. Battino, R.; Banzhof, M.; Bogan, M.; Wilheim, E. *Anal. Chem.* **1971**, *43*, 806
9. Norris, B.J.; Meckstroth, M.L.; Heineman, W.R. *Anal. Chem.* **1971**, *43*, 806.
10. Fox, M.A.; Staley, S.W. *Anal. Chem.* **1976**, *48*, 992.
11. Dell'Ova, V.E.; Denton, M.B.; Burke, M.F. *Anal. Chem.* **1974**, *46*, 1365.
12. Rollie, M.E.; Ho, C.-N.; Warner, I.M. *Anal. Chem.* **1983**, *55*, 2445.
13. MacCrehan, W.A.; May, W.E. *Anal. Chem.* **1984**, *56*, 625.
14. Reim, R. *Anal. Chem.* **1983**, *55*, 1188.
15. Rollie, M.E.; Patonay, G.; Warner, I.M. *Anal. Chem.* **1987**, *59*, 180.
16. McGown, L.B.; Warner, I.M. *Anal. Chem.* **1990**, *62*, 255R.
17. Peterson, J.I.; Fitzgerald, R.V.; Buckhold, D.K. *Anal. Chem.* **1984**, *56*, 62.
18. Wolfbeis, O.S.; Posch, H.E.; Kroneis, H.W. *Anal Chem.* **1985**, *57*, 2556.
19. Hieftje, G.M.; Haugen, G.R. *Anal. Chim. Acta.* **1981**, *123*, 255.
20. Alfano, A.J.; Fong, F.K.; Lytle, F.E. *Rev. Sci. Instrum.* **1983**, *54*, 967.
21. Demas, J.N.; Jones, W.M.; Keller, R.A. *Anal. Chem.* **1986**, *58*, 1717.

22. Holland, J.
1971.

23. Christmann
MI, 1980.

24. Ratzlaff, E.
1982.

25. Adamsons,

26. Adamsons,
1985.

27. Doherty, T.
1990.

28. Victor, M.A

29. Yappert, M.

30. Yappert, M.

31. Holland, J.F
706.

32. Yappert, M.

22. Holland, J.F. Ph. D. Dissertation, Michigan State University, East Lansing, MI, 1971.

23. Christmann, D.R. Ph. D. Dissertation, Michigan State University, East Lansing, MI, 1980.

24. Ratzlaff, E.H. Ph. D. Dissertation, Michigan State University, East Lansing, MI, 1982.

25. Adamsons, K. M.S. Thesis, Michigan State University, East Lansing, MI, 1982.

26. Adamsons, K. Ph. D. Dissertation, Michigan State University, East Lansing, MI, 1985.

27. Doherty, T.P. Ph. D. Dissertation, Michigan State University, East Lansing, MI, 1990.

28. Victor, M.A. unpublished work.

29. Yappert, M.C.; Schuyler, M.W.; Ingle, J.D. *Anal. Chem.* **1989**, *61*, 593.

30. Yappert, M.C.; Ingle, J.D. *Appl. Spectrosc.* **1989**, *43*, 759.

31. Holland, J.F.; Teets, R.E.; Kelley, P.M.; Timnick, A. *Anal. Chem.* **1977**, *49*, 706.

32. Yappert, M.C.; Ingle, J.D. *Appl. Spectrosc.* **1989**, *43*, 767.

CHAPTER 2:
BASED APPRO

While sat
sample absorptio
correction for the
based methods to
because the latter
time and capital i
methods do not p
beyond that needc
quenching is extre

Of the ins
Haugen method [1
fluorescence inten
methods reviewed
exactly correct the

A real-time
of correcting for t
lifetime and the s
latter quantity is re
of the excited-stat
acquiring fluoresce
implementation of

CHAPTER 2: DESIGN CONSIDERATIONS FOR AN INSTRUMENTATION-BASED APPROACH TO REAL-TIME CORRECTION FOR ERRORS DUE TO QUENCHING

While satisfactory methods exist to correct fluorescence measurements for sample absorption, a routine, instrumentation-based technique for the real-time correction for the effects of quenching has yet to be fully developed. Instrumentation-based methods to correct for quenching are preferable over chemically-based methods because the latter necessarily perturb the system under study and require investments of time and capital in the form of additional sample preparation. Instrumentation-based methods do not perturb the system under study, and do not require sample preparation beyond that needed for a routine fluorescence assay. Of course in situations where quenching is extreme, a combination of methods may be needed.

Of the instrumentally based methods to correct for quenching, the Hieftje-Haugen method [1] is one of the best to develop. It provides an exact means to correct fluorescence intensity for the reduction caused by collisional quenching. The other methods reviewed in chapter one only minimize the effects of quenching. They do not exactly correct the measured quantity.

A real-time or near real-time implementation of the Hieftje-Haugen method [1] of correcting for the effects of quenching requires rapid acquisition of the excited-state lifetime and the steady-state fluorescence intensity. The real-time acquisition of the latter quantity is relatively simple. The same cannot be said for the rapid determination of the excited-state lifetime. The criteria and choice of a measurement strategy for acquiring fluorescence intensity and excited-state lifetime data needed for the real-time implementation of the Hieftje-Haugen method are discussed in this chapter.

CR

In additio
lifetime, one ne
collisional quench

Linearity
response of the
"bending over" d
detector is a pho
proportional to fl
PMT in absolute
nanoamp or less
by cooling a PMT
the photocathode
detect is often lim
detection limits or

If correctio
range is limited b
typical value for t
tolerated with a
intensities, especia
not uncommon fo
magnitude in conc
instruments is ro
milliamps.

CRITERIA FOR THE DETERMINATION OF I AND τ

In addition to typical values for the fluorescence intensity and the excited-state lifetime, one needs to know the extent to which these quantities are reduced by collisional quenching to implement the Hieftje-Haugen method [1] intelligently.

Linearity in measured fluorescence intensity is generally limited by the dark response of the detector on the low end of the intensity scale and by the classical "bending over" due to self-absorption at the high end. In modern spectrometers, the detector is a photomultiplier tube (PMT), and the quantity measured and considered proportional to fluorescence intensity is the PMT's anode current. The response of a PMT in absolute darkness is referred to as the dark current, and it is on the order of a nanoamp or less for most PMTs. A dark current of picoamps or less can be achieved by cooling a PMT. The extent of this reduction depends on the degree of cooling and the photocathode material. The minimum detectable concentration an instrument can detect is often limited by the detector's dark current. State-of-the-art instruments have detection limits on the order of 10^{-12} M for strongly fluorescent compounds [2].

If corrections are made for self-absorption, the high intensity end of the linear range is limited by the PMT's maximum average anode current. One milliamp is a typical value for the maximum average current of a PMT. Higher light levels can be tolerated with a photodiode. However, PMTs are superior for detecting lower intensities, especially in the ultra-violet and the blue end of the visible spectrum. It is not uncommon for the linear range of a fluorometer to extend over six orders of magnitude in concentration [2]. Not surprisingly, the linear range in well-designed instruments is roughly equal to that of a room temperature PMT: nanoamps to milliamps.

Real-time

simply connect t

digital display o

simple oscillosc

covers the openi

leak in the form

time dependent

applying a bias v

More elaborate s

computer have b

In extrem

for *trans*-stilbene

Values of 1 to 1

for anthracene [5

The exte

reduced by collis

In this expressio

of quenching, k_q

of the fluorophor

concentration of

Real-time acquisition of fluorescence intensity is straightforward. One may simply connect the anode of a PMT to a common digital multimeter for a convenient digital display or to an oscilloscope for higher bandwidth, analog display. In fact a simple oscilloscope configuration is the suggested means of testing a PMT. One covers the opening in the PMT's housing with black electrical tape, and creates a light leak in the form of a pin hole in the tape. Fluorescent room lights provide a convenient time dependent light source. Triggering the oscilloscope from the power line and applying a bias voltage to the PMT yields a rough 60 Hz sine wave on the oscilloscope. More elaborate schemes for automated, high speed data acquisition using a laboratory computer have become not only possible, but increasingly affordable in recent years.

In extreme cases, excited-state lifetimes can range from picoseconds (e.g. 70 ps for *trans*-stilbene in hexane [3,4]) or faster to milliseconds for some transition metals. Values of 1 to 100 nanoseconds are more typical for aromatic compounds (e.g. 4.1 ns for anthracene [5] and 96 ns for naphthalene [6]).

The extent to which the fluorescence intensity and the excited state lifetime are reduced by collisional quenching can be deduced from the Stern-Volmer equation [7]:

$$\frac{F_o}{F} = 1 + k_q \tau_o [Q] \qquad (2\text{-}1)$$

In this expression, F_o and F are the fluorescence intensities in the absence and presence of quenching, k_q is the bimolecular quenching constant, τ_o is the excited state lifetime of the fluorophore in the absence of quenching (i.e. the natural lifetime), and [Q] is the concentration of quencher. By defining the Stern-Volmer quenching constant, K_D:

$$K_D = k_q \tau_o \qquad (2\text{-}2)$$

the Stern-Volmer

Because collisiona
lifetimes in the ab

$$\tau_o =$$

Where Γ is the n
expressed as :

The right-hand si
Hence collisional
lifetime to the san

It is inter
constant that the
the quencher is
collisional quenc
concentration of
Volmer plot, the p
slope of K_D. Mu
in a Stern-Volmer
amino acids in pro
accessible and, he

If the Stern
the expected redu

the Stern-Volmer equation can rearranged to yield:

$$\frac{F_o}{F} = 1 + K_D[Q] \qquad (2\text{-}3)$$

Because collisional quenching is a kinetic process that depopulates the excited state, the lifetimes in the absence (τ_o) and presence (τ) of quenching can be expressed as:

$$\tau_o = \Gamma^{-1} \qquad (2\text{-}4) \qquad\qquad \tau = (\Gamma + k_q[Q])^{-1} \qquad (2\text{-}5)$$

Where Γ is the natural rate of decay of the excited state The ratio of τ_o to τ can be expressed as :

$$\frac{\tau_o}{\tau} = 1 + k_q\tau_o[Q] = 1 + K_D[Q] \qquad (2\text{-}6)$$

The right-hand side of this expression is identical to that of the Stern-Volmer equation. Hence collisional quenching reduces the fluorescence intensity and the excited-state lifetime to the same extent.

It is interesting to note from the definition of the Stern-Volmer quenching constant that the fluorescence intensity is reduced by 50% when the concentration of the quencher is K_D^{-1}. The Stern-Volmer quenching constant and information on collisional quenching can be obtained by plotting F_o/F (or τ_o/τ) versus the concentration of quencher. In this classic graphical construct, known as a Stern-Volmer plot, the plotted data are linear, intercept the ordinate axis at unity, and have a slope of K_D. Multiple environments of the fluorophore are indicated by non-linearity in a Stern-Volmer plot. Such situations are often encountered in the fluorescence of amino acids in proteins where the amino acids on the surface of the protein are more accessible and, hence, more readily quenched than those in the interior [8].

If the Stern-Volmer quenching constant of the quencher in question is known, the expected reduction in fluorescence intensity due to collisional quenching can be

readily determine
containing values
the scientific liter

To get a g
excited-state lifeti
quencher. The di
cm^2/sec in water
Intermediate valu
translates to diffu
lifetimes of 4, 2
fluorophore is l
virtually impossib
tryptophan quenc
diffusion coefficie
constant of 32.4
oxygen of 1/(32
tryptophan by a f
naphthalene, the
by a factor of 3
significant when
values.

From the
fluorescence inter
Hiefije-Haugen m

readily determined from the Stern-Volmer equation. Unfortunately reference volumes containing values of k_q and K_D do not exist. However, such information is available in the scientific literature for a number of fluorophore-quencher pairs.

To get a grasp on the extent that quenching reduces fluorescence intensity and excited-state lifetime, consider quenching by oxygen, a well known and very effective quencher. The diffusion coefficient of oxygen is quite large, ranging from 2.5×10^{-5} cm^2/sec in water at 25°C [8] to 5.31×10^{-5} cm^2/sec in cyclohexane at 29.6°C [9]. Intermediate values are found for solvents of intermediate polarity. For water, this translates to diffusion distances of 44, 100 and 224 A° over the course of excited state lifetimes of 4, 20, and 100 ns [8]. Obviously quenching is most severe if the fluorophore is long-lived. In fact, room temperature phosphorescence (RTP) is virtually impossible if oxygen is present [10]. The bimolecular quenching constant for tryptophan quenched by oxygen in water is 1.2×10^{10} $\underline{M}^{-1}$ sec^{-1} [8]. From the diffusion coefficient for oxygen in water, one can calculate a Stern-Volmer quenching constant of 32.4 $\underline{M}^{-1}$ for tryptophan (τ_0 = 2.7 ns) [8]. Therefore a concentration of oxygen of $1/(32.4\ \underline{M}^{-1})$ or 0.03 $\underline{M}$ would be needed to quench fluorescence of tryptophan by a factor of two. Assuming the same bimolecular quenching constant for naphthalene, the same concentration of oxygen would reduce naphthalene fluorescence by a factor of 35. For most fluorophores (i.e. $\tau < 20$ ns), quenching becomes significant when the total concentration of quenching species approaches millimolar values.

From the preceding discussions, one can specify criteria for measuring fluorescence intensities and excited-state lifetimes which are needed to implement the Hieftje-Haugen method [1]. The linear range in fluorescence intensity should be

several orders of
wide range, and
quenching specie
lifetimes from 10
dependent, but d
determination of
fluorescenct spec
by a factor of 10
be on the order o
the determination

REVIEW

Fluorescer
instrument that is
such an approach
complex apparat
information. Ea
either a time dom

The simple
to excite the sam
decay with a devi
the advantage of
sufficient accurac

several orders of magnitude in order to determine fluorophore concentrations over a wide range, and correct for quenching in the presence of large concentrations of quenching species. The instrument should also be able to determine excited-state lifetimes from 100 ns to less than 1 ns. The excited-state lifetime is not concentration dependent, but does vary from fluorophore to fluorophore. This range allows the determination of excited-state lifetimes for many fluorophores, but not for all fluorescenct species. It also allows for a maximum reduction of excited state lifetime by a factor of 100. The time required for the measurement of these quantities should be on the order of seconds or less. The following section reviews existing methods for the determination of fluorescence intensity and excited-state lifetime.

REVIEW OF METHODS FOR THE MEASUREMENT OF I AND τ

Fluorescence intensity and excited-state lifetime can be determined in a single instrument that is essentially two instruments in a single housing. However pursuing such an approach would not accomplish anything new, and would result in a needlessly complex apparatus. Several methods exist that provide both of these pieces of information. Each has its own advantages and limitations, and can be classified as either a time domain method or a frequency domain method.

Time Domain Methods

The simplest and most intuitive means of determining an excited-state lifetime is to excite the sample with a brief pulse of light and directly record the fluorescence decay with a device such as a camera coupled to an oscilloscope [11]. This method has the advantage of simplicity in setup and operation. However it does not provide sufficient accuracy for the determination of an excited-state lifetime to several

significant figure
without the use
bandwidth in exc
nanosecond. It
before curve fittin
or a transient
complexity; it ca
is one part in 2^{12}

An impro
block diagram of

Figure 2-1. Blo

source is used to
passed through a
detector is ampl
oscilloscope or a

significant figures. In addition, determining extremely fast lifetimes is not possible without the use of equally fast oscilloscopes. For example, an oscilloscope having a bandwidth in excess of a gigahertz is needed to determine a fluorescence lifetime of a nanosecond. It is also not "user friendly", as the data must be digitized manually before curve fitting. Replacing the conventional oscilloscope with a digital oscilloscope or a transient digitizer removes the manual digitization step at the cost of added complexity; it can, however, improve accuracy if the resolution of the digitizing device is one part in 2^{12} or higher.

An improvement over direct recording is the pulse sampling method [12]. A block diagram of an apparatus for this method is shown in Figure 2-1. A pulsed light

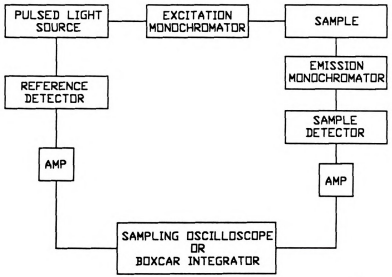

Figure 2-1. Block diagram of a pulse-sampling apparatus.

source is used to excite the sample, and fluorescence from the sample is collected and passed through a wavelength selection device prior to detection. The output of the detector is amplified and recorded with a sampling device such as a sampling oscilloscope or a boxcar integrator. These devices sample the detector response over a

narrow time win

fluorophore and

triggered by a t

decay by a contir

waveform. This

Figure 2-2. Sa
sequence of wav
show the pulse s
sampling.

acquires a single

the mean. Beca

obtained with a b

until the signal-t

fitting or less so

lifetime from the

fluorescence deca

One of the

state via fluoresc

recently recomme

The fluorescence

narrow time window. The fluorescence decay is recorded by repetitively exciting the fluorophore and sampling the fluorescence decay in step-wise fashion. Sampling is triggered by a temporal reference detector, and is scanned across the fluorescence decay by a continuously swept delay between the trigger signal and the sampling of the waveform. This methodology is illustrated in Figure 2-2. A sampling oscilloscope

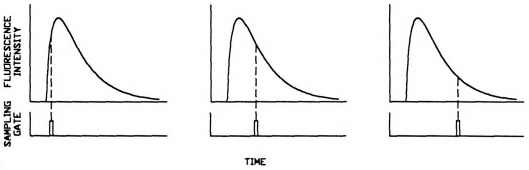

Figure 2-2. Sampling sequence used in the pulse sampling method. The upper sequence of waveforms is a series of fluorescence decays. The plots beneath them show the pulse sampling sequence and the increasing delay between the trigger and sampling.

acquires a single point while a boxcar averager acquires multiple samples and returns the mean. Because of its signal averaging nature, higher signal-to-noise data are obtained with a boxcar averager. In either case, successive decay curves are averaged until the signal-to-noise ratio is sufficient for curve fitting. Computer-based curve fitting or less sophisticated manual approaches are used to extract the excited-state lifetime from the raw data. The fluorescence intensity is obtained by integrating the fluorescence decay over time.

One of the most widely used techniques for recording the decay of an excited state via fluorescence is time-correlated single-photon counting [13, 14]. IUPAC recently recommended the name Single Photon Timing (SPT) for this method [15]. The fluorescence decay is acquired by measuring the time between excitation of the

sample and the e

light sources are

excitation flash is

shown in Figure

Figure 2-3. Blo

the light is direc

constant signal wi

sample. Fluores

spectrally selecte

detector. After a

converted to digit

START and ST

START/STOP pa

sample and the emission of a photon. Relatively weak, high repetition rate, pulsed light sources are used such that the probability of detecting a fluorescence photon per excitation flash is less than unity. A diagram of the instrumentation used in SPT is shown in Figure 2-3. The train of exciting pulses is split such that a small portion of

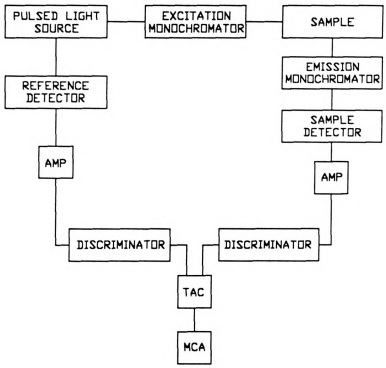

Figure 2-3. Block diagram of a single photon timing apparatus.

the light is directed toward to a reference detector, which provides a temporally constant signal with respect to the excitation pulse, while the remainder continues to the sample. Fluorescence photons from the sample are collected with a lens system, spectrally selected with a filter or monochromator, and detected with a very fast detector. After amplification, the smooth, analog pulses generated by the detectors are converted to digital pulses using discriminators. The edges of these pulses then provide START and STOP inputs to a time-to-amplitude-converter (TAC). For each START/STOP pair, the TAC provides a pulse having an amplitude that represents the

time between STA
by a multichannel
accumulating the
photon, the exci
methods, the exci
The fluorescence
or by integrating

Desilets a
state lifetimes th
fluorescence dec
sampling oscillos
the laser. The ar
of the oscilloscop
inserting a delay
oscilloscope. Th
excited-state lifet

where $I(t_1)$ and
constants, and τ i
t_2 was recorded f
curve. Once
determined "on-t
Their system wa
quinine sulfate i

time between START and STOP. The amplitude of pulses from the TAC is digitized by a multichannel analyzer (MCA) and stored in a buffer memory or a computer. By accumulating the time between the excitation pulse and the detection of a fluorescence photon, the excited-state decay can be constructed. As with the pulse sampling methods, the excited-state lifetime must be extracted from the raw data by curve fitting. The fluorescence intensity can be derived by measuring the sample detector pulse rate, or by integrating the acquired decay curve.

Desilets and coworkers [16] reported a simple method for determining excited-state lifetimes that acquires the fluorescence intensity at only two points on the fluorescence decay. Their instrument used a nitrogen laser and a dual-channel sampling oscilloscope. The oscilloscope was triggered by a photodiode illuminated by the laser. The anode current from the PMT was split and sent to both of the channels of the oscilloscope. Sampling the decay curve at two times was accomplished by inserting a delay cable between the power splitter and one of the channels of the oscilloscope. The ratio of the two intensities was recorded, and used to determine the excited-state lifetime by the equation:

$$\ln\left[\frac{I(t_1)}{I(t_2)}\right] = \ln\left[\frac{k_2}{k_1}\right] + \frac{t_1 - t_2}{\tau} \qquad (2\text{-}7)$$

where $I(t_1)$ and $I(t_2)$ are the intensities at times t_1 and t_2, k_1 and k_2 are instrumental constants, and τ is the excited-state lifetime. The ratio of the intensities at times t_1 and t_2 was recorded for fluorophores of known lifetime and used to construct a calibration curve. Once the calibration curve was constructed, lifetimes could easily be determined "on-the fly" with computer controlled acquisition and data manipulation. Their system was used to determine the excited-state lifetime of gentisic acid and quinine sulfate in static cells and in flowing streams. It was also used to determine

excited-state lifeti
method works w
intensity informat
intensities at the
expensive and so
requires optimiza
splitter and the
fluorophores hav
measurement cou

Rather th
observing the de
by continuously
comparing the e
utilize this princ
The waveforms
quantities derive
page 23 in Figu
frequency ω.
frequency, but s
the finite reside
lifetime increas
modulated than
demodulation fa

excited-state lifetimes for fluorescence detection in liquid chromatography [17]. This method works well for determining excited-state lifetimes, but it does not provide intensity information. In fact, one of the attributes of this method is that the ratio of intensities at the two times is concentration independent. It also requires moderately expensive and somewhat uncommon instrumentation. As presented, this method also requires optimization, or at least changing, the length of the delay cable between the splitter and the oscilloscope to change the temporal aperture to accommodate fluorophores having significantly different lifetimes. However the principle of the measurement could be implemented with other means.

Frequency Domain Methods

Rather than sequentially exciting the sample with a brief pulse of light and observing the decay of the excited-state, the same chemical information can be derived by continuously illuminating the sample with sinusoidally modulated light and comparing the emission waveform with that of the exciting light. Techniques that utilize this principle are broadly grouped as frequency domain fluorescence techniques. The waveforms used in a basic frequency domain fluorescence experiment and the quantities derived from them used to determine the excited-state lifetime are shown on page 23 in Figure 2-4. The excitation waveform is modulated at radial modulation frequency ω. This induces a modulation on the emitted fluorescence at the same frequency, but shifted in phase relative to excitation. The phase shift, ϕ, is a result of the finite residence time of the fluorophore in the excited state and increases as the lifetime increases for a given modulation frequency. The emission is also less modulated than the excitation, and the extent of this demodulation is expressed in the demodulation factor, m. Its value ranges from zero to unity with decreasing lifetime,

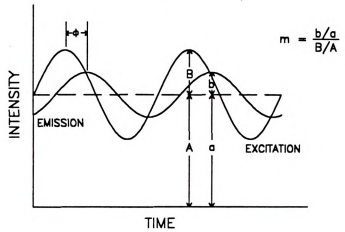

Figure 2-4. Excitation and emission waveforms for frequency domain fluorescence.

and it is the ratio of the AC to DC amplitudes of the emission waveform relative to the excitation waveform. The excited-state lifetime can be calculated directly from either the phase shift or the demodulation factor [8]:

$$\tau_p = \frac{\tan \phi}{\omega} \qquad (2\text{-}8)$$

$$\tau_m = \frac{1}{\omega}\left[\frac{1}{m^2} - 1\right]^{\frac{1}{2}} \qquad (2\text{-}9)$$

Modulation frequencies on the order of several tens of megahertz are required to measure excited-state lifetimes in the nanosecond range.

Various experimental approaches have been developed to extract the phase and demodulation information. A complete history of these is given in chapter four. Modern instrumentation uses cross-correlation detection [18] to step down the frequency of measurement from the high modulation frequencies used to resolve lifetimes in the nanosecond range. The highest modulation bandwidth reported is ten GHz [19] providing temporal resolution of 1 ps.

Almost all existing instruments use a cross-correlation frequency (i.e. the frequency at which phase and demodulation data are measured) of 30 Hz. This allows

real-time acquisit
computer controll
frequency is the
instrument, name
constructed by va

Of the ti
coworkers [16], i
is the only one th
also does not rec
the raw data. H
channel samplin
oscilloscope), an
approach based c
it would have to
fluctuations. In
small range of
computer-contro
appropriate dela

The dire
fluorescence an
domain techniqu
to extract the e
domain techniq

real-time acquisition of excited-state lifetime and fluorescence intensity through computer controlled instrumentation, The widespread use of a 30 Hz cross-correlation frequency is the result of incorporating the detection electronics of a commercial instrument, namely the Aminco model 4800 phase fluorometer, in instruments constructed by various research groups.

CONCLUSIONS

Of the time-domain methods, the method developed by Desilets, Lytle and coworkers [16], in which two points are acquired during the decay of the excited-state, is the only one that offers a means of rapid acquisition of the excited-state lifetime. It also does not require extensive curve fitting to extract the excited-state lifetime from the raw data. However it requires a somewhat rare and expensive instrument, a dual-channel sampling oscilloscope (one could also use a transient digitizer or digital oscilloscope), and it does not provide a means of obtaining fluorescence intensity. An approach based on their method could include acquisition of fluorescence intensity, but it would have to be normalized to the source intensity to compensate for amplitude fluctuations. In addition, because it uses a fixed delay line, it would be limited to a small range of lifetimes. This could be overcome to some extent by including a computer-controlled switch and multiple channel power splitter/combiner to select an appropriate delay cable for a sample having a given excited-state lifetime.

The direct relationship between the parameters measured in frequency domain fluorescence and the excited-state lifetime provides a distinct advantage over time domain techniques. Unlike most time domain techniques, which require curve fitting to extract the excited-state lifetime, curve fitting is not a requirement of frequency domain techniques. However to improve confidence when examining systems that

exhibit multi-expo

make measuremen

Frequency

the real-time imp

effects of quench

fluorescence was

experimentally de

time required for

most time domai

potential for real-

cross-correlation

possible. In ord

different lifetime

controlled appara

the modulation fr

Two mea

commercial frequ

and fabricated in

commercial ente

available for this

A comp

measurements w

also reduce reli

standards [21, 2

exhibit multi-exponential lifetimes or distributions in the lifetime data, many workers make measurements at multiple modulation frequencies and curve-fit the acquired data.

Frequency domain fluorescence was chosen as the best technique to pursue for the real-time implementation of the Hieftje-Haugen method [1] of correcting for the effects of quenching in molecular fluorescence spectroscopy. Frequency domain fluorescence was chosen for several reasons. The direct relationship between the experimentally determined quantities and the excited-state lifetime greatly reduces the time required for the measurement and the amount of data manipulation compared to most time domain techniques. Consequently, frequency domain fluorescence has the potential for real-time acquisition of the excited-state lifetime. In fact, increasing the cross-correlation frequency could make data acquisition on the stopped flow time scale possible. In order to make accurate measurements on samples having significantly different lifetimes, the modulation frequency must be changed. However, a computer controlled apparatus that incorporates commercial frequency synthesizers could change the modulation frequency in a few microseconds [20].

Two means are possible to implement the Hieftje-Haugen method [1]. A commercial frequency domain fluorometer could be modified, or one could be designed and fabricated in-house. Either route could be reproduced by other laboratories or by commercial enterprises. As a commercial frequency domain fluorometer was not available for this work, the latter approach was undertaken.

A complementary method to confirm or refute excite-state lifetime measurements would be advantageous. The availability of such instrumentation would also reduce reliance on compounds or mixtures accepted as excited-state lifetime standards [21, 22]. It has been shown that doing so may not be a wise practice as the

fluorescence deca

Because funds ar

apparatus, SPT w

fluorescence decay of accepted standards may not be as quantitatively certain [23]. Because funds and equipment were available to construct a single photon timing apparatus, SPT was chosen as the complementary method.

1. Hieftje, G.M

2. Ingle, J.D.
Cliffs, NJ,

3. Courtney, S

4. Hochstrasse

5. Birks, J.B.;

6. Berlman, I.
Academic P

7. Stern, O.;

8. Lakowicz,
York, 1983

9. Weast, R.C
FL, 1980,

10. Kraus, P.F
1988.

11. Demas, J.M
1983.

12. Ware, W.
Lamola, Ed

13. O'Connor,
Academic

14. Fleming,
University

15. Comission

16. Desilets, D
Chem. 198

17. Desilets, D

CHAPTER 2 REFERENCES

1. Hieftje, G.M.; Haugen, G.R. *Anal. Chim. Acta.* **1981**, *123*, 255.
2. Ingle, J.D.; Crouch, S.R. *Spectrochemical Analysis* Prentice Hall: Englewood Cliffs, NJ, 1988.
3. Courtney, S.H.; Flemming, G.R. *J. Chem. Phys.* **1980**, *83*, 215.
4. Hochstrasser, R.M. *Pure Appl. Chem.* **1980**, *52*, 2683
5. Birks, J.B.; Munro, I.H. *Prog. Reac. Kinetics* **1967**, *4*, 239.
6. Berlman, I.B *Handbook of Fluorescence Spectra of Aromatic Molecules* 2nd Ed. Academic Press: New York, 1971.
7. Stern, O.; Volmer, M. *Z. Physik*, **1919**, *20*, 183.
8. Lakowicz, J.R. *Principles of Fluorescence Spectroscopy* Plenum Press:New York, 1983.
9. Weast, R.C. Ed. *Handbook of Chemistry and Physics* CRC Press: Boca Raton, FL, 1980, p. F-61.
10. Kraus, P.R. Ph.D. Dissertation, Michigan State University, East Lansing, MI 1988.
11. Demas, J.N. *Excited State Lifetime Measurements* Academic Press: New York, 1983.
12. Ware, W.R. in *Creation and Detection of the Excited State* vol 1A, A.A. Lamola, Ed. Marcel Dekker, Inc.: New York, 1971, chapter 5.
13. O'Connor, D.V.; Phillips, D. *Time-Correlated Single Photon Counting* Academic Press, Inc: London, 1984.
14. Fleming, G.R. *Chemical Applications of Ultrafast Spectroscopy* Oxford University Press: New York, 1986.
15. Comission on Photochemistry, *Pure Appl. Chem.* **1990**, *62*, 1632.
16. Desilets, D.J.; Coburn, J.T.; Lantrip, D.A.; Kissinger, P.T.; Lytle, F.E. *Anal. Chem.* **1986**, *58*, 1123.
17. Desilets, D.J.; Kissinger, P.T.; Lytle, F.E. *Anal. Chem.* **1987**, *59*, 1830.

18. Birks, J.B.;

19. Lackzo, G.;
J.R.*Rev. Sci*

20. Technical Li

21. Chen, R.F.

22. Lampert, R
Meech, S.R

23. O'Connor,

18. Birks, J.B.; Little, W.A. *Proc. Phys. Soc.* **1953**, *66(A)*, 921.

19. Lackzo, G.; Gryczynski, I.; Gryczynski, Z.; Wiczk, W.; Malak, H.; Lakowicz, J.R.*Rev. Sci. Instrum.* **1990**, *61* 2331.

20. Technical Literature, Programmed Test Sources, Littleton, MA.

21. Chen, R.F. *Anal. Biochem.* **1974**, *57*, 593.

22. Lampert, R.A.; Chewter, L.A.; Phillips, D.; O'Connor, D.V.; Roberts, A.J.; Meech, S.R. *Anal. Chem.* **1983**, *55*, 68.

23. O'Connor, D.V.; Meech, S.R.; Phillips, D. *Chem. Phys. Let.* **1982**, *88*, 22.

Popularly

Timing (SPT) is t

of electronically

described in chapt

and Thomas [2] to

scintillators. Late

decay data [3,4].

instrumentation ar

excited-state deca

Information on the

devoted exclusively

fluorescence decay

attention must be p

on this level. Su

excited-state decays

instrument was cor

compound that has

existing system tha

component was de

instrument more ve

of the theory of the

described, and the

discussed. This

determination. Ex

CHAPTER 3: SINGLE−PHOTON TIMING

Popularly known as time−correlated single−photon counting, Single−Photon Timing (SPT) is the most widely used technique for recording the fluorescence decay of electronically excited species. It is generally agreed that the technique, briefly described in chapter two, was developed independently by Koechlin [1] and Bollinger and Thomas [2] to study the temporal characteristics of the pulses of light generated in scintillators. Later, biochemists used the method to acquire molecular fluorescence decay data [3,4]. Since its introduction many improvements have been made in instrumentation and methodology, providing a means to study fast and complex excited-state decays. Several reviews have appeared in the literature [5-8]. Information on the technique can also be found in various books [9-13] including one devoted exclusively to the technique [14]. State-of-the-art instrumentation can record a fluorescence decay having a lifetime of less than 20 picoseconds [15]. Careful attention must be paid to seemingly insignificant details to achieve temporal resolution on this level. Such items and concerns for accurately recording multi-exponential excited-state decays are discussed at appropriate points in this chapter. A modern SPT instrument was constructed. This instrument can record the fluorescence decay of a compound that has an excited-state lifetime less than 50 picoseconds. It is similar to an existing system that is restricted to recording only very fast fluorescence decays. A component was designed and fabricated to remove this limitation, making the new instrument more versatile than many modern SPT instruments. After a brief discussion of the theory of the measurement, the instrumentation used in state-of-the-art SPT is described, and the restrictions imposed by various instrumental configurations are discussed. This is followed by a description of typical excited-state lifetime determination. Example data from the constructed instrument is presented, and

application of the

quenching is discu

The basic

rationale behind t

the sample is an a

This probability d

measurements of t

emitted photon. (

excited-state deca

These restrictions

photocathode of th

collisions will resu

As the stat

[6, 17], only a br

given here.

At each cy

photons will strike

distribution, and is

where m is the av

flash. There is th

application of the SPT technique to the Hieftje-Haugen method [16] of correcting for quenching is discussed.

THEORY

The basic measurement scheme was briefly described in chapter two. The rationale behind the method is that the probability distribution of photons emitted by the sample is an accurate representation of the excited state decay of the fluorophore. This probability distribution is obtained by summing the results of a large number of measurements of the time difference between an excitation flash and the detection of an emitted photon. Certain restrictions must be taken into consideration to assure that the excited-state decay is accurately represented by the acquired probability distribution. These restrictions arise from the nature of the probability of photons impinging on the photocathode of the detector following an excitation flash, and the probability that these collisions will result in the emission of electrons from the photocathode.

As the statistics of the SPT technique have been thoroughly discussed elsewhere [6, 17], only a brief condensation following Pfeffer et al. [18] and Ware [9] will be given here.

At each cycle of the excitation source, we can define the probability, P_1, that n photons will strike the photocathode of the detector. This probability follows a Poisson distribution, and is given by:

$$P_1 = \frac{m^n e^{-m}}{n!} \tag{3-1}$$

where m is the average number of photons that strike the detector after an excitation flash. There is then the probability P_2 that these n photons striking the photocathode

will generate x pho

where ϕ is the q
electrons will be g
of P_1 and P_2 sum

If an electron is g
rate R for a source

R

The detector count
photocathode per u

Hence the fluores
between the detect
photons to source
below one percent.
distorted in propor
minor distortion.
fluorescence photon
upper limit of on
experiments are co
lasers are used.

will generate x photoelectrons. P_2 follows a binomial distribution, and is given by:

$$P_2 = \frac{n!}{x!(n-x)!}\ \phi^x\ (1-\phi)^{n-x} \tag{3-2}$$

where ϕ is the quantum efficiency of the photocathode. The probability that x electrons will be generated following each excitation cycle is then the joint probability of P_1 and P_2 summed over all possible values of n:

$$P_x = \sum_{n=x}^{\infty} P_1\, P_2 \quad = \quad \frac{(\phi m)^x\, e^{-m\phi}}{x!} \tag{3-3}$$

If an electron is generated, one can assume that a count will be recorded. The count rate R for a source repetition rate of v is:

$$R = v\,(1-P_{x=0}) = v\,(1-e^{-m\phi}) = v\left[m\phi - \frac{(m\phi)^2}{2} + \cdots\right] \tag{3-4}$$

The detector count rate will be proportional to the number of photons incident on the photocathode per unit time when

$$m\phi >> \frac{(m\phi)^2}{2} \tag{3-5}$$

Hence the fluorescence should be weak such that several excitation cycles occur between the detection of two fluorescence photons. In practice the ratio of detected photons to source flashes per unit time is the monitored parameter and is often kept below one percent. It has been shown [7] that the recorded fluorescence decay will be distorted in proportion to this ratio, and a ratio of up to five percent will cause only minor distortion. As the acceptable level of distortion decreases, so must the ratio of fluorescence photons to source flashes per unit time. It is commonly accepted that an upper limit of one or one-half percent is suitable for most work. In practice experiments are conducted at much lower ratios, especially when high repetition rate lasers are used.

Before dis
considerations co
figure by which
referred to as the
exists, it is gen
instantaneous sig
temporal jitter of
limit of excited-st
determine a lifeti
there is some dis
components of a
Aside from the i
The ultimate dete
sensitivity. In SI
sufficient data fo
efficiency at whic
parameters such a
illuminated and
instrumental detai

An accura
as a means of j
deconvolute the d
instrument respon
decay. This dis

THE INSTRUMENT RESPONSE

Before discussing the instrumentation used in modern SPT, a few general considerations concerning instrument performance should be mentioned. The primary figure by which SPT instruments are judged is the instrument response, sometimes referred to as the instrument response function (IRF). Although some disagreement exists, it is generally reported as the FWHM of the instrument's record of an instantaneous signal such as Raman scattering. It is essentially the rms sum of the temporal jitter of each component in the instrument. It defines time zero and the lower limit of excited-state lifetimes that can be determined. With proper techniques one can determine a lifetime that is roughly one-half of the instrument response. Here again there is some discrepancy on this issue. Some workers claim an ability to resolve components of a fluorescence decay one fifteenth of the instrument response [19, 20]. Aside from the instrument response, few other performance parameters are reported. The ultimate detectability of single photons defies the common definition of the term sensitivity. In SPT, sensitivity is essentially a measure of the time needed to acquire sufficient data for fitting the decay of a given sample. Hence it approximates the efficiency at which photons are collected and detected when the figure is normalized for parameters such as source power, sample quantum yield, and the volume of the sample illuminated and viewed. Sensitivity as such is almost never reported. Rather all instrumental details are reported.

An accurate measurement of the instrument response is of importance not only as a means of judging the performance of the instrument, it is also necessary to deconvolute the distortion of the fluorescence decay caused by the instrument. A finite instrument response, in SPT or another technique, will distort the acquired fluorescence decay. This distortion is minor for the case of a fluorescence decay that is long

compared to the

response is not n

is discussed towa

A block

accompanying di

configuration de

Although

have been con

research groups.

often the majori

limiting compo

necessarily the

SPT apparatus

clear, and the n

complete listing

given in Appen

The firs

the light source

however some

respects. The

compared to the instrument response, but becomes important when the instrument response is not negligible compared to the lifetime of the fluorophore. Deconvolution is discussed toward the end of this chapter in a section on data analysis.

INSTRUMENTATION

A block diagram of a SPT apparatus was shown in Figure 2-3. The accompanying discussion was intentionally not highly detailed because the instrumental configuration depends on several factors.

Although a few commercial systems exist, most of the SPT instruments in use have been constructed from home-built and commercial components by various research groups. Each component affects the instrument response to some degree, but often the majority of the temporal jitter is due to a single component. Historically the limiting component has been either the light source or the detector. This is not necessarily the case with modern instrumentation. In this section each component of an SPT apparatus is described, its appropriate configuration in the instrument is made clear, and the nature and extent of its effect on the instrument response is discussed. A complete listing of the components of the SPT instrument constructed in this work is given in Appendix 1.

Light Sources

The first consideration in any instrument used for fluorescence spectroscopy is the light source. SPT is no exception. Of course a perfect light source does not exist; however some of the light sources in use today approach ideal behavior in some respects. The ideal light source for SPT would emit a highly collimated, controllable,

high repetition trai
frequencies of ligh
light is not as criti
the absolute tempo
the shortest pulse
instruments use
disadvantages, an
instrument, dictat

The flash
generate nanosecc
pulse results fro
Other gases have
below atmospher
choice of gas an
most dependent
the temporal pr
duration is norm
followed by a sl
thorough review
and Phillips [14]

Mode-loc
[22] have been
these sources, a
profile is quite
matched. A mi

high repetition train of infinitely reproducible light pulses that contain a broad range of frequencies of light or can be tuned to a specific frequency. The width of the pulses of light is not as critical as the reproducibility. In the light sources manufactured to date, the absolute temporal jitter decreases with pulse width. Hence the interest in obtaining the shortest pulse width sources. While early instruments used a flashlamp, modern instruments use a laser. Each type of light source has inherent advantages and disadvantages, and certain characteristics, when coupled with other components in the instrument, dictate different instrumental configurations.

The flashlamps used in the past, and still used in some instruments today, generate nanosecond pulses of light at a repetition rate in the kilohertz range. The light pulse results from a high voltage discharge in a gas such as hydrogen or deuterium. Other gases have also been used. Lamps have been constructed that operate above and below atmospheric pressure. The spectral distribution of the lamp depends on the choice of gas and pressure. The pulse width also depends on these factors, but it is most dependent on the repetition rate. Gating has also been investigated. In general the temporal profile of the pulses generated by these sources is not smooth. The duration is normally a few nanoseconds, and it is not uncommon for the fast pulse to be followed by a slowly decaying tail that may last for several tens of nanoseconds. A thorough review of the flashlamps used in SPT can be found in a book by O'Connor and Phillips [14] .

Mode-locked lasers [21] and cavity dumped, synchronously pumped dye lasers [22] have been used in SPT. Unit picosecond or shorter pulses are obtainable with these sources, although pulses of five picoseconds are more common. The temporal profile is quite clean provided the cavity lengths of the pump and dye laser are exactly matched. A mismatch can cause "satellite" pulses on both sides of the primary pulse.

As these can be a
be monitored and
rate can be chan
Because the ligh
monochromatic, a
provided that a r
tuneable over the
dye laser. Natu
typical value fo
wavelengths is
"frequency doub
collimation are h
sources used in S

In contra
$10,000, a las
instrumentation
required to moni
require continuo
However, the e
justified if the e
flashlamp syster
multiple excitati
single laser dye/
during the cours
Providing the n
based SPT app

As these can be a source of systematic error in an SPT measurement, the output must be monitored and appropriate steps must be taken to eliminate satellites. The repetition rate can be changed through the appropriate control on the cavity dumper driver. Because the light source is a laser, the spectral output is necessarily highly monochromatic, allowing one to detect emission within a few nanometers of excitation provided that a monochromator of sufficient resolution is used. This output is also tuneable over the limits of the laser and saturable absorber dye combination used in the dye laser. Naturally this range varies with the dye combination used; however, a typical value for this range is 40 nm. Another range of the available output wavelengths is possible through second harmonic generation (SHG); so-called "frequency doubling". Other properties of laser light such as the high degree of collimation are helpful. O'Connor [14] and Fleming [12] have reviewed laser light sources used in SPT.

In contrast to a flashlamp light source that can be purchased for less than $10,000, a laser source can cost in excess of $150,000. In addition, the instrumentation required to monitor a laser source is much more expensive than that required to monitor the output of a flashlamp. Indeed, flashlamp-based systems do not require continuous monitoring and more closely approximate a turn-key system. However, the expense and maintenance requirements of a laser-based system can be justified if the excited state decay of the system of interest is too fast for study with a flashlamp system. Of course the successful study of a chemical system may require multiple excitation wavelengths, and those needed may lie outside the tuning range of a single laser dye/saturable absorber combination. This can necessitate changing the dyes during the course of the experiment - a most inconvenient task with some laser systems. Providing the needed excitation wavelengths can be a trivial matter for a flashlamp-based SPT apparatus. However, mode-locked laser sources routinely operate at

repetition rates in
and below. This
laser based SPT ap

Other light
nitrogen and excir
they are rarely use

A mode-lo
SPT instrument b
time needed to acc
locked Nd:YAG
specific componer

The select
made with only t
and emission. Sp
designed cells. Fo
attachment to va
considerations hol
resolution in the p

The photo
aqueous solution
response of this

repetition rates in the megahertz range while flashlamps operate in the kilohertz range and below. This greatly reduces the time required for a given measurement with a laser based SPT apparatus compared to a flashlamp based system.

Other light sources such as synchrotrons and low repetition rate lasers (e.g. nitrogen and excimer) have been used. However they will only be mentioned here as they are rarely used.

A mode-locked laser system was chosen for the light source in the constructed SPT instrument because of the high time resolution possible with it, and the reduced time needed to acquire a fluorescence decay. The specific laser system used is a mode-locked Nd:YAG laser and a synchronously pumped, cavity dumped, dye laser. The specific components are listed in Appendix 1.

Sample Cells

The selection of the sample cell in most fluorescence experiments is normally made with only the criteria of high transmittance in the spectral regions of excitation and emission. Special sample requirements are usually accommodated with specially designed cells. For example, air tight cells fitted with ground glass joints are used for attachment to vacuum lines for handling air sensitive compounds. The same considerations hold for SPT, but one should consider additional factors when temporal resolution in the picosecond range is needed.

The photon transit time through a standard one cm cuvette filled with an aqueous solution is roughly 40 picoseconds. When one is striving for an instrument response of this magnitude, one needs to take this into account since the detected

fluorescence photo
of the exciting lig
originate from a
effectively doubli
collection optics s
the contribution t
reflected exciting
to use a smaller cu
quartz. The cell
window and is al
collected through
light. Hence, this
reduce reflected s
minimize the volu
the laser light awa
position the cell
minimized.

Although t
sources of tempor
fabricated cells. I
of the cell is view
addition to cells fa

fluorescence photon could originate from a molecule excited anywhere along the path of the exciting light pulse. Consider also that the detected fluorescence photon could originate from a molecule excited by light reflected from the wall of the cuvette, effectively doubling the contribution to the instrument response. Adjustment the collection optics so that only a small area of the solution is viewed will help minimize the contribution to the instrument response from this source, but the problem of reflected exciting light remains. A solution suggested by Steiner and coworkers [13] is to use a smaller cuvette (e.g. four mm path length) having two adjacent walls of black quartz. The cell is oriented so that the exciting light enters through one transparent window and is absorbed when it reaches the opposite wall. Fluorescence is then collected through the other transparent window which is 90 degrees to the exciting light. Hence, this approach provides a way to minimize the photon transit time and to reduce reflected source light and sample fluorescence. One may also use masks to minimize the volume of the solution viewed and a sample cell geometries that reflects the laser light away from the region of the solution viewed. However it is difficult to position the cell such that reflected source light and reflected fluorescence are minimized.

Although the special cuvette used by Steiner and coworkers [13] minimizes both sources of temporal broadening, funds could not be obtained to purchase these specially fabricated cells. Instead the collection optics were arranged so that only a small region of the cell is viewed. This way standard 1.0 cm fluorescence cuvettes could be used in addition to cells fabricated for use on a vacuum line.

In order t
insure that only f
scattered laser ra
decay will be dist
be skewed toward
be added if the co
instruments, and
filter, and a sma
light rejection wh
of the Czerny-Tu

In the cas
solution viewed
fluorescent light
through the mon
because rays tra
The difference in
the grating. Thi
of a SPEX Indu
solid and a dashe
grating. The fig
model the mono
from the blue to
the transit time

Wavelength Selection

In order to record the decay of the fluorophore accurately, it is necessary to insure that only fluorescent light reaches the detector. If stray light originating from scattered laser radiation and/or Raman scattering reaches the detector, the recorded decay will be distorted. If the contribution from these sources is small, the decay will be skewed toward a shorter lifetime. A false, fast, second component to the decay will be added if the contribution from these sources of stray light is significant. Many SPT instruments, and the one constructed in this work, use a longpass filter, an interference filter, and a small Czerny-Turner single monochromator to achieve the needed stray light rejection while maintaining a reasonable throughput. The temporal characteristics of the Czerny-Turner monochromator are, however, not ideal for SPT.

In the case of the sample cell, the photon *transit time* through the volume of solution viewed increases the instrument response. When wavelength selection of the fluorescent light is accomplished with a monochromator, the *transit time spread* of light through the monochromator is the critical parameter. The transit time spread arises because rays traced through the monochromator have different optical path lengths. The difference in optical path length increases as the ray's path approaches the edge of the grating. This is illustrated on the next page in Figure 3-1. The figure is top view of a SPEX Industries model 1681 Czerny-Turner monochromator (f/n = 3.9) with a solid and a dashed line representing rays that strike the extreme edges of the diffraction grating. The figure was generated with a commercial software package [23] used to model the monochromator. As the monochromator is adjusted to pass wavelengths from the blue to the red region of the spectrum, the grating angle increases and hence the transit time spread increases. One means to minimize the transit time spread is to

Figure 3-1. Mod
strike the left and

place a mask in t

In essence one

characteristics.

tabulated in Tabl

TABLE 3-1. TH
INCREMENTS I

WAVELENGT
300
400
500
600
700

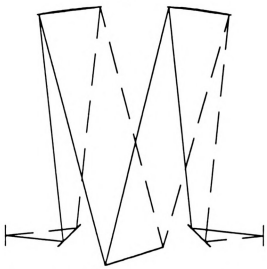

Figure 3-1. Model of a SPEX 1681 Czerny-Turner monochromator showing rays that strike the left and right edges of the grating. The wavelength of the rays is 500 nm.

place a mask in the monochromator such that only the central grooves are illuminated. In essence one sacrifices the monochromator's throughput to improve its temporal characteristics. The transit time spread of the SPEX model 1681 monochromator is tabulated in Table 3-1 for full grating illumination and for a mask that blocks all but 10

TABLE 3-1. TRANSIT TIME SPREAD (TTS) FROM 300 TO 700 NM IN 100 nm INCREMENTS FOR A SPEX 1681 CZERNY-TURNER MONOCHROMATOR.

WAVELENGTH (nm)	TTS (ps) Full Grating Width (48mm)	TTS (ps) 10 mm Exposed Width
300	48	12
400	63	16
500	79	20
600	96	24
700	113	28

mm of the gratin

The mask reduces

Other mea

wavelength select

additional filters,

the Czerny-Turne

the filter approac

must be taken a

compensator pla

approach, and it

optical componer

Selection of a mo

the contribution

In theory

spread of zero.

monochromator

Holographic mo

page 41 in Fig

approach has the

stray light rejec

samples that st

particulate matte

mm of the grating's width. Values are given for wavelengths from 300 to 700 nm. The mask reduces the transit time spread by a factor of four.

Other means of reducing the contribution to the instrument response from the wavelength selection device include removing the monochromator and replacing it with additional filters, placing compensator plates in the monochromator [24], and replacing the Czerny-Turner single monochromator with a monochromator of another design. If the filter approach is chosen, additional steps to achieve the needed stray light rejection must be taken and a means to vary the throughput must be included. The use of compensator plates achieves a slightly better transit time spread than the mask approach, and it only reduces the throughput by the loss that results from the additional optical components. It is also more difficult to implement than the mask approach. Selection of a monochromator of another design provides a better means of minimizing the contribution of the wavelength selection system to the instrument response.

In theory, a subtractive dispersion double monochromator has a transit time spread of zero. This is because the optical path length for all rays that pass through the monochromator are identical. The optical layout of such a device, an American Holographic model DB10-S subtractive dispersion monochromator [25], is shown in on page 41 in Figure 3-2. In addition to its desirable temporal characteristics, this approach has the advantage that additional filters are not needed to achieve the level of stray light rejection required for most work. However, filters may be needed for samples that strongly scatter source light, such as those that contain suspended particulate matter.

Figure 3-2. Fl
dispersion double

Had it be
have been chosen
unit that is suitab
that time.

The instru
risetime of detect
transit time sprea
of interest is the
consideration, a
narrow PHD. T
side-on photomul

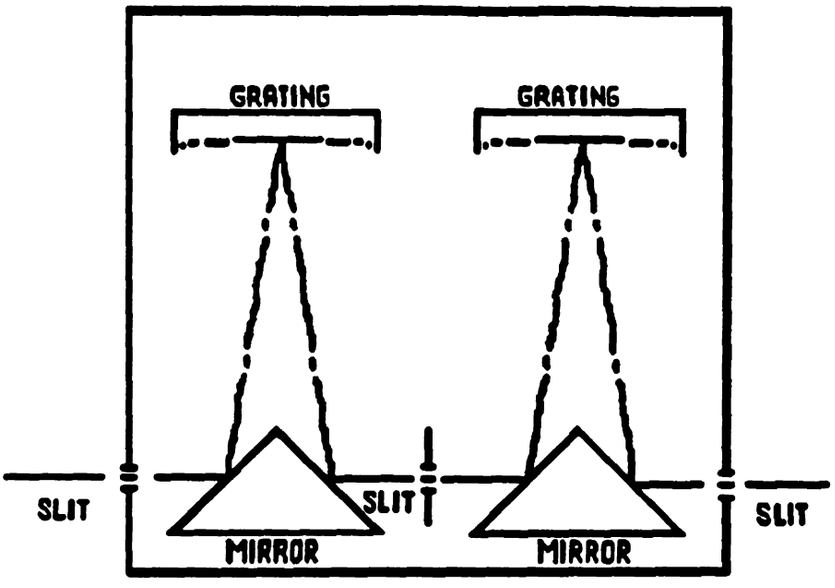

Figure 3-2. Floor plan view of an American Holographic DB10-S subtractive dispersion double monochromator. From [25].

Had it been an option, a subractive dispersion double monochromator would have been chosen for the constructed instrument. Unfortunately, the only commercial unit that is suitable for SPT, the American Holographic DB10-S, was not available at that time.

Detectors

The instrument response is often tied to the risetime of the detector signal. The risetime of detectors that contain an electron multiplier is largely a function of the *transit time spread* (TTS) of the pulse of electrons as it passes through the device. Also of interest is the *pulse height distribution* (PHD) of the detector. Similar to the TTS consideration, a narrow instrument response is obtained with a detector that has a narrow PHD. The most widely used detectors in SPT instruments are conventional, side-on photomultiplier tubes (PMTs) and microchannel plate photomultiplier tubes

(MCP-PMTs). I

specific detectors

For a con

2.2 ns [26]. Th

and is not strongl

response of one t

Although

information whe

devices has allow

packaged with a

lost, but the signa

PMT that contain

The risetime is r

PMT are six micr

The PHD

relatively low ap

However a peak

gain saturation [2

PHD, and hence

MCP-PMT near

counts is greater

one is recording t

other components

(MCP-PMTs). Both are available in the instrument constructed in this work, and the specific detectors used are listed in Appendix 1.

For a conventional side-on PMT such as the Hamamatsu R928, the risetime is 2.2 ns [26]. The PHD of a conventional PMT follows an exponential function [27], and is not strongly dependent on the applied voltage. These factors yield an instrument response of one to two nanoseconds when a conventional PMT is used.

Although microchannel plates were originally designed for preserving spatial information when amplifying a photocurrent, the extremely fast risetime of these devices has allowed a significant reduction in the instrument response for SPT. When packaged with a common anode, the spatial information of the micro-channel plate is lost, but the signal bandwidth is preserved, yielding a risetime of 220 ps for an MCP-PMT that contains two micro-channel plates composed of twelve micron channels [26]. The risetime is reduced further to 150 ps when the micro-channel plates in the MCP-PMT are six microns in diameter.

The PHD of MCP-PMTs is strongly dependent on the applied voltage. At relatively low applied voltages, the PHD is exponential like a conventional PMT. However a peak in the PHD appears as the bias voltage is increased. This is due to gain saturation [27, 28] and is illustrated on page 43 in Figure 3-3. To obtain a narrow PHD, and hence a narrow instrument response, one needs to apply a bias voltage to the MCP-PMT near the device's maximum rated voltage. Naturally the number of dark counts is greater at higher applied voltages, but this is generally not a problem when one is recording the decay of moderately efficient fluorophores. By carefully adjusting other components in the instrument to benefit from the narrower PHD at high bias

Figure 3-3. Puls
The bias voltage

voltages, an inst
micron MCP-PM
response of 20 ps

The riseti
as fast as that for
fluorescence in
efficiency in the
the spectrum is s
where they are il
avalanche photoc
The circuit used

These pho
interest emits nea
beyond the breal
avalanche of ele
tube counterparts
dark counts resu

Figure 3-3. Pulse height distribution of an MCP-PMT as a function of applied voltage. The bias voltage increases from left to right.

voltages, an instrument response of 50 picoseconds or less is possible when a 12 micron MCP-PMT is used [27]. A six micron MCP-PMT can yield an instrument response of 20 ps [15].

The risetime of the current generation of silicon avalanche photodiodes is almost as fast as that for the MCP-PMT. These devices are not as widely used as detectors of fluorescence in SPT because they are generally optimized for maximum quantum efficiency in the infrared. However, their quantum efficiency in the visible region of the spectrum is sufficient for them to be used as temporal reference detectors in SPT, where they are illuminated with a comparatively large number of photons. The silicon avalanche photodiode used in the constructed SPT apparatus is listed in Appendix 2. The circuit used to bias it is also described therein.

These photodiodes can also be used as sample detectors when the fluorophore of interest emits near the red region of the spectrum, or in the infrared [29]. When biased beyond the breakdown voltage, a single photon can, as the name implies, trigger an avalanche of electrons yielding single photon detectability. Similar to their vacuum tube counterparts, an avalanche can also result from dark noise. In this case however, dark counts result from leakage of an electron across the photoactive junction. This

noise source can

reduce dark noise

The detec

change in the tem

a PMT or MCP-

spread with a cha

difference in kine

photons of differ

work function o

cause the ejection

the difference b

Hence, the kinet

than the kinetic e

shift in time resp

an MCP-PMT. S

color effect of

picosecond range

PMTs [28].

The impro

over the past ten

However, these

components of a

these component

noise source can be reduced by cooling the detector, analogous to cooling a PMT to reduce dark noise.

The detectors mentioned above exhibit a color effect. This is observed as a change in the temporal characteristics of the detector with a change in wavelength. For a PMT or MCP-PMT, one observes a change in the transit time and/or transit time spread with a change in wavelength. It is generally agreed that this effect is due to a difference in kinetic energy of photoelectrons emitted by the photocathode for incident photons of different wavelengths. When a photon having an energy greater than the work function of the photocathode material collides with the photocathode, it may cause the ejection of an electron. The kinetic energy of the ejected electron will equal the difference between the photon's energy and the photocathode work function. Hence, the kinetic energy of an electron resulting from a blue photon will be greater than the kinetic energy of an electron resulting from a red photon. This effect causes a shift in time response of a PMT of less than one nanosecond [10]. The effect is less for an MCP-PMT. Silicon avalanche photodiodes also exhibit a color effect. Although the color effect of MCP-PMTs is not well documented, it is considered to be in the picosecond range for a wavelength shift of 100 nm, much less than that observed for PMTs [28].

Electronics

The impressive improvements in the temporal resolution of SPT instrumentation over the past ten years is largely a result of progress in light sources and detectors. However, these developments would not be possible without progress in the other components of an SPT instrument, and the careful incorporation and configuration of these components in the instrument. Each of the components must be properly

configured and it
a specific compo
These are discus
neglected compo

Although
instrument are nc
can, if ignored,
expected to accu
mate the compo
conducted throug
signal (e.g. one
For example, a
frequencies in ex
a mode-locked, s

In order
cables and conne
component of the
sufficient bandwi
connectors should
PMT contains m
adequate coaxial
name arises becau
a solid copper or

configured and its placement in the instrument must be arranged such that limitations of a specific component do not adversely affect the overall performance of the instrument. These are discussed in this section. However the importance of simple, yet often neglected components is discussed first.

CABLES AND CONNECTORS

Although the coaxial cables and connectors used to conduct the signals in a SPT instrument are not active electronic components, they are part of the overall system and can, if ignored, adversely affect the instrument response. If an electronic system is expected to accurately measure a given quantity, the cables and the connectors used to mate the components must have sufficient bandwidth such that no part of the signal conducted through the system is attenuated. A significant portion of a rapidly rising signal (e.g. one approximating a square wave) is contained in higher order harmonics. For example, a signal having a risetime of one nanosecond can contain harmonic frequencies in excess of one GHz. Consider that the harmonic content of the output of a mode-locked, synchronously pumped dye laser extends beyond 50 GHz [30].

In order to maintain the integrity of the fast signals in a SPT apparatus, the cables and connectors used must have bandwidths greater than the highest frequency component of the signal. Common RG 58/U coaxial cable and BNC connectors have a sufficient bandwidth for PMT based systems. However higher bandwidth cables and connectors should be used in MCP-PMT systems. This is especially true if the MCP-PMT contains microchannel plates composed of six micron channels. A more than adequate coaxial cable is semi-rigid coax, which is used for microwave signals. The name arises because rather than having a braided shield, the outer jacket of this cable is a solid copper or stainless steel tube. Its bandwidth extends to several GHz (e.g. 70 dB

per 100 feet @ 1

immunity of the

0.250" diameter

Even though it i

instrument becau

As ment

risetime systems

SMA connector

SMA connector

The sign

must be ampli

important facto

However an ar

MCP-PMT.

available at v

instrument, the

The faster six

amplifier havi

bandwidth, the

exceed the inpu

It is co

before the inpu

per 100 feet @ 10 GHz) [31]. Also, its shielding is absolute, thus improving the noise immunity of the system. Common sizes of semi-rigid coax are 0.085", 0.141", and 0.250" diameter. The bandwidth generally increases with the diameter of the cable. Even though it is the lowest bandwidth semi-rigid cable, 0.085" cable was used in this instrument because it is the most easily shaped.

As mentioned above, connectors for coaxial cable are also important for fast risetime systems. An excellent connector for SPT with an MCP-PMT detector is the SMA connector. The bandwidth closely approximates that of semi-rigid coax, and SMA connectors are used for the semi-rigid cable in this instrument.

AMPLIFIERS

The signal from the detector in the fluorescence channel (PMT or MCP-PMT) must be amplified before it reaches the discriminator. Again, bandwidth is an important factor. For PMTs a bandwidth of 500 MHz is more than sufficient. However an amplifier having a bandwidth of 2 GHz is needed for a twelve micron MCP-PMT. Fortunately, low noise amplifiers having bandwidths of 2 GHz are available at very reasonable cost. For example, the amplifier chosen for this instrument, the model ZFL-2000 2 GHz amplifier from Minicircuits, is priced at $200. The faster six micron MCP-PMTs require faster amplifiers. For these detectors, an amplifier having a bandwidth of 4 to 6 GHz should be used. Regardless of its bandwidth, the amplifier should be chosen such that its maximum output does not exceed the input range of the discriminator.

It is common practice to insert a one dB feedthrough attenuator immediately before the input of the amplifier in the fluorescence channel. This provides a constant

DC leakage for
detector and the

Because
pulse produce a
not needed, and

The co
This device ha
a threshold val
NIM negative
removed. Th
instrument, ar
made properly
of discriminat
and most imp
on the tempor

The o
respect to th
insensitive to
realizes this
in one of the
the signal su
delayed sign

DC leakage for the capacitor that is the short length of coaxial cable between the detector and the amplifier.

Because the silicon avalanche photodiodes used to detect the temporal reference pulse produce a signal that is sufficient for the discriminator, an amplifier is generally not needed, and one is not used in this instrument.

THE CONSTANT FRACTION DISCRIMINATOR

The component in the instrument following either detector is the discriminator. This device has three functions in an SPT instrument. It not only blocks signals below a threshold value, it also generates a NIM negative logic signal from the analog input. NIM negative logic is essentially emitter coupled logic (ECL) with the DC offset removed. These logic levels are recognized by the next active component in the instrument, and the signals need to be in this form for the time measurement to be made properly. In order to achieve high speed and low temporal jitter, a special type of discriminator known as a constant fraction discriminator (CFD) is used. The third and most important function of the CFD is to lessen the dependence of signal amplitude on the temporal output.

The object of a CFD is to produce a logic pulse that is exactly timed with respect to the analog input. The method of accomplishing this task should be insensitive to the amplitude of the input. The constant fraction technique [32, 33] realizes this by splitting the unipolar input pulse. The signal is attenuated and inverted in one of the paths and delayed in the other. The delay is matched to the risetime of the signal such that the attenuated signal is at its peak at the desired fraction of the delayed signal. The two signals are then recombined. The zero-crossing of the

resulting bipola
A conventional
constant fractio
the amplitude o

In order
before the com
proper length o
coaxial cable p
risetime of the
modified. This
455. Although
300 ps. Hence
MCP-PMT. T
optimize the C
concerning the

The Ter
discrete, some
been observed
channel, the w
can generate sp
insure that inp
changes that thi

resulting bipolar pulse coincides with a constant fraction of the of the original signal. A conventional zero-crossing detector generates a logic pulse corresponding to a constant fraction of the original signal. The output is not strongly subject to changes in the amplitude of the input with this technique.

In order to minimize walk (time dependence on amplitude) in a CFD, the delay before the comparator must be carefully matched to the input pulse risetime. The proper length of this delay is best determined experimentally. Most often the delay is a coaxial cable patched between two connectors on the front panel of the CFD. If the risetime of the signal is less than the internal delay of the CFD, the CFD must be modified. This was the case with the CFD used in this instrument, the Tennelec model 455. Although it is the fastest CFD commercially available, its internal delay is about 300 ps. Hence the unit from the factory must be modified if it is to be used with an MCP-PMT. The suggested modifications from the manufacturer [34] were followed to optimize the CFD used in this instrument for the 12 micron MCP-PMT. Information concerning the modifications needed can also be found in the scientific literature [35].

The Tennelec model 455 has four independent channels. Although they are discrete, some cross-talk does occur between channels [13]. This phenomenon has also been observed with other multi-channel CFDs [15]. When a signal is received in one channel, the walk in the others is degraded for approximately 40 nanoseconds. This can generate spurious signals in the system if one does not take appropriate steps to insure that inputs to the CFD are sufficiently separated in time. The configuration changes that this imposes are fully discussed later in this chapter.

The fun
difference betw
pulse is then di
personal compu
is to count the s
interest. The
oscillations are
and known. Al
make, present
measure the tim
alternate measu

As ment
having an ampl
the data channe
3-4. A fast,
received at the
negative logic s
and hold ampli
the next pair of

Conside
TACs available
concerns a Ten

THE TIME-TO-AMPLITUDE CONVERTER

The function of the time-to-amplitude converter (TAC) is to encode the time difference between the two data channels as a unipolar voltage pulse. This voltage pulse is then digitized and stored by the multichannel analyzer housed in a laboratory personal computer. The conventional strategy by which a time difference is measured is to count the signal from a precision oscillator during the time between the signals of interest. The time difference can be accurately determined if a large number of oscillations are counted and the frequency of the precision oscillator is highly constant and known. Although this technique is one of the most accurate measurements one can make, present technology cannot provide oscillators and counters fast enough to measure the time difference between the data channels in an SPT instrument. Hence an alternate measurement strategy is used.

As mentioned above, the purpose of the TAC is to generate an analog voltage having an amplitude that is proportional to the time difference between the signals in the data channels. This is accomplished by the scheme illustrated on page 50 in Figure 3-4. A fast, linear voltage ramp is started when a NIM negative logic signal is received at the START input. The internal voltage ramp continues until a NIM negative logic signal is received at the STOP input. This event also triggers a sample and hold amplifier. A brief, unipolar pulse is then generated and the TAC resets for the next pair of input signals.

Consider the signal throughput of a TAC. Because it is representative of the TACs available and it is the TAC used in this instrument, the following discussion concerns a Tennelec model 862. The output voltage range of the TAC is zero to 10

Figure 3-4. Me

volts. The time
width can be va
TAC reset time
When the time
throughput of al
This limitation i
that uses a TAC

The thro
flashlamp is use
high repetition r
can be obviated
called reversed
reference channe
the acquired exc

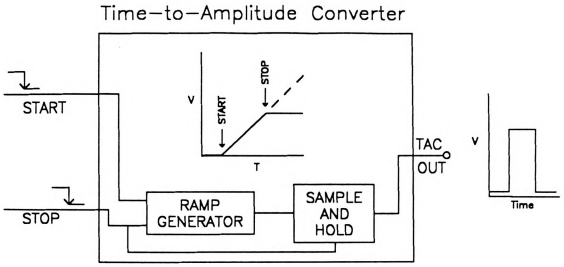

Figure 3-4. Method of operation of a time-to-amplitude converter.

volts. The time base can be varied continuously from 25 ns to 3 ms. The output pulse width can be varied from 1 to 10 ms and can be delayed for 250 ns to 25 ms. The TAC reset time ranges from 0.5 μs to 5 μs for the fastest to the slowest time base. When the time required for all of these tasks is summed, a best-case instrument throughput of about 500 kHz is realized. In practice this figure is in the tens of kHz. This limitation imposes a restriction on the overall configuration of an SPT instrument that uses a TAC.

The throughput limitation of the TAC is generally not a problem when a flashlamp is used. However, it does impose a constraint when the instrument uses a high repetition rate laser. When this is the case, the throughput limitation of the TAC can be obviated if the fluorescence channel provides the START input to the TAC, so-called reversed timing [36, 37]. The high repetition rate signal in the temporal reference channel then serves as the STOP signal. This configuration does not distort the acquired excited-state decay. It merely reverses the direction of increasing time in

the recorded d
instrument, a co

From thi
limiting factor i
has been shown
are functions of
tested, an ORT
they measured a
kHz to 100 kH
when one is str
constraint when
decays even if
following this re

The amplitude
multichannel an
a conventional
this device to b
addresses in m
received, the p
voltage is incre
number of inp
number. After
number yields

the recorded data. It does, however, require an additional component in the instrument, a coaxial cable delay.

From this discussion one might assume that the TAC conversion rate is not a limiting factor in an SPT experiment. Although this assumption is valid to an extent, it has been shown by Hallam and Imhof [38] that the linearity and calibration of a TAC are functions of the conversion rate. The linearity and calibration of the TAC they tested, an ORTEC 457, degraded with an increase in conversion rate. For example, they measured a shift of 90 picoseconds when the conversion rate was increased from 1 kHz to 100 kHz. They recommended that the conversion rate be kept below 1 kHz when one is striving for maximum temporal resolution. One should also observe this constraint when one is studying chemical systems that exhibit complex excited-state decays even if the species under study is long-lived. IUPAC recently recommended following this restriction on acquisition rate for all measurements [39].

THE MULTICHANNEL ANALYZER

The amplitude of the unipolar pulse generated by the TAC is digitized by a multichannel analyzer (MCA), and stored in memory. This device operates faster than a conventional analog-to-digital converter. One can consider the analog input range of this device to be partitioned into some number of equally spaced "channels" - actually addresses in memory. A channel is essentially a counter. When an input pulse is received, the pulse amplitude is determined, and the channel corresponding to that voltage is incremented. After some number of input pulses, each channel contains the number of input pulses that have had a pulse height corresponding to that channel number. After a large number of excitation flashes, a plot of count versus channel number yields a histogram, the outline of which is the summed result of the time

between excitatio

words the fluores

The temp

divided by the r

consideration the

of the TAC. Of

This is the case

voltage range is

MCAs, has varia

the MCA.

The const

inserted in both c

are separated by

that the excited-s

accomplishes this

shown on page 5

similar to their in

the beam splitter.

optic which prov

detector, a silico

through a short le

CFD. The digita

between excitation and emission for all of the detected fluorescence photons, in other words the fluorescence decay.

The temporal resolution of the acquired data is the time base of the TAC divided by the number of channels in the MCA. One may also need to take into consideration the analog input range of the MCA compared to the analog output range of the TAC. Often an MCA's input range is less than the output range of the TAC. This is the case for the MCA used in this instrument, a Nucleus PCA/8K. Its input voltage range is zero to about 8.2 volts, and it has 8,196 channels (8K). It, like many MCAs, has variable gain, actually a variable number of channels up to the maximum of the MCA.

Delays and Relative Timing

The constraints on the configuration of the instrument require that delays be inserted in both of the data channels. These delays must be placed such that the signals are separated by at least 40 ns when they reach the CFD, but arrive at the TAC such that the excited-state decay is properly recorded. An instrumental configuration that accomplishes this was reported by Steiner and coworkers [13]. Their configuration is shown on page 53 in Figure 3-5. The configuration of the instrument constructed is similar to their instrument with one important exception. Each data channel begins at the beam splitter. Laser light in the temporal reference channel is coupled into a fiber optic which provides a delay before the pulse of light reaches the temporal reference detector, a silicon avalanche photodiode. The signal from the photodiode travels through a short length of 0.085" diameter semi-rigid coax to one of the channels of the CFD. The digital pulse generated by the CFD is used as the STOP signal for the TAC.

Figure 3-5. Dia

Light not deflec
harmonic gener
from the sampl
optics - an f/n
plano-convex fo
a polarization a
detected with th
semi-rigid coax
amplifier. Th
channel of the
cable delay befo
TAC is digitize

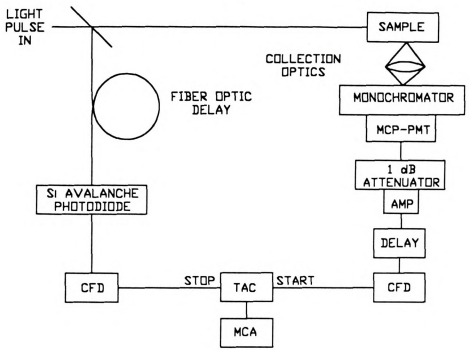

Figure 3-5. Diagram of the optimum instrumental configuration.

Light not deflected by the beamsplitter continues to the sample. If needed, a second harmonic generator is inserted between the beamsplitter and the sample. Fluorescence from the sample is collected, and directed into the monochromator by the collection optics - an f/n = 2 quartz, plano-convex collecting lens and an f/n = 3.9 quartz, plano-convex focussing lens which matches the f/n of the monochromator. Filters and a polarization analyzer may be inserted between the lenses. Fluorescence photons are detected with the MCP-PMT. The anode current pulse travels through a short length of semi-rigid coax to a 1 dB attenuator connected to the input of a 2 GHz, 22 dB amplifier. The amplified signal is conducted through semi-rigid coax to another channel of the CFD. The output from the CFD is delayed through a switched coaxial cable delay before reaching the START input of the TAC. The pulse generated by the TAC is digitized and stored in the MCA.

The len

reaches the CF

This ensures th

the fluorescenc

over the fastes

the time range

CFD and the

occurs near th

time difference

limit of the TA

excitation and

This cc

for acquiring

nanoseconds.

desired, a me

increase the le

window, but

that could be

fiber optics to

switched fibe

fluorophore u

the switched

The length of the fiber optic delay is such that the temporal reference signal reaches the CFD 80 nanoseconds after the pulse of light is split at the beam splitter. This ensures that the temporal reference signal is sufficiently separated from pulses in the fluorescence channel at the CFD, provided the fluorescence has decayed completely over the fastest setting of the TAC time base. The two signals are brought to within the time range of the TAC by adjusting the switched coaxial cable delay between the CFD and the TAC in the fluorescence channel. This delay is set such that time zero occurs near the upper limit of the TAC timebase. Since the timing is reversed, short time differences between excitation and emission produce TAC outputs near the upper limit of the TAC timebase, and the TAC output decreases with increasing time between excitation and emission.

This configuration works well for very fast fluorescence decays, but it is limited for acquiring the decays of fluorophores that have lifetimes greater than five nanoseconds. Because an ability to determine longer excited-state lifetimes was desired, a means of removing this limitation was developed. One solution could be to increase the length of the fiber optic delay. This way one can collect data over a larger window, but temporal resolution would be reduced, thus limiting the fastest lifetimes that could be determined A crude way around this would be to have a collection of fiber optics to insert as optical delays. A more "user friendly" approach was chosen - a switched fiber optic delay. This allows the user to change the optical delay to suit the fluorophore under study. Complete details concerning the design and construction of the switched fiber optic delay are given in Appendix 2.

The det
measurements.
response, and th
performed for e
response should
is by no means
of an experimen

A time c
TAC in a config
known, stepwise
START/STOP p
START/STOP p
START and ST
resumed, and th
covered. This is
signals such as t
function generato
the signal in the
TAC's STOP inp
for the TAC-MC
the MCA. When
of 1 kHz as mea
calibration need
should be done w

A TYPICAL SPT EXPERIMENT

The determination of an excited-state lifetime by SPT consists of three measurements. These are a time calibration, a measurement of the instrument response, and the acquisition of the fluorescence decay. A time calibration need not be performed for each excited-state lifetime determination, but recording the instrument response should be a routine part of the experiment. The order of these measurements is by no means fixed, and one may, in fact, repeat one or two of them over the course of an experiment.

A time calibration is performed by sending pairs of START/STOP pulses to the TAC in a configuration where the time between START and STOP can be adjusted in a known, stepwise fashion. The TAC output is recorded with the MCA for a series of START/STOP pulses having a constant time difference. After a sufficient number of START/STOP pulses have been acquired, the MCA is paused and the delay between START and STOP is incremented by a known quantity. Acquisition by the MCA is resumed, and the process is repeated until the temporal range of interest has been covered. This is most easily accomplished by splitting a source of NIM negative logic signals such as the output of one of the channels of the CFD or a properly adjusted function generator. One leg of the split leads directly to the TAC's START input, and the signal in the other leg is passed through a switched delay card before it reaches the TAC's STOP input. If the time increment of the delay is known, the time calibration for the TAC-MCA settings used is determined by a linear least squares fit of the data in the MCA. When performing a time calibration, one should use a TAC conversion rate of 1 kHz as mentioned in the discussion on the TAC. As mentioned above, a time calibration need not be carried out for each excited-state lifetime determination, but it should be done whenever the TAC time base is changed. Even if the TAC time base

has not changed
proper laborator

The acq
follow a few gu
the delays, the
the data channe
time zero. Wh
range of the M
delays are set,
decay is brack
preceding the
channels at the
five lifetimes.
attempting to f
MCA gain nee
than simple d
lower channel
can achieve v
(e.g., 2 ns) fo

The c
kept below c
section on th
accuracy pos
decays. How
additional un

has not changed, a time calibration should be done every few days, consistent with proper laboratory practice.

The acquisition of a fluorescence decay is straightforward, but one should follow a few guidelines when adjusting instrumental parameters such as the setting of the delays, the TAC timebase, MCA gain and offset, and the count rate. The delays in the data channels should be set such that the TAC is near the end of its time base at time zero. When setting the delays one must also keep in mind that the input voltage range of the MCA may be less than the output voltage range of the TAC. Once the delays are set, the TAC timebase and MCA parameters should be adjusted such that the decay is bracketed by dark noise. That is, the number of counts in the channels preceding the decay should be roughly the same as the number of counts in the channels at the extreme tail of the decay. Hence, one should acquire data over four or five lifetimes. This is not absolutely necessary, but it is important when one is attempting to fit a fluorescence decay to a bi-exponential or more complex model. The MCA gain need not exceed 512 or 1024 channels, except if one is striving to fit other than simple decays. The MCA offset allows one to block a selectable range of the lower channels (TAC pulse amplitudes) while maintaining a high gain. In this way one can achieve very high time resolution (about 2.7 ps/channel) over a small window (e.g., 2 ns) for the acquisition of very fast fluorescence decays.

The count rate, the number of valid TAC conversions per second, should be kept below one kHz to maintain integrity in the acquired data as mentioned in the section on the TAC. This is of greatest concern when one is striving for the highest accuracy possible and when attempting to characterize multi-exponential excited-state decays. However, one can operate at higher count rates if one is willing to tolerate the additional uncertainty in the acquired data.

If it is n

that excites the

parameters in t

the monochrom

instrument resp

Recordi

accomplished

containing cycl

sample compa

filters to pass

instrument resp

Of course the

fluorescence w

This effect car

The m

method is sho

scatterer. Be

impurities in s

in the ultra-vi

by passing the

In the

an intense ela

method work

If it is necessary, the best means to reduce the count rate is to attenuate the light that excites the sample (e.g. by narrowing an iris). This is preferred to changing parameters in the optical path between the sample and the detector such as narrowing the monochromator slits or inserting neutral density filters. These will change the instrument response.

Recording the instrument response is straightforward and is normally accomplished within one minute. A convenient procedure is to place a cuvette containing cyclohexane or another compound that is an efficient Raman scatterer in the sample compartment. One then resets the monochromator and selects appropriate filters to pass Raman scattered light from the sample. One should collect the instrument response using the same parameters used to collect the fluorescence decay. Of course the instrument response will be shifted relative to what it would be at the fluorescence wavelength due to the color effect of the detector and the monochromator. This effect can be taken into account and corrected for during the data analysis.

The major source of difficulty in obtaining an instrument response by this method is short-lived fluorescence from impurities in the solvent used as a Raman scatterer. Because SPT is so sensitive, one can readily detect fluorescence from impurities in spectrophotometric grade solvents. This is especially true with excitation in the ultra-violet. Fluorescence from impurities in cyclohexane can be reduced greatly by passing the cyclohexane through a column of silica gel and basic alumina [40].

In the past a common means of obtaining an instrument response has been to use an intense elastic scattering solution such as Ludox or diluted dairy milk. Although this method works to a point, it produces intense after pulses in the instrument response.

These are prim
used because li
satisfactory wh

Now th
is appropriate
of these is the
This is showr
was degassed
excited at 29(
is not shown
acquired in th
this display.
IUPAC recor
the complexi
A more com
also that the

As ev
of naphthale
bengal. Its
page 60 Fig
at 585 nm.
figure, was
Like naphth
Note the dif

These are primarily due to reflections. This method is attractive when a weak source is used because little time is required to obtain the instrument response. However it is not satisfactory when one is using a laser source.

Now that the configuration of the instrument has been thoroughly discussed, it is appropriate to present examples of excited-state decays acquired by SPT. The first of these is the decay of naphthalene obtained with a conventional photomultiplier tube. This is shown in Figure 3-6 on page 59. The sample is 10 μM in cyclohexane, and was degassed using the method suggested by Matsuzawa et al. [41]. The sample was excited at 290 nm, and fluorescence was detected at 350 nm. The instrument response is not shown because it is much shorter than the fluorescence decay. The data were acquired in the reversed timing configuration, and the time axis was reversed prior to this display. Note that the data are presented as log counts versus time following the IUPAC recommendation [39]. Presenting the data in this fashion aids in establishing the complexity of the decay. A straight line is indicative of a single exponential decay. A more complex decay mechanism is probable if the slope of the decay changes. Note also that the complete fluorescence decay is recorded.

As evidenced by the time interval in the abscissa in Figure 3-6, the excited-state of naphthalene is a relatively long-lived. A molecule that decays much faster is rose bengal. Its fluorescence decay and the instrument response function are shown in on page 60 Figure 3-7. The sample was excited at 570 nm and fluorescence was detected at 585 nm. The instrument response, the narrow "peak" on the left-hand side of the figure, was obtained by collecting Raman scattered light at 677 nm from cyclohexane. Like naphthalene, the decay of rose bengal appears to follow a single exponential. Note the difference in the time axis. The decay of rose bengal is complete in less than

Figure 3-6. F

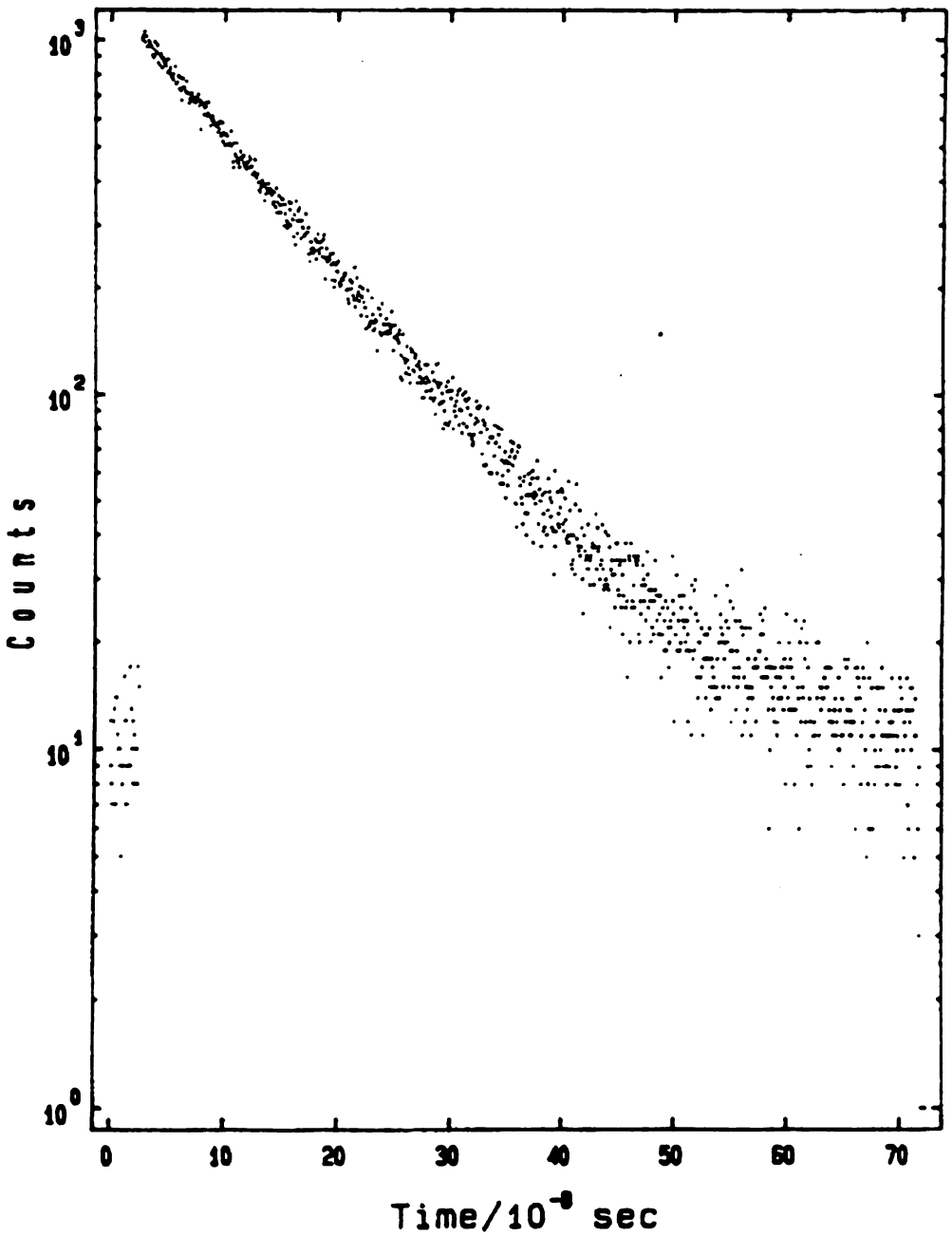

Figure 3-6. Fluorescence decay of naphthalene, 10 μM in degassed cyclohexane.

Figure 3-7. F
response.

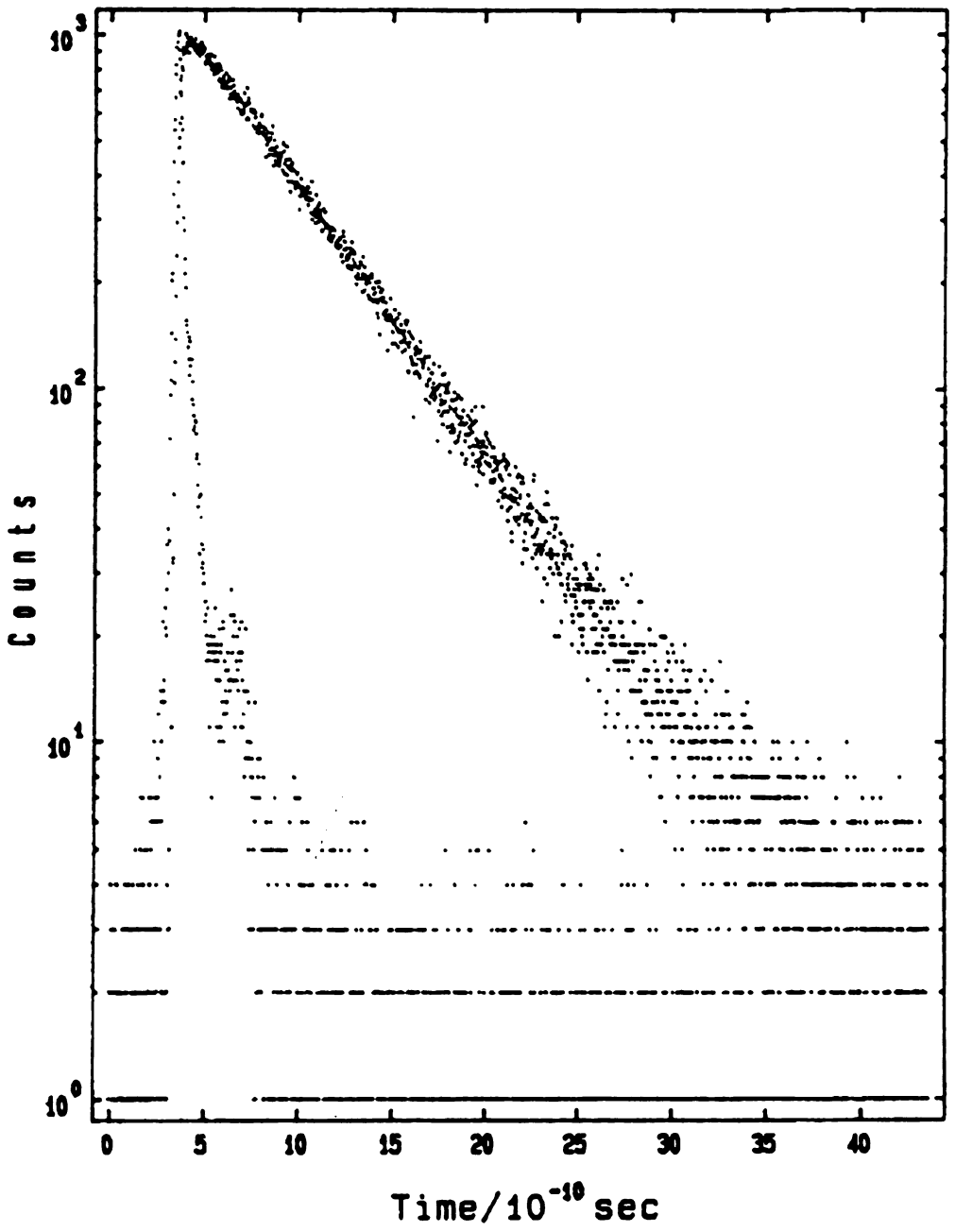

Figure 3-7. Fluorescence decay of rose bengal, 10 μM in methanol, and instrument response.

four nanoseconds.
FWHM, and is fol
reflections from the

Naphthalene
different decay tim
on most laser-base
fiber optic delay
measurements easi
proper data analys

Once the i
acquired, one det
a model (e.g. a s
the fluorescence
task, the method
iteration of the fi

where i is the c
experimental da
the standard de
follows a Poissc

four nanoseconds. The instrument response is quite narrow, about 50 picoseconds FWHM, and is followed by a bit of a tail. This is not fluorescence, but is due to reflections from the cuvette walls as mentioned earlier.

Naphthalene and rose bengal were used as examples because of their vastly different decay times. Acquisition of the fluorescence decays of these two compounds on most laser-based SPT instruments would be quite difficult. However, the switched fiber optic delay discussed in Appendix 2 allows one to perform both of these measurements easily. Yet the ease of data acquisition is of no consequence without proper data analysis. This topic is discussed in the next section.

DATA ANALYSIS

Once the instrument response and the fluorescence decay of a sample have been acquired, one determines the excited-state lifetime by comparing the obtained decay to a model (e.g. a single exponential). The model is successively refined until it matches the fluorescence decay. Although many methods have been used to accomplish this task, the method of least squares [11, 42, 43] is the most widely used. With each iteration of the fitting procedure, the parameter χ^2 is determined:

$$\chi^2 = \sum_{i=1}^{n} \left[\frac{Y(i) - M(i)}{\sigma(i)} \right]^2 \qquad (3\text{-}6)$$

where i is the channel number (the natural unit of time in SPT), Y(i) values are the experimental data, M(i) values are those predicted by the model, and the $\sigma(i)$ values are the standard deviations in the experimental data. Since the uncertainty in SPT data follows a Poisson distribution, $\sigma(i)$ can be estimated from the experimental data:

$$\sigma(i) \cong (Y(i))^{\frac{1}{2}} \qquad (3\text{-}7)$$

The value of χ^2 at e

exist for optimizin

advantages and dis

commercial softwa

variable step size g

In addition

account for the di

important when th

lifetime. The acqu

fluorescence decay

related by the conv

If L(t) and R(t) a

instrument respons

have been used [11

[46, 47]. In recc

model before com

approach than atte

acquired data.

No matter

acquired data, one

data. When least

of fit", as it is com

to the number of d

The value of χ^2 at each iteration is used to guide the search procedure. Many strategies exist for optimizing the model to find a minimum in χ^2, and each strategy has advantages and disadvantages, especially with respect to speed and stability. The commercial software package [44] purchased for use with this instrument uses a variable step size grid search followed by parabolic interpolation.

In addition to fitting a model to the fluorescence decay, one also needs to account for the distortion of the decay caused by the instrument. This is most important when the instrument response is significant compared to the excited-state lifetime. The acquired fluorescence decay, R(t) is actually a convolution of the true fluorescence decay, F(t), and the instrument response, L(t). These three functions are related by the convolution integral [7, 10]:

$$R(t) = \int_0^t L(t')\, F(t-t')\, dt \qquad (3\text{-}8)$$

If L(t) and R(t) are known, the true fluorescence decay, four nanoseconds. The instrument response is quite F(t) can be determined. Although a variety of techniques have been used [11, 39, 45], the method of iterative reconvolution is the most common [46, 47]. In reconvolution analysis, the instrument response is convolved with the model before comparing the model to the acquired decay. This is a more stable approach than attempting to deconvolve the effect of the instrument response on the acquired data.

No matter which technique is used to adjust the model so that it matches the acquired data, one must have objective means to judge how well the model fits the data. When least squares is used, the most basic means of determining the "goodness of fit", as it is commonly referred to, is the reduced value of χ^2. This is χ^2 normalized to the number of degrees of freedom (i.e., the number of data points less the number of

fitted parameters)

the confidence in

values above 1.5.

This is the ratio o

the expected diffe

weighting factor

indicates a systen

residuals is neces

is not obvious ir

subjective inspect

One such test of

(i.e., are half o

standard deviati

parameter [48,49

where $r(t_i)$ is th

chosen for the c

determine trends

(DU and DL) for

Durbin and Wats

fitted parameters

one must extrapo

this parameter to

fitted parameters). A value of unity for the reduced χ^2 is indicative of a good fit, and the confidence in the fit decreases with an increase in χ^2. Most workers seldom accept values above 1.5. After χ^2, it is common to examine a plot of the weighted residuals. This is the ratio of the actual difference between the experimental data and the model to the expected difference (standard deviation of the data). Since the data are Poisson, the weighting factor is determined directly from the data. A non-randomness in this plot indicates a systematic difference between the data and the model. Because a plot of the residuals is necessarily noisy, an autocorrelation of the residuals can reveal a trend that is not obvious in the plot of the residuals. As both of these are visual, and hence subjective inspections, one should also test the randomness of the data by other means. One such test of the residuals is to see if they are distributed in a Gaussian fashion (i.e., are half of the residuals positive, are 68 percent of the residuals within one standard deviation, etc.). Beyond this, one can determine the Durbin-Watson parameter [48,49]:

$$DW = \frac{\sum_{i=n1+1}^{n2} \left(r(t_i) - r(t_{i-1}) \right)^2}{\sum_{i=n1}^{n2} \left(r(t_i) \right)^2}$$

where $r(t_i)$ is the weighted residual, and n1 and n2 are the first and last channels chosen for the curve fit.. The Durbin-Watson parameter was originally developed to determine trends in econometric data, and the authors generated upper and lower limits (DU and DL) for data sets of varying size and parameters. In their original work [48], Durbin and Watson reported limits for DW for data sets of up to 100 points and five fitted parameters. As the number of channels in a SPT experiment often exceed 100, one must extrapolate values for DU and DL from the original work if one wishes to use this parameter to judge the residuals from a curve fit. Although some deem it a more

sensitive judgmen

Watson parameter

Other mea

of skew [50] and

distributed about

the analysis of SP

Figure 3-

naphthalene deca

model (i.e. A +

= 0.49 ns) was

values of 107 ns

instrument respo

seems to be succ

decay, appear to

residuals are neg

standard deviatio

An autoc

Although no maj

of about 13 ns.

driver which ope

sensitive judgment of the goodness of fit than χ^2 [14], few workers report the Durbin-Watson parameter for SPT data, and IUPAC does not yet recommend its use [39].

Other means of judging randomness in the weighted residuals are the measures of skew [50] and kurtosis [51]. The former indicates deviations that are not evenly distributed about zero while the latter indicates convexity. Neither is widely used in the analysis of SPT data.

Figure 3-8 on page 65 shows the results of a least squares curve fit of the naphthalene decay shown in Figure 3-6. The decay was fitted to a single exponential model (i.e. A + Bexp-(i/τ)) over 855 channels (0.708 ns/ch). A lifetime of 110 ns (σ = 0.49 ns) was determined. This is in excellent agreement with modern literature values of 107 ns [41] and 100 ns [52]. Reconvolution was not necessary because the instrument response was negligible compared to the fluorescence decay. The curve fit seems to be successful because χ^2 is nearly unity. The residuals, plotted beneath the decay, appear to be random and evenly distributed about zero. In fact, 45.8% of the residuals are negative, 65.8% are within one standard deviation, 94.7% are within two standard deviations, and 99.5% are within three standard deviations.

An autocorrelation of the residuals is shown on page 66 in Figure 3-9. Although no major trends are evident in this plot, there is a small oscillation at a period of about 13 ns. This corresponds to radio frequency interference from the mode locker driver which operates at 38.25 MHz.

Figure 3-8.

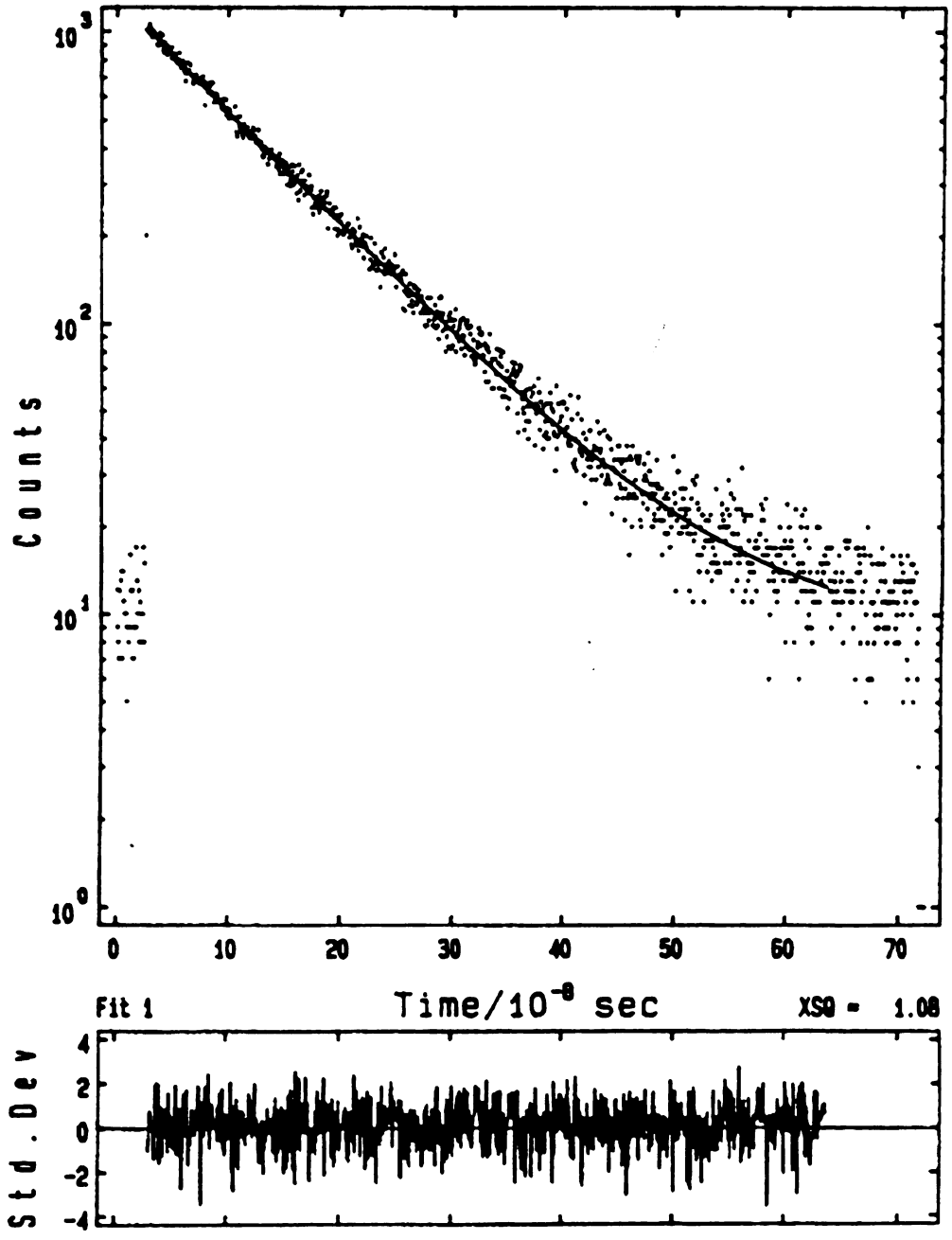

Figure 3-8. Fitted decay of naphthalene. The lower plot shows the weighted residuals.

Figure 3-9. Auto

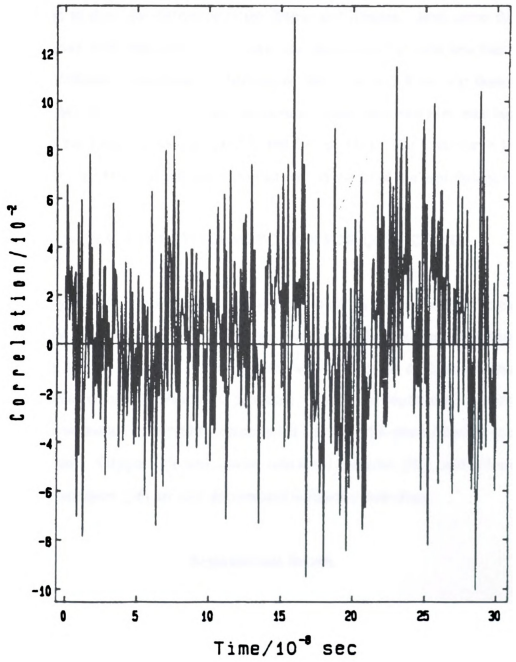

Figure 3-9. Autocorrelation of weighted residuals from fit of naphthalene decay.

Since the i

hengal, one should

hengal was fit t

reconvolution to s

carried out over 1

each case. Witho

A value of 549 p

Values from the l

distribution of the

API

Steady-sta

SPT was used to

of correcting for

Data from three

oxygen, quinine

by nitromethane.

[16] and nitrome

Fluoresc

model LS-5 flu

Since the instrument response is not negligible compared to the decay of rose bengal, one should include reconvolution during the data analysis. The decay of rose bengal was fit to a single exponential model, and analyzed with and without reconvolution to show the difference in the determined lifetime. Both curve fits were carried out over 1400 channels (2.77 ps/ch), and the value of χ^2 was less than 1.1 in each case. Without reconvolution, a lifetime of 564 ps (σ = 1.8 ps) was determined. A value of 549 ps (σ = 1.7 ps) was determined when reconvolution was included. Values from the literature are 549 ps [53] and 543 ps [54]. For both curve fits, the distribution of the residuals was similar to that seen in the fit of the naphthalene data.

APPLICATION TO CORRECTION FOR QUENCHING

Steady-state fluorescence intensity was measured on a common fluorometer and SPT was used to determine excited-state lifetimes by the Hieftje-Haugen method [16] of correcting for the reduction in fluorescence intensity due to collisional quenching. Data from three chemical systems are presented. These are naphthalene quenched by oxygen, quinine sulfate quenched by chloride ion and dansyl-L-phenylalanine quenched by nitromethane. Oxygen is a well known collisional quencher [55], and chloride ion [16] and nitromethane [56] are also documented collisional quenchers.

Experimental Details

APPARATUS

Fluorescence intensities were measured with a Perkin-Elmer (Norwalk, CT) model LS-5 fluorometer. Excited-state decays were obtained with the SPT apparatus

described in this cl

package (199M soft

Certified gr

of roughly equal qu

was recrystallized t

from the certified

purified cyclohexa

A 1.0 mM

in 0.1 M sulfuric

(Malinckrodt) in o

Dansyl-L-phenylal

was prepared in

potassium chloride

(Malinckrodt) was

A degasse

following manner

in a valved, qua

degassed with se

fluorescence inte

atmosphere briefl

described in this chapter and lifetimes were determined with a commercial software package (199M software library, IBH Consultants Ltd., Edinburgh, UK).

REAGENTS

Certified grade cyclohexane (Fisher) was purified by passing through a column of roughly equal quantities of silica gel and basic alumina. Naphthalene (Malinckrodt) was recrystallized twice from cyclohexane. The first crop of crystals was recrystallized from the certified cyclohexane, and the second crop was recrystallized from the purified cyclohexane.

A 1.0 m$\underline{M}$ stock solution of quinine sulfate monohydrate (Aldrich) was prepared in 0.1 $\underline{M}$ sulfuric acid (prepared by diluting 5.5 ml of concentrated sulfuric acid (Malinckrodt) in one liter of distilled and deionized water (Corning millipure system)). Dansyl-L-phenylalanine (Sigma) was used as received, and a 1.0 m$\underline{M}$ stock solution was prepared in 2-propanol (Burdick and Jackson). A 1.0 $\underline{M}$ stock solution of potassium chloride (J.T. Baker) was prepared in 0.1 M sulfuric acid. Nitromethane (Malinckrodt) was used as received.

PROCEDURES

A degassed solution of naphthalene in cyclohexane was prepared in the following manner. A small crystal of naphthalene (approximately 0.07 mg) was placed in a valved, quartz cuvette designed for use on a vacuum line. Cyclohexane was degassed with several freeze-pump-thaw cycles, and transferred to the cuvette. The fluorescence intensity and lifetime were measured. The cuvette was exposed to the atmosphere briefly, and the measurements were repeated. This sequence was carried

out six times, and

measurements.

For the qun

systems, working so

fluorophore and ap

volumetric flask, ar

solutions were prep

quencher in these s

For the flu

wavelengths were

nm for the quinir

phenylalanine solu

measurements. A

uncertainty in the

same wavelengths

wavelength was 28

Various de

SPT measurement

peak channel wer

channels. The M

1481) slit widths

monochromator a

A cutoff filter (O

out six times, and oxygen was briefly bubbled through the solution for the last two measurements.

For the qunine sulfate - chloride and dansyl-L-phenylalanine - nitromethane systems, working solutions were prepared by combining 1.0 ml of the stock solution of fluorophore and appropriate volumes of the stock solution of quencher in a 100 ml volumetric flask, and diluting to the mark with the appropriate solvent. Nine working solutions were prepared for each fluorophore-quencher system. The concentration of quencher in these solutions was 0, 0.005, 0.001, 0.05, 0.01, 0.5, 0.1, 0.5, and 1.0 M.

For the fluorescence intensity measurements, the excitation and emission wavelengths were 290 nm and 330 nm for the naphthalene solution, 282 nm and 450 nm for the quinine sulfate solutions and 350 nm and 505 nm for the dansyl-L-phenylalanine solutions. The excitation and emission bandpasses were 3 nm for all measurements. A single intensity measurement was made on each solution, and the uncertainty in the measurement was estimated from fluctuations in the readout. The same wavelengths were used for the lifetime determinations, except that the excitation wavelength was 282 nm for the dansyl-L-phenylalanine solutions.

Various delays, TAC time base settings, and MCA parameters were used in the SPT measurements. Three decay curves having approximately 1,000 counts in the peak channel were obtained for each sample. All decays were acquired over 1024 channels. The MCP-PMT was biased at -3,100 volts. The monochromator (SPEX 1481) slit widths were 0.5 mm for all measurements. A mask was placed in the monochromator at the grating surface to block all but the central ten mm of grooves. A cutoff filter (Oriel KV418 or WG305) and a bandpass filter (Oriel 57560 or 57540)

were included in

minutes per solu

Each dec

was not include

The poorest fit

and the dansyl-

were randomly

the weighted r

The f

lifetime deter

TABLE 3-2.
I/τ OF NAP
OXYGEN.

Exposure N	
complet	
degass	
1	
2	
3	
4	
5	
6	

were included in the collection optics. Acquisition times were on the order of a few minutes per solution.

Each decay curve was fit to a single exponential model. Reconvolution analysis was not included. The reduced χ^2 for all but four of the curve fits was less than 1.1. The poorest fits were obtained for the quinine sulfate solution that was 1.0 M in KCl and the dansyl-L-phenylalanine solution that was 1.0 M in nitromethane. The residuals were randomly distributed for all of the curve fits as judged by inspections of plots of the weighted residuals.

Results and Discussion

The fluorescence intensity measurements and the results of the excited-state lifetime determinations for naphthalene quenched by oxygen are given in Table 3-2.

TABLE 3-2. FLUORESCENCE INTENSITIES, LIFETIMES AND THE RATIO OF I/τ OF NAPHTHALENE IN CYCLOHEXANE SUCCESSIVELY QUENCHED BY OXYGEN.

Exposure Number	Intensity	Lifetime (ns)	Intensity/Lifetime
completely degassed	8970	109.9	81.6
1	3010	39.9	75.4
2	1590	20.7	76.2
3	1530	18.9	81.0
4	1370	16.3	84.1
5	510	5.80	87.9
6	330	3.68	89.7

As one would expe

with the number o

oxygen to enter the

quenching by ratio

3-10. The steadi

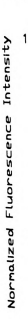

Figure 3-10. St
excited-state life
mM).

intensities by div

bars on the co

deviation in both

intensity data be

The correction i

trend with incr

during exposure

As one would expect, the fluorescence intensity and the excited state lifetime decrease with the number of exposures to the atmosphere. These exposures presumably allow oxygen to enter the solution. The steady-state intensity and the intensity corrected for quenching by ratioing to the excited-state lifetime are compared graphically in Figure 3-10. The steady-state fluorescence intensities were normalized to the corrected

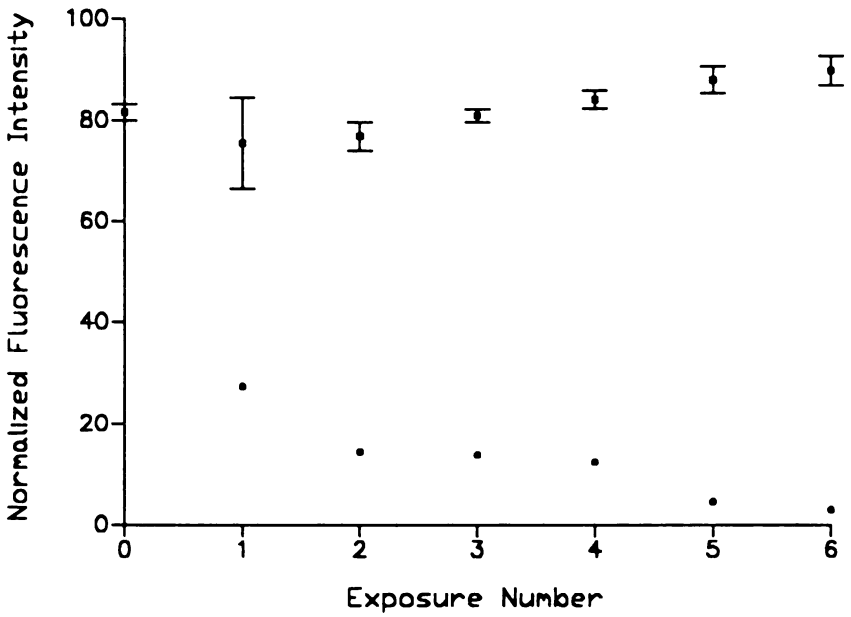

Figure 3-10. Steady-state fluorescence intensity (circles) and intensity ratioed to the excited-state lifetime (squares) for naphthalene in degassed cyclohexane (approx 0.1 mM).

intensities by dividing all values by the unquenched lifetime of naphthalene. The error bars on the corrected intensities indicate propagated uncertainty for one standard deviation in both lifetime and intensity. Error bars are not shown for the steady-state intensity data because they would be on the order of the size of the plotted characters. The correction is almost ideal within the limits of the error bars. The general upward trend with increasing exposure is probably due to evaporation of the cyclohexane during exposure to the atmosphere. This process will increase the concentration of

naphthalene in the

this deviation is g

solution.

The fluore

lifetime determina

3-3. The normali

TABLE 3-3. FL
I/τ OF QUININ
VARYING CON

$[Cl^-]$
0.0
0.005
0.01
0.05
0.1
0.5

ratioing to the e

11. As in Figu

by dividing all c

system, the flu

concentration o

independent on

concentration o

naphthalene in the solution, and hence, increase the intensity. As one might expect, this deviation is greatest for the exposures in which oxygen was bubbled through the solution.

The fluorescence intensity measurements and the results of the excited-state lifetime determinations for the quinine sulfate - chloride ion system are given in Table 3-3. The normalized steady-state intensity and the intensity corrected for quenching by

TABLE 3-3. FLUORESCENCE INTENSITIES, LIFETIMES, AND THE RATIO OF I/τ OF QUININE SULFATE, 10 μM 0.1 M SULFURIC ACID, QUENCHED BY VARYING CONCENTRATIONS OF CHLORIDE ION.

$[Cl^-]$	Intensity	Lifetime (ns)	Intensity/Lifetime
0.0	8980	18.7	481
0.005	5070	10.9	466
0.01	3600	8.0	449
0.05	1025	2.5	418
0.1	550	1.4	404
0.5	118	0.31	385

ratioing to the excited-state lifetime are compared graphically on page 73 in Figure 3-11. As in Figure 3-10, the fluorescence intensities were normalized to the ratio of I/τ by dividing all of the values by the unquenched lifetime. Like the naphthalene-oxygen system, the fluorescence intensity and the excited state lifetime decrease as the concentration of quencher increases. But unlike that system, the ratio of I/τ is not independent on the concentration of quencher. In fact, this quantity decreases as the concentration of quencher increases. However, the corrected intensity does not

Figure 3-11. P
intensity correcte
quinine sulfate in

decrease as rapi

discussed later in

The data

74 in Table 3-4.

decrease as the

like the quinine

quencher increas

in Figure 3-12

unquenched I/τ

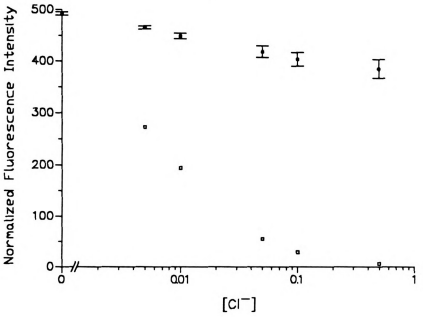

igure 3-11. Plot of steady-state fluorescence intensity (circles) and fluorescence tensity corrected for quenching by ratioing to the excited-state lifetime (squares) for uinine sulfate in 0.1 M sulfuric acid quenched by chloride ion.

ecrease as rapidly as the uncorrected intensity. Possible reasons for this trend are scussed later in this chapter.

The data for the dansyl-L-phenylalanine - nitromethane system is shown on page in Table 3-4. Again, both the fluorescence intensity and the excited-state lifetime crease as the concentration of quencher, nitromethane in this case, increases. And e the quinine sulfate system, the ratio of I/τ also decreases as the concentration of encher increases, but more rapidly. These data are presented graphically on page 74 Figure 3-12. The fluorescence intensities here are also normalized to the quenched I/τ value.

TABLE 3-4. FLU
I/r OF DANSYL-
BY VARYING CO

$[CH_3NO_2]$
0.0
0.005
0.01
0.05
0.1
0.5
1.0

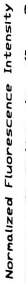

Figure 3-12. P
intensity correcte
dansyl-L-phenyla

TABLE 3-4. FLUORESCENCE INTENSITIES, LIFETIMES, AND THE RATIO OF I/τ OF DANSYL-L-PHENYLALANINE, 10 μM IN 2-PROPANOL, QUENCHED BY VARYING CONCENTRATIONS OF NITROMETHANE.

$[CH_3NO_2]$	Intensity	Lifetime (ns)	Intensity/Lifetime
0.0	8980	15.0	598
0.005	6520	11.8	554
0.01	5280	10.3	513
0.05	3755	7.7	487
0.1	1830	4.4	417
0.5	120	0.76	158
1.0	37	0.44	84

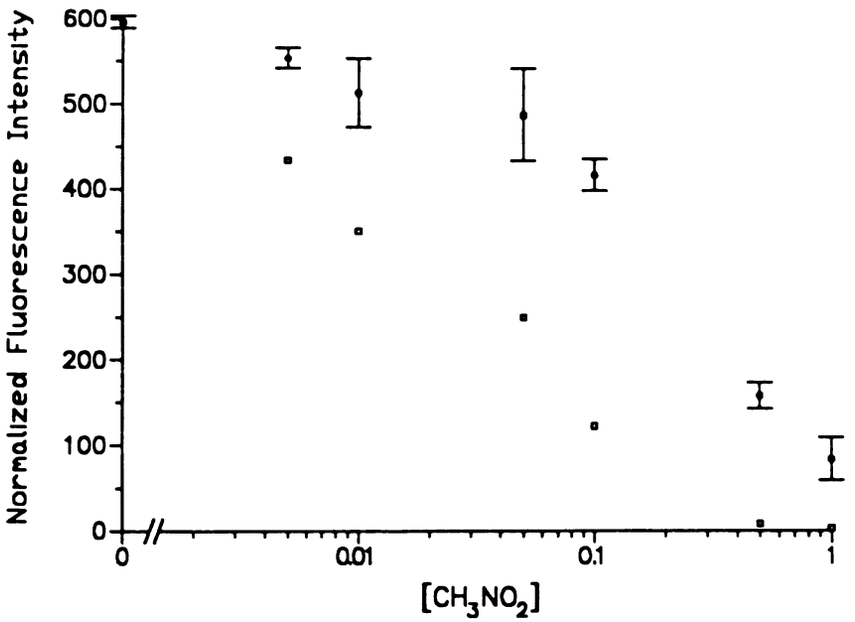

Figure 3-12. Plot of steady-state fluorescence intensity (circles) and fluorescence intensity corrected for quenching by ratioing to the excited-state lifetime (squares) for dansyl-L-phenylalanine in 2-propanol quenched by nitromethane.

The Hieft
degree, but it d
correction it pro
quenching mecha

The nap
Although the ac
from the steady
occurring. The
by oxygen is w
above, the con
of an accurate S

The oth
mechanisms o
Hieftje-Hauge
quencher is h
concentration
quinine sulfat

In bo
concentration
radiative rate
disagreement
constant is p
Hence, the
intensity wil

The Hieftje-Haugen method [16] corrects for quenching in these systems to a degree, but it does not work well with all of the chemical systems studied. The correction it provides is most accurate when collisional quenching is the dominant quenching mechanism.

The naphthalene-oxygen system is the most well-behaved system studied. Although the actual concentration of oxygen in the solution is not known, it is evident from the steady-state intensity and the excited-state lifetime data that quenching is occurring. The most likely mechanism is collisional quenching as collisional quenching by oxygen is well known. A Stern-Volmer plot would verify this. However, as stated above, the concentration of oxygen in the solution is not known, making construction of an accurate Stern-Volmer plot impossible.

The other fluorophore-quencher systems tested are cases where other quenching mechanisms or other factors that affect the quantum yield are possible. Here the Hieftje-Haugen method is not highly accurate, especially when the concentration of quencher is high. The decrease in the ratio of I/τ with an increase in quencher concentration is greater in the dansyl-L-phenylalanine - nitromethane system than in the quinine sulfate - chloride ion system. This could be due to several phenomena.

In both systems, the refractive index of the solution increases with the concentration of quencher. This also affects the excited-state lifetime because the radiative rate constant is dependent on the refractive index. Although there is some disagreement on this in the literature, it is generally thought that the radiative rate constant is proportional to the square of the refractive index of the solution [14]. Hence, the excited-state lifetime should decrease as η^2 increases. The fluorescence intensity will be coupled to this because the quantum yield, Q, is also dependent on the

radiative rate

intersystem cr

If k_{NR} remain

quantum yield

obviously dep

ratio of I/τ to

explain a pos

observed for t

If, for

quencher incr

the ratio of I

quenching.

Even

quenchers, a

formation of

static quenchi

be reduced, b

from both st

concentration

fluorophore

intensity mor

dansyl-L-phe

system owing

radiative rate constant, k_R, and the rate constant for all non-radiative processes (e.g. intersystem crossing, internal conversion etc...), k_{NR}:

$$Q = \frac{k_R}{k_R + k_{NR}} \tag{3-9}$$

If k_{NR} remains constant, an increase in the refractive index will also increase the quantum yield, and hence, the fluorescence intensity. The extent of the increase obviously depends on the relative values of k_R and k_{NR}. One would expect that the ratio of I/τ to increase as the refractive index of the solution increases. This would explain a positive deviation in the ratio of I/τ, but not a negative deviation as is observed for these systems.

If, for some reason, k_{NR} increases faster than k_R as the concentration of quencher increases, the quantum yield will decrease. This will cause the intensity and the ratio of I/τ to decrease by an amount greater than that due to simple, collisional quenching.

Even though chloride ion and nitromethane are documented collisional quenchers, a possible explanation for the observed deviation is static quenching: the formation of a non-fluorescent "dark complex" at high concentrations of quencher. If static quenching were the only quenching mechanism, the fluorescence intensity would be reduced, but the excited-state lifetime would not be affected. If quenching occurs from both static and dynamic quenching, the ratio of I/τ should decrease as the concentration of quencher increases. This is due to the fact that a larger fraction of the fluorophore will be complexed at high concentrations of quencher, thus reducing the intensity more than the extent due to collisional quenching. This is more likely for the dansyl-L-phenylalanine-nitromethane system than for the quinine sulfate - chloride ion system owing to the strong electron withdrawing nature of the nitro group. Indeed the

déviation is g
nitromethane.
Stern-Volmer p

Anothe
fluorophore m
quencher is m
instantaneous q

Perhaps
a semi-quantita
quenching is
quencher will
quenching mec
would constru
mechanism of
of quencher
demonstrated
quencher is n
method.

deviation is greater for the π electron rich dansyl-L-phenylalanine quenched by nitromethane. One could determine the extent of static quenching by constructing Stern-Volmer plots of both F_o/F and τ_o/τ at different temperatures [10].

Another possible explanation for the observed deviation is that some of the fluorophore molecules are quenched immediately at high concentrations. That is a quencher is more likely to be an immediate neighbor to a fluorophore, resulting in instantaneous quenching that may appear to be static quenching [10].

Perhaps another application of the Heiftje-Haugen measurement scheme [16] is a semi-quantitative method of determining the mechanism of quenching. If collisional quenching is the dominant mechanism, a plot of I/τ versus the concentration of quencher will be a straight line with a slope of zero. A deviation will indicate other quenching mechanisms such as static quenching or energy transfer. Traditionally one would construct Stern-Volmer plots at different temperatures to establish the mechanism of quenching. However one needs accurate knowledge of the concentration of quencher in the solution to construct meaningful Stern-Volmer plots. As demonstrated with the naphthalene-oxygen study, the absolute concentration of quencher is not needed to interpret measurements made using the Hieftje-Haugen method.

1. Koechlin,
2 Bollinger
3. Wahl, Ph
4. Blumberg
5. Birks, J.E
6. Morton, (
7. Yguerabi
8. Knight, A
9. Ware, W
A.A., Ed
10. Lakowicz
York, 19
11. Demas, J
1983.
12. Fleming,
University
13. Steiner, E
Complexe
Fouassier,
14. O'Connor
Academic
15. Dr. Gary
Communi
16. Hieftje, G
17. Wahl, P.E
18. Pfeffer, G

CHAPTER THREE REFERENCES

1. Koechlin, Y. Ph.D. Dissertation, University of Paris, 1961
2. Bollinger, L.M.; Thomas, G.E. *Rev. Sci. Instrum.* **1961**, *32*, 1044.
3. Wahl, Ph.; Lami, H. *Biochim. Biophys. Acta*, **1967**, *133*, 233.
4. Blumberg, W.E.; Eisinger, J.; Nonen, G. *Biophys. J. Soc. Abs.* **1968**, *12*, A106.
5. Birks, J.B.; Munro, I.H. *Prog. React. Kinetics* **1967**, *4*, 239.
6. Morton, G.A. *Appl. Optics*, **1968**, *7*, 1.
7. Yguerabide, J. *Meth. Enzymol.* **1972**, *26*, 498,
8. Knight, A.E.W.; Selinger, B.K. *Aust. J. Chem.* **1973**, *26*, 1.
9. Ware, W.R. in *Creation and Detection of the Excited State* vol 1A, Lamola, A.A., Ed. Marcel Dekker, Inc.: New York, 1971, chapter 5.
10. Lakowicz, J.R. *Principles of Fluorescence Spectroscopy* Plenum Press: New York, 1983.
11. Demas, J.N. *Excited State Lifetime Measurements* Academic Press: New York, 1983.
12. Fleming, G.R. *Chemical Applications of Ultrafast Spectroscopy* Oxford University Press: New York, 1986.
13. Steiner, R.F.; Holtom, G.H.; Kubota, Y. *Laser Spectroscopy of Nucleic Acid Complexes* in *Lasers in Polymer Science and Technology: Applications*, vol 4. Fouassier, J.P. and Rabex, J.F. Eds. CRC Press: Boca Raton, FL, 1989
14. O'Connor, D.V.; Phillips, D. *Time-Correlated Single Photon Counting* Academic Press: London, 1984
15. Dr. Gary Holtom, Pacific Northwest Laboratories, Richland, WA. Personal Communication, December 1990.
16. Hieftje, G.M.; Haugen, G.R. *Anal. Chim. Acta.* **1981**, *123*, 255.
17. Wahl, P.R. *New Tech. Biophys. Cell. Biol.* **2**, 233. 1975
18. Pfeffer, G.; Lami, H.; Laustriat, G.; Coche, A. *Compt. Rend.* **1962**, *4*, 1035.

19. Cramer, I

20. Grinwald,

21. Kinoshita,

22. Phillips,
1985, *14*,

23. BEAM4,

24. Bebelaar,

25. Technical

26. Catalog o

27. *Applicati*
Related
February

28. *Characte*
RES-079

29. Lacaita,

30. Lakowic

31. Technica

32. Gedcke,

33. Leskova
1113.

34. Graves,
TN. Se

35. Anfinru

36. Spears,

37. Haugen,

38. Hallam,

39. Comissi

19. Cramer, L.E.; Spears, K.G. *J. Am. Chem. Soc.* **1978**, *100*, 221.

20. Grinwald, A. *Anal. Biochem.* **1976**, *75*, 260.

21. Kinoshita, S.; Ohta, H.; Kushida, T. *Rev. Sci. Instrum.* **1981**, *52*, 572.

22. Phillips, D.; Drake, R.C. O'Connor, D.V.; Christensen, R.L. *Anal. Instrum.* **1985**, *14*, 267.

23. BEAM4, Stellar Software, Berkeley, CA.

24. Bebelaar, D. *Rev. Sci. Instrum.* **1986**, *57*, 1686.

25. Technical Literature, American Holographic, Littleton, MA, 1990.

26. Catalog of Photomultipliers, Hamamatsu Photonics K.K., Japan, January 1988.

27. *Application of MCP-PMTs to Time Correlated Single Photon Counting and Related Precautions* Technical Literature, Hamamatsu Photonics K.K., Japan, February 1987.

28. *Characteristics and Applications of Microchannel Plates* Technical Manual RES-0795. Hamamatsu Photonics K.K., Japan, January 1987.

29. Lacaita, A.; Cova, S.; Ghioni, M *Rev. Sci. Instrum.* **1988**, *59*, 1115.

30. Lakowicz, J.R.; Laczko, G.; Gryczynski, I; *Rev. Sci. Instrum.* **1986**, *57*, 2499.

31. Technical Literature, Precision Tube Company, North Wales, PA, 1988.

32. Gedcke, D.A.; McDonald, W. J. *Nucl. Instr. Meth.* **1968**, *58*, 253.

33. Leskovar, B.; Lo, C.C.; Hartig, P.R.; Sauer, K. *Rev. Sci. Instrum.* **1976**, *47*, 1113.

34. Graves, W.; Coyne, B. In-house Correspondence, Tennelec, Inc. Oak Ridge, TN. September 26, 1986.

35. Anfinrud, P.A.; Struve, W.S. *Rev. Sci. Instrum.* **1989**, *60*, 800.

36. Spears, K.G.; Cramer, L.E. Hofland, L.D. *Rev. Sci. Instrum.* **1978**, *49*, 255.

37. Haugen, G.R.; Wallin, B.W. Lytle, F.E. *Rev. Sci. Instrum.* **1979**, *50*, 64.

38. Hallam, A.; Imhof, R.E. *J. Phys. E.* **1980**, *13*, 520.

39. Comission on Photochemistry, *Pure Appl. Chem.* **1990**, *62*, 1632.

40. Lampert,
Meech, S

41. Matsuzaw

42. Bevington
McGraw

43. Press, W
Recipies

44. 199M So

45. Lopez-De

46. O'Conno

47. McKinno

48. Durbin, J

49. Durbin, J

50. Irvin, D.

51. Pearson,

52. Comissio

53. Ware, W

54. Cramer,

55. Kautsky,

56. Dreeskar

40. Lampert, R.A.; Chewter, L.A.; Phillips, D.; O'Connor, D.V.; Roberts, A.J.; Meech, S.R. *Anal. Chem.* **1983**, *55*, 68.

41. Matsuzawa, S.; Wakisaka, A.; Tamura, M. *Anal. Chem.* **1990**, 62, 2645.

42. Bevington, P.R. *Data Reduction and Error Analysis for the Physical Sciences* McGraw Hill: New York, NY 1969.

43. Press, W.H.; Flannery, B.P.; Teukolsky, S.A.; Vetterling, W.T. *Numerical Recipies* Cambridge University Press: New York, NY, 1986. chapter 14.

44. 199M Software Library, IBH Consultants Ltd., Edinburgh, Scotland, UK.

45. Lopez-Delgado, R.; Tramer, A, Munro, I.H. *Chem. Phys.* **1974**, *5*, 72.

46. O'Connor, D.V.; Ware, W.R.; Andre, J.C. *J. Phys. Chem.* **1979**, *83*, 1333.

47. McKinnon, A.E.; Szabo, A.G.; Miller, D.R. *J. Phys. Chem.* **1977**, *81*, 1564.

48. Durbin, J.; Watson, G.S. *Biometrika* **1950**, *37*, 409.

49. Durbin, J.; Watson, G.S. *Biometrika* **1951**, *38*, 159.

50. Irvin, D.J.G.; Livingston, A.E. *Comp. Phys. Commun.* **1974**, *7*. 95.

51. Pearson, K. *Biometrika*, **1905**, *1V*, 181.

52. Comission on Photochemistry, *Pure Appl. Chem.* **1988**, *60*, 1108.

53. Ware, W.R.; Pratinidhi, M.; Bauer, R.K. *Rev. Sci. Instrum.* **1983**, *54*, 1148.

54. Cramer, L.E.; Spears, K.G. J. *Am. Chem. Soc.* **1978**, *100*, 221.

55. Kautsky, H. *Trans. Faraday Soc.* **1939**, *35*, 216.

56. Dreeskamp, H.; Koch, E Z. *Naturforch.* **1975**, *30*, 1311.

Fre

[1], and v

excited mo

not as int

FDF is n

nature, th

time-dom

Th

followed

described

excited-s

frequenc

and the r

at a sing

determin

method

in Figu

demodu

expressi

discussi

CHAPTER 4: FREQUENCY DOMAIN FLUORESCENCE

Frequency domain fluorescence (FDF) was first reported by Gaviola in 1921 [1], and was the first technique capable of measuring the decay of an electronically excited molecule with nanosecond resolution. Briefly described in chapter two, FDF is not as intuitive as the various time-domain methods such as pulse sampling. Hence FDF is not as widely used as the time-domain methods. Despite its non-intuitive nature, the capabilities of modern FDF instrumentation are comparable to those of the time-domain techniques.

This chapter begins with a brief treatment of the basic theory of FDF. This is followed by a historical survey of the technique. A frequency domain fluorometer is described which is designed to simultaneously acquire fluorescence intensity and excited-state lifetime in near real time. This fluorometer is similar to existing frequency domain fluorometers, and differs primarily in the cross-correlation frequency and the method used to measure the phase shift. The constructed fluorometer operates at a single modulation frequency and, hence, the range of excited-state lifetimes it can determine is rather narrow. Application of this instrument to the Hieftje-Haugen method [2] of correcting for the effects of collisional quenching is discussed.

THEORY

The waveforms used in FDF and quantities derived from them were illustrated in Figure 2-4. The excited state lifetime can be determined from either the demodulation factor, m, or the phase shift, ϕ, and several routes exist to derive the expressions that relate the excited-state lifetime to these experimental parameters. The discussion on the theory of FDF presented here is logically straightforward,

algebraically c

additional treat

Conside

initial populatio

from the initial

where γ and k

dependent inte

where a and

modulation fr

the emission t

and has redu

population of

A and B repr

shift between

modulated lig

Substitution o

The temporal

algebraically complex, and follows that of Lakowicz [3]. Readers interested in additional treatments are referred to those by Ware [4] and Demas [5].

Consider a fluorophore excited by an infinitely short pulse of light generating an initial population of the excited state. The population of the excited-state will decrease from the initial value following:

$$\frac{dN(t)}{dt} = -(\gamma + k)\, N(t) \tag{4-1}$$

where γ and k are the respective rates of non-radiative and radiative decay. The time dependent intensity of a sinusoidally modulated source is given by:

$$f(t) = a + b \sin \omega t \tag{4-2}$$

where a and b indicate the degree of modulation (Figure 2-4) and ω is the radial modulation frequency. A sinusoidally modulated source used to excite a sample causes the emission to be modulated at the same frequency, but the emission is phase-shifted and has reduced modulation. When such a source is used, we can express the population of the excited-state as:

$$N(t) = A + B \sin(\omega t - \phi) \tag{4-3}$$

A and B represent modulation parameters of the emission waveform and ϕ is the phase shift between excitation and emission. When the sample is excited with sinusoidally modulated light, the rate of decay of the excited state becomes:

$$\frac{dN(t)}{dt} = -\frac{1}{\tau} N(t) + f(t) \tag{4-4}$$

Substitution of (4-3) and (4-2) into (4-4) yields:

$$\frac{dN(t)}{dt} = \frac{1}{\tau}(A + B \sin(\omega t - \phi)) + a + b \sin \omega t \tag{4-5}$$

The temporal dependence of the excited-state can also be expressed as:

$$\frac{dN(t)}{dt} = \omega B \cos(\omega t - \phi) \tag{4-6}$$

After expandi

and the consta

The relation

(4-8) and sub

That for mod

yield:

From (4-7),

Or in direct t

Hence the ex

or the demod

One a

the relative

frequency do

After expanding the sine and cosine functions, equating coefficients of sin ωt, cos ωt and the constant terms, we obtain from (4-5) and (4-6):

$$a - \left[\frac{1}{\tau}\right] A = 0 \tag{4-7}$$

$$\omega \cos\phi - \frac{1}{\tau} \sin\phi = 0 \tag{4-8}$$

$$\omega \sin\phi + \frac{1}{\tau} \cos\phi = \frac{b}{B} \tag{4-9}$$

The relation between excited-state lifetime and phase shift is obtained by rearranging (4-8) and substituting:

$$\frac{\sin\phi}{\cos\phi} = \tan\phi = \omega\tau_p \tag{4-10}$$

That for modulation is obtained after squaring (4-8) and (4-9) followed by addition to yield:

$$\omega^2 + \left[\frac{1}{\tau}\right]^2 = \left[\frac{b}{B}\right]^2 \tag{4-11}$$

From (4-7), $A = a\tau$ and (4-11) can be expressed as:

$$m = \frac{B/A}{b/a} = (1 + \omega^2 \tau_m^2)^{\frac{-1}{2}} \tag{4-12}$$

Or in direct terms of τ_m:

$$\tau_m = \frac{1}{\omega}\left[\frac{1}{m^2} - 1\right]^{\frac{1}{2}} \tag{4-13}$$

Hence the excited-state lifetime can be determined directly from either the phase shift or the demodulation factor.

One additional topic that should be mentioned here is the fundamental limit on the relative standard deviation (RSD) in an excited-state lifetime determined with frequency domain techniques. A simple relationship between the RSD of an excited-

state lifetime

derived as foll

Writte

The relative

variables ϕ a

After taking

Multiplying

This express

approaches (

Taking squa

state lifetime determined from phase shift data and the absolute phase shift can be derived as follows.

Written directly in terms of the excited-state lifetime, (4-10) becomes

$$\tau_p = \frac{\tan\phi}{\omega} \tag{4-14}$$

The relative uncertainty in τ_p can be determined by propagation of error in the variables ϕ and ω:

$$\frac{\Delta\sigma_{\tau_p}^2}{\tau_p^2} = \frac{\frac{\partial}{\partial\phi}\left[\frac{\tan\phi}{\omega}\right]^2 \Delta\phi^2 + \frac{\partial}{\partial\omega}\left[\frac{\tan\phi}{\omega}\right]^2 \Delta\omega^2}{\left[\frac{\tan\phi}{\omega}\right]^2} \tag{4-15}$$

After taking partial derivatives the equation becomes:

$$= \frac{\frac{\sec^4\phi}{\omega^2}\Delta\phi^2 + \frac{\tan^2\phi}{\omega^4}\Delta\omega^2}{\frac{\tan^2\phi}{\omega^2}} \tag{4-16}$$

Multiplying by ω^2/ω^2, we have:

$$= \frac{\sec^4\phi\,\Delta\phi^2 + \frac{\tan^2\phi}{\omega^2}\Delta\omega^2}{\tan^2\phi} \tag{4-17}$$

This expression can be further simplified because as ω approaches ∞ , $(\tan^2\phi\ /\ \omega^2)$ approaches 0 and

$$= \frac{\sec^4\phi\,\Delta\phi^2}{\tan^2\phi} \tag{4-18}$$

Taking square roots to obtain the RSD:

$$\frac{\sigma_{\tau p}}{\tau_p} = \frac{\sec^2\phi\,\sigma_\phi}{\tan\phi} \tag{4-19}$$

And from the c

Upon inspectio

One can also

graphically in

Figure 4-1.
determined
an RSD in t

figure, one

shift is betv

A s

dependenc

And from the definitions of secant and tangent, we can finally write:

$$\frac{\sigma_{\tau_p}}{\tau_p} = \frac{\sigma_\phi}{\sin\phi \cos\phi} \tag{4-20}$$

Upon inspection we find that as ϕ approaches 0° or 90°, the RSD in τ_p approaches ∞. One can also estimate the RSD in τ_p for a known σ_ϕ. Such an estimation is shown graphically in Figure 4-1 for a typical value of 0.2 degrees for σ_ϕ. According to this

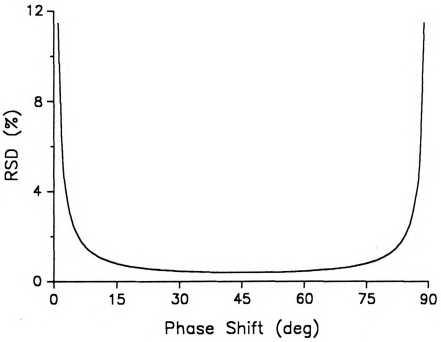

Figure 4-1. Plot of the relative standard deviation (RSD) in an excited-state lifetime determined from phase shift data as a function of the phase shift. This plot is based on an RSD in the phase shift of 0.2 degrees.

figure, one should arrange the experimental parameters such that the measured phase shift is between 10 and 80 degrees. to obtain an RSD of two percent or less

A similar approach has been attempted for the RSD in the excited-state lifetime dependence on the demodulation factor, but a simple relationship has not been found.

However, plot

similar to Figu

A simp

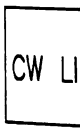

Figure 4-2. S

dependence

modulator dr

wavelength s

is split with

exciting light

appropriate c

However, plots of the RSD in τ as a function of m have been constructed and they are similar to Figure 4-1 with respect to shape and relative value of the RSD in τ.

REVIEW

A simplified apparatus for FDF experiments is shown in Figure 4-2. A time

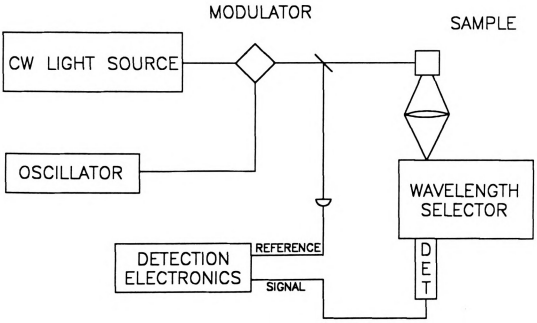

Figure 4-2. Simplified apparatus for frequency domain fluorescence.

dependence is impressed on the output of a continuous wave light source by a modulator driven at a radial modulation frequency ω by an appropriate oscillator. A wavelength selector may or may not be used in the excitation path. The exciting light s split with a portion directed toward a reference detector while the remainder of the exciting light continues to the sample. Fluorescence from the sample is collected with appropriate collection optics and passed through a wavelength selector before reaching

the sample de

signals by the

A nece

modulated sou

Pockels cells

optic (AO) r

modulators [

devices, esp

frequencies

end of the vi

modulators t

value for lig

modulation

modulated s

One

be generate

a pulsed wa

fundamenta

Although th

pulses of li

high repet

component

modes are

3. Note th

the sample detector. The frequency domain parameters are derived from the two signals by the detection electronics.

A necessary component of an FDF instrument is a modulator or an intrinsically modulated source. Various electro-optic (EO) modulators such as Kerr cells [6,7] and Pockels cells [6,7] have been used to modulate a continuous wave source. Acousto-optic (AO) modulators such as those of the Debye-Sears [7,8] type and solid state modulators [9,10] have also been used for this purpose. Although some of these devices, especially those of the EO family, have been used to modulate light at frequencies of several GHz [6], they are somewhat restricted to light toward the red end of the visible spectrum and the near infra-red. The modulation bandwidth for those modulators that do not significantly absorb light at ca. 400 nm is much less. A typical value for light of this wavelength is 200 MHz. A means of achieving a much higher modulation bandwidth for many regions of the spectrum is to use an intrinsically modulated source.

One of the basic concepts of Fourier theory is that any complex waveform can be generated by summing a sufficiently large number of harmonic components. Hence a pulsed waveform contains frequency components that are higher in frequency than the fundamental frequency of the waveform. Consider the output of a mode-locked laser. Although they are expensive and not widely available, mode-locked lasers can generate pulses of light that are less than 100 ps FWHM. These pulses are generated at a very high repetition rate (e.g., 100 MHz) and contain a large number of harmonic components. The temporal output of a mode-locked laser in which 50 longitudinal modes are phase-locked and its frequency spectrum are shown on page 88 in Figure 4-3. Note that the temporal output consists of very narrow pulses and that the frequency

Figure 4
spectrum
longitudi

spectrum

longitud

the "pea

of the

Figure

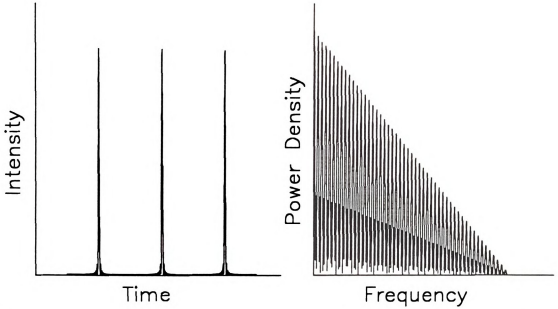

Figure 4-3. Calculated temporal output of a mode-locked laser (left) and its frequency spectrum (right). These waveforms are for a mode-locked laser in which 50 longitudinal modes are phase-locked.

spectrum shows a large number of harmonic components, 50 to be exact - one for each longitudinal mode. One can also see evidence of the higher harmonics at the base of the "peaks" in the temporal output. To emphasize this, an enlarged view of this region of the temporal output is shown in Figure 4-4. The higher harmonics are readily

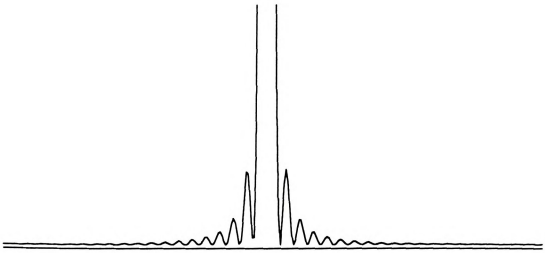

Figure 4-4. Enlarged view of the temporal output of a mode-locked laser.

apparent in

greater than

several GHz.

Follo

Dushinsky

Szymanowsk

In that year,

accuracy of

excited-state

factor. The

frequency d

instruments

number of f

In

correlation

shift and d

shift betwe

fluorophor

of 45 degre

frequency

heterodyni

apparent in this illustration. Quite often the number of longitudinal modes is much greater than 50, and the useful harmonic content of a mode-locked laser can extend to several GHz.

Early Work

Following the work of Gaviola [1], the theory of FDF was refined by Dushinsky [11] and minor improvements in instrumentation were made by Szymanowsky [12]. Modest improvements were made by various workers until 1953. In that year, Schmillen [13] reported a crude heterodyne technique which improved the accuracy of phase shift measurements and Birks and Little [14] reported the first excited-state lifetime measurements from both the phase shift and the demodulation factor. The first review of FDF was that of Bonch-Bruevich [15] in 1956. By 1961 frequency domain parameters could be measured directly at 10 MHz [16], but FDF instruments were limited to measurements at a single frequency or one of a small number of frequencies.

Modern FDF

In 1969, Spencer and Weber [17] published a landmark paper on cross-correlation detection. This method greatly reduces the frequency at which the phase shift and demodulation factor are measured. It is difficult to directly measure a phase shift between two signals at the high frequencies used in FDF. Consider that a fluorophore that has an excited-state lifetime of ten nanoseconds will have a phase shift of 45 degrees when the modulation frequency is 16 MHz. Cross-correlation is actually frequency mixing of two different frequencies. This process is also known as heterodyning. In cross-correlation detection, the gain of the detector is modulated at a

frequency sli
detector esse
light source,
and differenc
exciting ligh
same source
present in b
signal can is
easier to me
frequencies
correlation,

Ano
Their work
resolved" c
in the litera
the techniq
resolution.
P(t), is mu
integrated.
ϕ_D, is varia

where A i
excitation
modulatio
when F(t)

frequency slightly higher than that of the exciting light. The resulting signal from the detector essentially contains four frequencies: one at the modulation frequency of the light source, one at the modulation frequency of the detector, and one at each the sum and difference of the two modulation frequencies. The signals used to modulate the exciting light and the gain of the detector must be phase locked or derived from the same source to eliminate phase. The phase shift and modulation information are present in both the sum and difference frequency. Simple low pass filtering of this signal can isolate the difference frequency which can be as low as 30 Hz. It is much easier to measure the phase shift and demodulation factor at 30 Hz than it is at the high frequencies used in FDF. Because of the greater accuracy and simplicity of cross-correlation, almost all FDF instruments reported since its introduction use it.

Another major advance was initiated in 1970 by Veselova and coworkers [18]. Their work marked the beginning of a detection methodology known as "phase resolved" or "phase sensitive" fluorescence. The two names have used synonymously in the literature, and it has been recommended [19] that the former be used to refer to the technique and to spectra, and the latter to the detection used to accomplish phase resolution. In phase resolved fluorescence, the AC portion of the detector response, $P(t)$, is multiplied by a digital, periodic waveform of the same frequency, $F(t)$, and integrated. The phase angle between the periodic waveform and the detector response, ϕ_D, is variable from 0 to 360 degrees, and the integrated signal follows:

$$F(\phi_D) = A\, m_{ex}\, m \cos(\phi_D - \phi) \qquad (4\text{-}21)$$

where A is the observed steady-state emission intensity, ϕ is the phase shift between excitation and emission, m_{ex} is the excitation modulation, and m is the emission modulation. The integrated signal reaches a maximum when ϕ equals ϕ_D. That is when $F(t)$ is exactly in phase with $P(t)$. The methodology is illustrated in Figure 4-5.

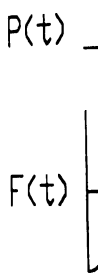

Figure 4-5.
represents th
0 degrees o
phase (right
intermediate

By adjustin
fluorophore
that detecto
exponential

Sinc
[18], nume
include ins
instrument
or of pulse
television
optics [28
exponentia
37] have
frequency
resolved [

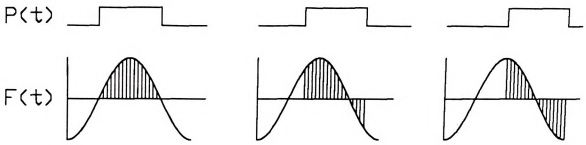

Figure 4-5. Integration scheme used in phase resolved fluorescence. The shaded area represents the integrated signal. As the phase shift between F(t) and P(t) is varied from 0 degrees or in phase (left), to slightly out of phase (middle), to 90 degrees out of phase (right), the integrated signal decreases from the maximum value (left) to an intermediate value (middle) to zero (right).

By adjusting the phase shift between F(t) and P(t) to 90 degrees beyond that of a given fluorophore, the signal from that fluorophore can be eliminated from the total signal at that detector phase angle. One can use this means of "phase nulling" to resolve multi-exponential fluorescence decays or mixtures of fluorophores.

Since the introduction of cross-correlation [17] and phase resolved detection [18], numerous improvements in instrumentation have been reported. Some of these include instruments capable of a continuously variable modulation frequency [20-23], instruments that use the harmonic content of the output of a mode-locked laser [24, 25] or of pulses of light generated by a synchrotron [22]. Instruments based on a UHF television tuner [26], gain-modulated silicon avalanche photodiodes [27], and fiber optics [28] have also been reported. Several reports of the resolution of multi-exponential fluorescence decays [29-33] and of complex mixtures of fluorophores [34-37] have appeared in the literature. At present, the highest reported modulation frequency is 10 GHz [38], and mixtures containing up to six fluorophores have been resolved [37]. The most recent review of FDF was that of McGown and Bright [19].

The

FDF provid

figures in re

chosen for

instrument

quenching

specific ins

the literatu

Hieftje-Hau

As

state lifetir

this decisi

instantane

capable of

possible,

been fully

Be

the detect

and demo

determini

resolution

decays ar

angle res

The direct relationship between the phase shift and the demodulation factor in FDF provides a means to determine an excited-state lifetime to two or three significant figures in real or near real time. Because of this unique ability, FDF was the technique chosen for determining excited-state lifetimes in the instrument described here. This instrument corrects for the reduction in fluorescence intensity caused by collisional quenching using the Hieftje-Haugen method [2]. As there are choices with respect to specific instrumental configuration and detection methods, specific instruments from the literature are surveyed in the next section with an emphasis on application to the Hieftje-Haugen method [2].

Survey of Previous Instruments

As mentioned above, FDF was chosen as the method for determining excited-state lifetimes with the Hieftje-Haugen method [2]. Although the primary criterion for this decision is the ability of FDF to determine an excited state lifetime virtually instantaneously, not all molecular fluorescence spectrometers designed for FDF are capable of this. While some workers have strived for the highest modulation frequency possible, other improvements in the technique such as rapid data acquisition have not been fully developed.

Before considering specific instruments, a choice needs to be made concerning the detection methodology, phase resolution or direct measurement of the phase shift and demodulation factor. The chosen method must be consistent with the goal of determining the excited state lifetime instantaneously. Although the method of phase resolution is very powerful for the determination of multi-exponential fluorescence decays and mixtures of fluorophores, the requirement of scanning the detector phase angle restricts this detection method from making excited-state lifetime measurements

in real time
automated,

Alth
common co
shift and de
FDF instru
arc lamp ar
uses two ph
and the oth
only opera
cross-corre
frequency
noise. Ar
integer nu
during on
accomplis
dynode.
of modula
an LED d

M
of the mo
modulato
frequenci
PMTs.
workers

in real time. Since direct measurements of phase shift and demodulation can be automated, this means of detection was chosen.

Although it is not capable of determining an excited-state lifetime in real time, a common commercial frequency domain fluorometer that directly measures the phase shift and demodulation factor is the Aminco 4800 phase fluorometer. Many modern FDF instruments are in fact upgraded Aminco 4800s. This spectrometer uses a xenon arc lamp and Debye-Sears modulators [8] to generate intensity modulated light. It also uses two phase-locked frequency synthesizers, one to drive the Debye-Sears modulators and the other for cross-correlation detection [17]. Although the frequency synthesizers only operate at three frequencies, they are stable and of sufficient resolution that the cross-correlation frequency in this instrument is 30 Hz. Setting the cross-correlation frequency so that it is an integer fraction of 60 Hz helps minimize AC power line noise. Any effect the power line has will exactly cancel at, say, 30 Hz because an integer number of cycles of the AC line frequency, two in this case, will have occurred during one period of the cross-correlation frequency. This method of detection is accomplished within the PMTs by adding a modulating voltage to the bias at the second dynode. This instrument uses a ratio digital voltmeter to determine intensity and depth of modulation and a phase meter to measure the phase shift. The output is presented on an LED display, and the user then calculates the excited state lifetime.

Many workers have replaced one or two, or many parts of this instrument. One of the most common modifications is replacing the xenon arc lamp and Debye-Sears modulators with a laser and either an AO or EO modulator. The number of modulation frequencies can be increased by replacing the frequency synthesizers and re-wiring the PMTs. While these modifications can increase the modulation bandwidth, very few workers have attempted to improve the detection electronics. Indeed, where workers

have replac

controllable

process.

Alth

and cowork

capabilities

and the d

reported b

mode-lock

detection e

REFER

SAM

Figure 4.

reported

integrator

the figur

sample,

describe

have replaced the frequency synthesizers with completely variable and computer controllable commercial units, few have bothered to automate the measurement process.

Although it was reported a few years ago, the instrument described by Alcala and coworkers [24] is the most advanced frequency domain fluorometer with respect to capabilities for rapid data acquisition. With the exception of the modulated light source and the detection electronics, it is similar to the Aminco 4800. The instrument reported by Alcala and coworkers [24] uses the harmonic content of the output of a mode-locked laser as an intensity-modulated light source. A simplified version of the detection electronics used in their instrument is shown in figure 4-6. As is evident in

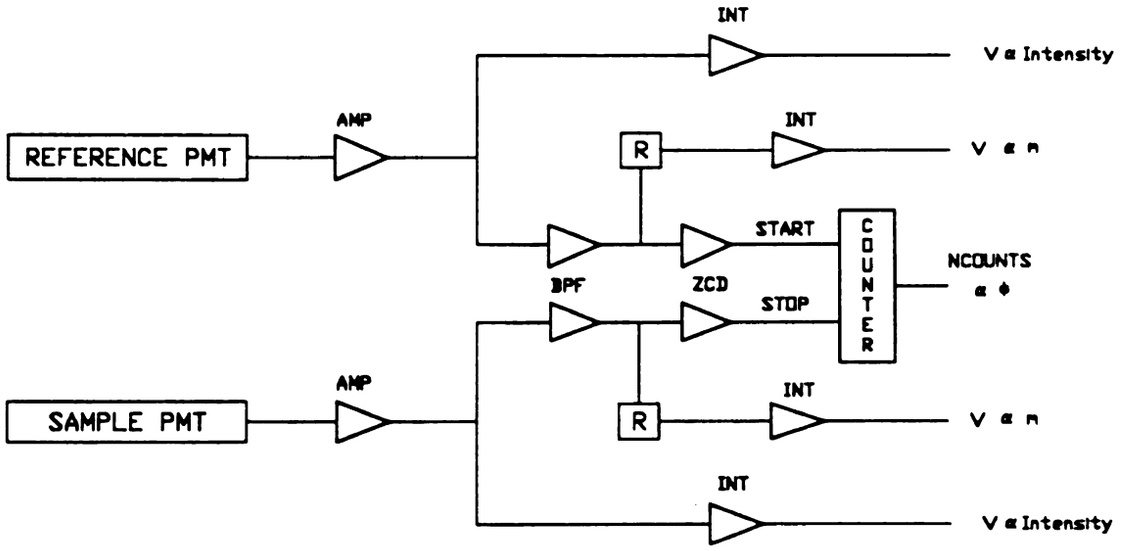

Figure 4-6. Simplified diagram of the detection electronics used in the instrument reported by Alcala and coworkers [24]. AMP: amplifier, BPF: bandpass filter, INT: integrator, ZCD: zero-crossing detector, R: rectifier.

the figure, the instrument has two identical channels, one each for reference and the sample, for deriving the frequency domain information. In order to more clearly describe the operation of the detection electronics, one of the channels and the signal at

various poi

Figure 4-7
by Alcala
operation.
rectifier, 2

current wl
the figure
determine
and the
integration
connected
signal fro
a counter
crossing
stopping

various points in it is shown in Figure 4-7. The signal from the detector, a PMT, is a

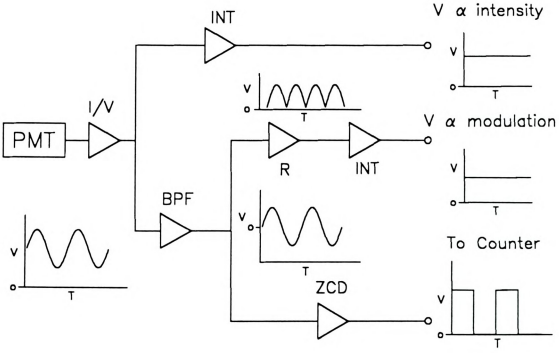

Figure 4-7. Single channel of the detection electronics used in the instrument reported by Alcala and coworkers [24]. The signal is shown at key points to illustrate its operation. I/V: current-to-voltage converter, BPF: bandpass filter, INT: integrator, R: rectifier, ZCD: zero-crossing detector.

current which is converted to a voltage by a current-to-voltage converter. As shown in the figure, the signal contains an AC and a DC component. The DC voltage is determined by integrating the signal. The AC signal is isolated with a bandpass filter, and the depth of modulation is determined by rectifying the signal followed by integration. The determination of the phase shift is accomplished with a counter connected to both channels. A zero-crossing detector is used to generate a digital signal from the filtered AC signal. These digital signals provide start and stop inputs to a counter (Figure 4-6). With the edges of the digital signal corresponding to the zero crossing point of the AC waveform and the reference and sample signals starting and stopping the counter, the phase shift is proportional to the number of counts. The

counter cou

measured p

are acquire

Afte

determinati

analysis.

modulation

the cell h

lifetime.

available

Haugen [2

A MO

In

quantity

assemble

these are

resolutio

radio-fre

One als

Althoug

all, of t

could n

counter counts oscillations from a 10 MHz oscillator providing high accuracy in the measured phase shift. All four of the analog voltages and the contents of the counter are acquired with a computer, automating the measurement and calculation processes.

After calibration of the instrument, this design allows a virtually instantaneous determination of an excited state lifetime through computer data acquisition and analysis. Since the reference is used to provide a continuous signal of the excitation modulation in addition to the phase reference, one merely needs to place a sample in the cell holder and "push a button" to obtain a direct readout of the excited-state lifetime. Because the information needed to directly determine the ratio of I/τ is available with this design, it was chosen for real-time implementation of the Hieftje-Haugen [2] method of correcting for the effects of collisional quenching.

A MOLECULAR FLUORESCENCE SPECTROMETER THAT CORRECTS FOR THE EFFECTS OF COLLISIONAL QUENCHING

In order to construct an instrument capable of a real-time, direct readout of the quantity I/τ using the overall design reported by Alcala and coworkers [24], one must assemble several expensive components not found in a typical fluorometer. Among these are an intensity modulated light source, a frequency synthesizer having 0.1 Hz resolution and capable of synchronization to the modulation of the light source, and a radio-frequency amplifier capable of delivering several watts of power to a modulator. One also needs access to test and measurement equipment to aid in construction. Although funds could not be obtained to purchase the needed equipment, most, but not all, of the above-mentioned components were acquired. The need for one item that could not be obtained, the frequency synthesizer, was satisfied by constructing a crude,

single fre

synthesize

Th

many mod

harmonic

dumped d

reported b

accomplis

cross-corr

coworkers

detector is

of mixing

modulatio

correlatio

gain-modu

require a

instrumen

it created.

correlatio

frequency

measuring

single frequency device. The limitations imposed by the constructed frequency synthesizer result in a less accurate method of measuring the phase shift.

General Features

The instrument constructed to directly determine the quantity I/τ is similar to many modern frequency domain fluorometers. A dual channel instrument, it uses the harmonic content of the output of a synchronously pumped, mode-locked, cavity dumped dye laser as an intensity modulated source, and is similar to the instrument reported by Alcala and coworkers [24]. Unlike their instrument, cross-correlation is accomplished external to the PMT with a doubly balanced mixer. This method of cross-correlation detection was used in an instrument reported by Lakowicz and coworkers [25]. In general, cross-correlation accomplished by modulating the gain of a detector is the preferred method, because one can realize almost theoretical efficiency of mixing when a PMT used. This is because one can achieve nearly perfect modulation with a PMT. The use of a doubly balanced mixer to generated the cross-correlation signal is less desirable because these devices are less efficient mixers than gain-modulated PMTs. External cross-correlation was chosen because it does not require a high power RF amplifier. Although such an amplifier was obtained for this instrument, it was not suitable because of ground loop problems and other interferences it created. The instrument described here is unique in that it uses a very high cross-correlation frequency of 325 kHz and is restricted to operation at a single modulation frequency, 76.5 MHz. Because of the high cross-correlation frequency, a method for measuring the phase shift was developed.

A d

Figure 4-8
directly de
locker driv
mixer, BB

mode-lock
intensity m
in Chapter
scattering s
needed, th
Scattered l
reference l
monochron
DC and A
the signal
input of a
PMT is sy

A diagram of the instrument is shown in Figure 4-8. As mentioned earlier, a

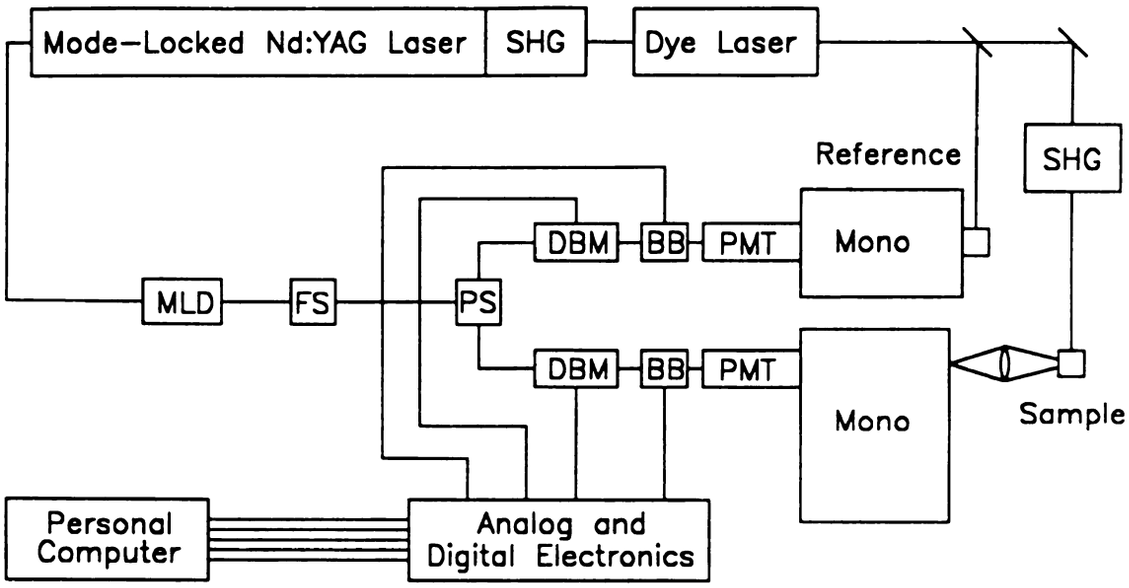

Figure 4-8. Diagram of the constructed frequency domain fluorometer capable of directly determining the quantity I/τ. SHG: second harmonic generator, MLD: mode-locker driver, FS: frequency synthesizer, PS: power splitter, DBM: doubly balanced mixer, BB: black box.

mode-locked, synchronously pumped, cavity dumped dye laser is used to provide an intensity modulated source. This is the same laser used in the SPT apparatus described in Chapter three. Light from the dye laser is split with a portion directed to a scattering solution and the remainder to the sample. If excitation in the ultra-violet is needed, the laser light can be frequency doubled with a second harmonic generator. Scattered laser light is filtered with a small monochromator and detected with the reference PMT. Fluorescence from the sample is collected and passed through a monochromator before reaching the sample PMT. The outputs from the PMTs contain DC and AC components. These are separated in a black box with the DC portion of the signal fed directly to the detection electronics and the AC portion fed to the RF input of a doubly balanced mixer. The frequency that is mixed with the signal from the PMT is synthesized in the frequency synthesizer which derives its frequency reference

from the n

power spli

generated i

the analog

coworkers

five DC vo

Th

presented

The freque

Th

AC and D

Figure 4-9
signal fro
mixer.

from the mode-locker driver. The output from the frequency synthesizer is split by a power splitter and fed to the LO port of the DBM. The cross-correlation frequency is generated in the DBM and accessed at the DBM's IF port. This signal is analyzed with the analog and digital electronics. As in the instrument reported by Alcala and coworkers [24], the intensity and the frequency domain information are contained in five DC voltages that are acquired with a laboratory personal computer.

Detection Electronics

The detection electronics are discussed in two stages. A general overview is presented first, and this is followed by a more detailed description of the circuits used. The frequency synthesizer is fully described in Appendix 3.

BLACK BOX AND MIXER

The contents of the "black box" indicated in Figure 4-8 and used to separate the AC and DC portions of the signal from the PMTs are shown in Figure 4-9. The AC

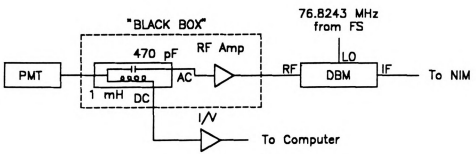

Figure 4-9. Diagram of the circuit used to separate the AC and DC components of the signal from the PMTs. I/V: current-to-voltage converter, DBM: doubly balanced mixer.

and DC si
capacitor (
the laser or
to-voltage
acquisition
amplified
mentioned
the signal
the light is
laser.

Th
extracted
nuclear ir
NIMs are
converted
correlatio
termed a
does not
circuit th
The phas
describe
by a ze
correspo

and DC signals from the PMT are separated with an inductor (passes DC) ar capacitor (passes AC). The DC signal represents the intensity of light, either tha the laser or of fluorescence, and is converted to a voltage and amplified with a curr to-voltage converter. This voltage is acquired with a personal computer in which a acquisition board is installed. The AC portion of the signal is high frequency an amplified with an RF amplifier before being fed to the doubly balanced mixer. mentioned previously, the cross-correlation frequency is generated in the mixer f the signal from the frequency synthesizer, 76.8243 MHz, and the frequency at w the light is modulated, 76.5 MHz - a harmonic of the fundamental repetition rate of laser.

NIM ELECTRONICS

The output of the mixer is filtered and the frequency domain informatio extracted by the rest to the detection electronics which are housed in two single-w nuclear instrumentation modules (NIMs) situated in a NIM bin. The contents of NIMs are in shown on page 101 in Figure 4-10. The signals from the mixers a converted to voltages and amplified with current-to-voltage converters. The cross correlation signal is isolated with a bandpass filter that is perhaps more appropriatel termed a tuned amplifier, as it provides gain over a narrow band of frequencies does not attenuate outside the passband. The depth of modulation is derived fro circuit that provides a DC voltage at the peak voltage of the cross-correlation sig The phase shift is measured using a time-to-amplitude converter. This device described in Chapter three. The cross-correlation signal is converted to a digital sig by a zero-crossing detector [39] such that the rising edge of the digital sig corresponds to the - to + transition of the cross-correlation signal. The refere

REFE

Figure 4-1
converter,
crossing d

signal prov
The heigh
between th
them. Th
and-hold
equipped

M
have cros
frequency
this instru
used in th

A
the DC si

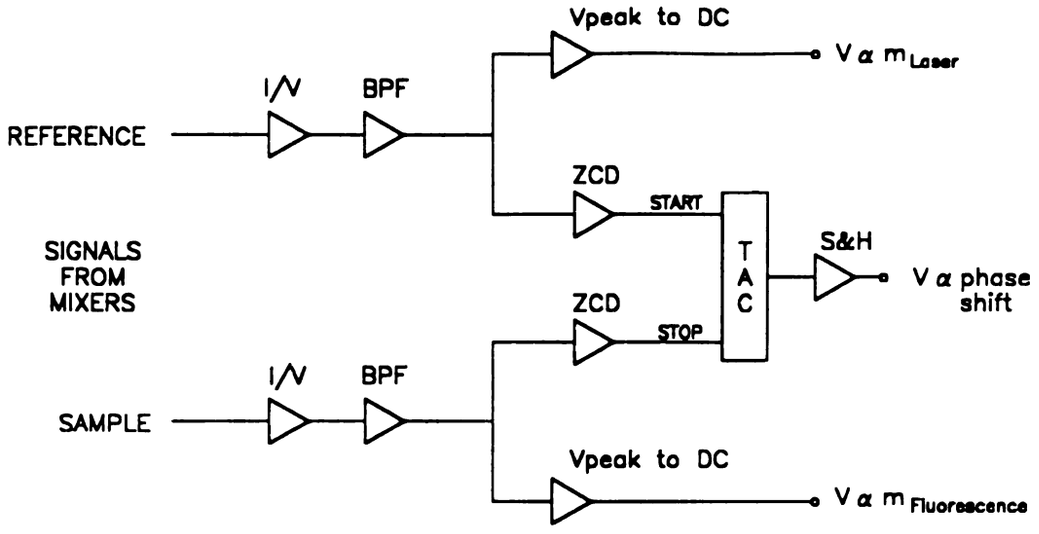

Figure 4-10. Overview of the circuits housed in the NIMs. I/V: current-to-voltage converter, BPF: bandpass filter, Vpeak to DC: Vpeak-to-DC converter, ZCD: zero-crossing detector, TAC: time-to-amplitude converter, S&H: sample-and-hold amplifier.

signal provides the start input to the TAC and the signal input provides the stop input. The height of the pulses generated by the TAC is proportional to the time difference between the start and stop inputs and hence is proportional to the phase shift between them. The pulses generated by the TAC are converted to a DC voltage with a sample-and-hold amplifier. The three DC voltages are acquired with a personal computer equipped with a data acquisition board.

Most frequency domain instruments that have been reported in the literature have cross-correlation frequencies near 30 Hz. While working with circuits for this frequency is straightforward, constructing circuits for the cross-correlation frequency in this instrument is much more challenging. Indeed, many of the operational amplifiers used in this instrument were introduced by manufacturers in the last three years.

A schematic diagram of the circuits housed in the NIM modules and those for the DC signals that are housed separately is shown on page 102 in Figure 4-11. The

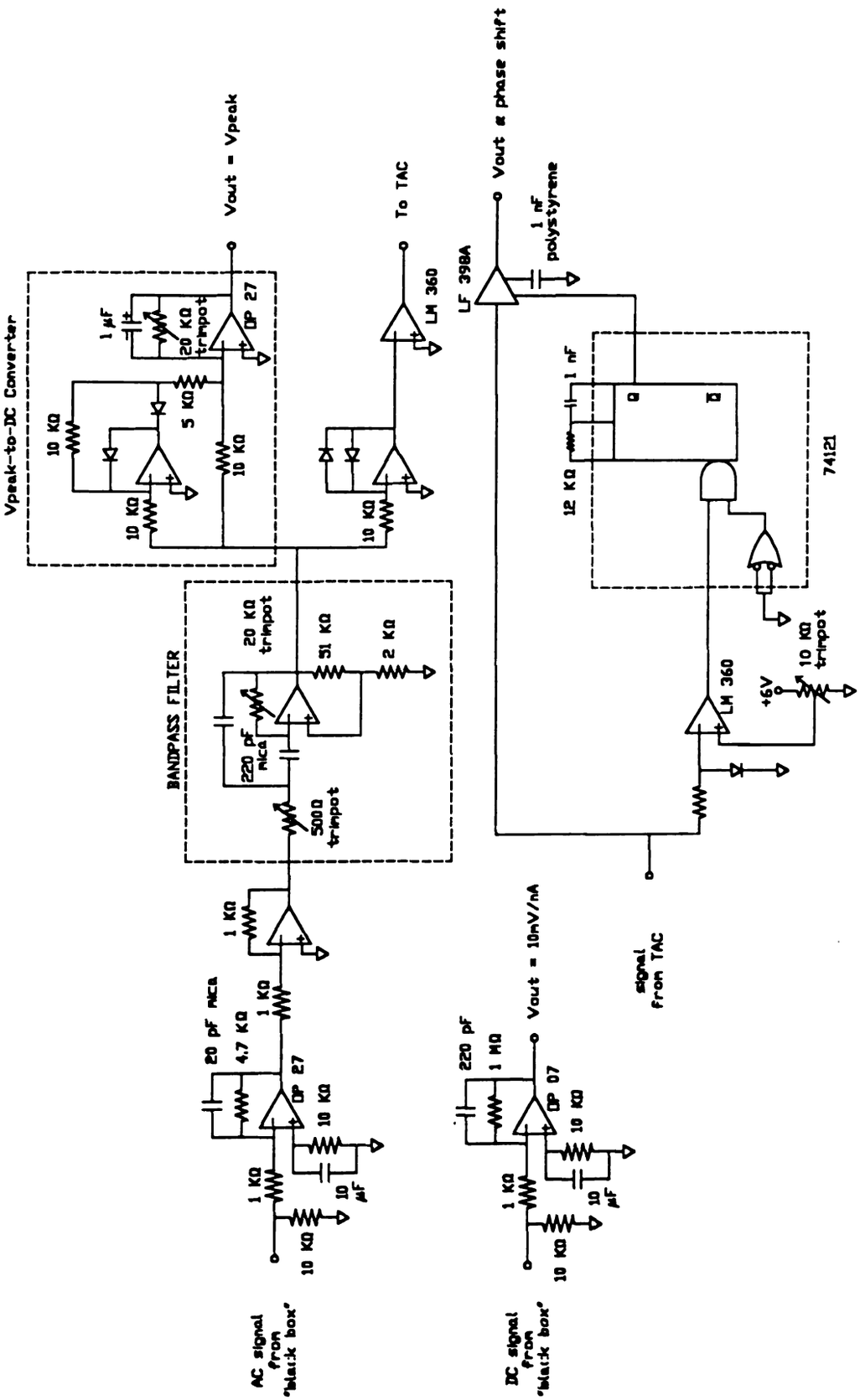

Figure 4-11. Schematic diagram of the detection electronics.

current-to-

left corner

through a

an inverti

feedback r

the input c

07, is not

μV [40].

a measure

Th

the top of

"black bo

also used

gain-band

[40]. Thi

first ampl

the next c

amplifiers

845s. Th

power ban

[41]. It v

are not qu

current-to-voltage converter and amplifier for the DC signals are shown in the lower left corner of the figure. The DC current from the "black box" is shunted to ground through a 10 kΩ resistor. The voltage developed across this resistor is amplified with an inverting amplifier having a gain of 1,000. A capacitor is placed across the feedback resistor to attenuate the high frequency response of the amplifier. Trimming the input offset voltage of this amplifier, a Precision Monolithics (Santa Clara, CA) OP 07, is not necessary because of this amplifier's extremely low input offset voltage of 25 μV [40]. This circuit generates 10 mV per nA of input current, and is used to provide a measure of the intensity of the sample or of the reference.

The circuit for deriving the depth of modulation of the AC signal is shown at the top of the figure. Like the circuit for the DC signal, the input current from the "black box" is shunted to ground through a 10 kΩ resistor. An inverter with gain is also used to amplify the voltage created by the IR drop, but the gain is five because the gain-bandwidth product of this amplifier, a Precision Monolithics OP 27, is eight MHz [40]. This amplifier is followed by an inverter of unity gain. It is needed because the first amplifier does not have sufficient power to drive the active bandpass filter which is the next component in the circuit. The amplifiers used for the inverter and all other amplifiers except the first one in the circuit are Analog Devices (Norwood, MA) AD 845s. This amplifier was chosen because of its excellent AC characteristics. The full power bandwidth of the AD 845 is 16 MHz and it is stable when operated at unity gain [41]. It was not used as the first amplifier in the circuit because its DC characteristics are not quite as good as those of the OP 27.

To

with a dash

from the

necessarily

large numb

that the co

signal afte

searching

Daryanani

negative a

and a pea

design of

that the ga

and cutof

was found

capacitors

variable r

optimize

285 Ω an

Figure 4-

BANDPASS FILTER

To aid in identifying it in the figure, the bandpass filter is labeled and outlined with a dashed line. A bandpass filter is necessary to isolate the cross-correlation signal from the other frequencies generated in the mixer. The signal from the mixer is necessarily rich in frequency components since the signal from the PMT contains a large number of harmonics. The filter must isolate the cross-correlation signal such that the contribution from the other frequencies comprises only a small fraction of the signal after the filter. A filter was developed to satisfy this need after a great deal of searching and experimentation. The filter design chosen is described in a book by Daryanani [42]. It is a second-order bandpass filter with gain derived from both negative and positive feedback. The filter was designed with a quality factor, Q, of 20 and a peak gain of 40 dB. A circuit simulation program [43] was used to aid in the design of this filter. Although amplifiers used in active filters are usually chosen such that the gain-bandwidth (GBW) product it at least ten times the product of the filter's Q and cutoff frequency [42] (a GBW of 65 MHz would be needed according to this), it was found that the AD 845, which has a GBW of 16 MHZ was sufficient. Mica capacitors were used because of their nearly ideal behavior at high frequencies. The variable resistors were initially set to values predicted by theory, and then adjusted to optimize the performance of the filter. The final values of the variable resistors were 285 Ω and 14.26 kΩ. A Bode plot of the constructed filter is shown on page 105 in Figure 4-12.

Figure 4-

T
converte
enclosed
is quite
to the ne
the orig
phase o
the non-
voltage
respons
convert
measure

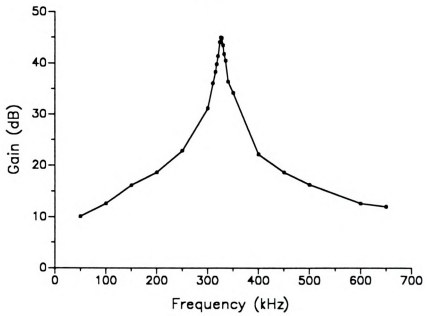

Figure 4-12. Bode plot of the bandpass filter.

PEAK DETECTOR

The signal from the active filter is fed to two circuits. These are a V_{peak}-to-DC converter and a zero-crossing detector. The V_{peak}-to-DC converter is also labeled and enclosed with dashed lines. This circuit was described in a book by Hufault [44], and is quite simple. The diodes in the feedback loop of the first amplifier limit the output to the negative half of the waveform. The output from this amplifier is combined with the original waveform in a summing integrator. Since the first amplifier shifts the phase of the waveform by 180 degrees, its output exactly cancels the positive half of the non-limited waveform. The value of the variable resistor is set so that the output voltage equals the peak voltage of the original signal. The circuit works well, but its response is slightly dependent on the signal level. Because of this, each V_{peak}-to-DC converter was calibrated, and the results of the calibration were used to correct measurements made with this circuit.

ZCD AND TAC

The zero-crossing detector is the only other part of the circuit shown in the upper portion of Figure 4-11 that has not been discussed. It consists of a log amp and a comparator [39]. The log amp provides a nearly constant amplitude waveform to the comparator and minimizes saturation and time shift with signal amplitude. The output of the comparator is used to provide start and stop inputs to the TAC.

The TAC was described in the chapter three. The amplitude of the pulses generated by the TAC represents the time difference between the reference and sample signals and hence is indicative of the phase shift. The TAC output pulse width was set to its maximum value of 10 μs. Since this is much faster than the conversion time of the analog-to-digital converter on the data acquisition board housed in the computer, a sample-and-hold (S&H) amplifier was used. The circuit used to sample and hold the output pulses from the TAC is shown in the lower right portion of Figure 4-12.

SAMPLE-AND-HOLD

A fast S&H amplifier, a National Semiconductor (Santa Clara, CA) LF 398A was used. The minimum acquisition time of this S&H is four μs [45]. However, in order to operate properly, the signal applied to its logic input must return to ground at least 250 ns before the analog signal level changes [45]. In order to satisfy this condition, a circuit was designed to provide an appropriate logic signal to the S&H. The circuit consists of a comparator and a monostable. In addition to being fed to the S&H, the signal from the TAC is fed to through a 1 kΩ resistor to the input of a fast comparator, a National Semiconductor LM360. The input to the comparator is shunted

to ground

reduces th

height. T

minimize

monostabl

the S&H.

Th

informati

ratio I/τ i

can have

two IBM

compatib

and mod

the S&H

common

acquired

This is

interrupt

Before c

mention

SPT ap

to ground through a diode. This limits the signals that reach the comparator input and reduces the dependence of temporal response of the comparator on the input pulse height. The threshold voltage is set slightly above the noise level in the circuit to minimize spurious signals. The output from the comparator is used to trigger a monostable (74121) which is configured to generate a 7 μs pulse which then triggers the S&H.

Data Acquisition

The five analog voltages derived from these circuits represent all of the information needed to measure fluorescence intensity and excited-state lifetime. The ratio I/τ is easily calculated by the data acquisition software. The five analog voltages can have values from zero to about 11 volts. All of these voltages are acquired with two IBM Data Acquisition and Control Adapters (IBM DACAs) housed in an IBM-compatible personal computer (Zenith Data Systems). While the voltages for intensity and modulation are essentially constant and can be acquired at will, the voltage from the S&H decays slightly with time from acquisition - a behavior termed droop that is common with S&H amplifiers. To reduce this source of error, the output voltage is acquired immediately after S&H acquisition with an interrupt service routine [45]. This is triggered by the Q output of the monostable which is used to generate an interrupt request pulse on the PC's bus.

Other Components

Before discussing the operation of the instrument, the other components used should be mentioned. Several of the components used in this instrument were also used in the SPT apparatus described in Chapter three. These include the light source and the

equipment
2000). T
Johnson.
(Newport,
(Metuche
signal, an
fluorescen
1P28. Th
biased usi
coworkers
was accor
Boca Rat
Systems,
(Redmond
5.1. Th
fluorescen
for correc
the subjec

Th
and refer
monochro
roughly e
with exci
detectors,

equipment used to monitor it, the TAC, and two RF amplifiers (Minicircuits ZFL-2000). The doubly balanced mixers (Minicircuits ZAD-1) were donated by Kermit Johnson. The collection optics consisted of two achromatic doublets, f/n = 2 and 6.8 (Newport, Fountain Valley, CA). The monochromators were an Instruments SA (Metuchen, NJ) model H10, used to filter the scattered laser light for the reference signal, and a Heath-McPherson (Benton Harbor, MI) model EU-700, used to isolate fluorescence from the sample. The PMTs were Hamamatsu (Bridgewater, NJ) model 1P28. These were housed in simple aluminum boxes with shutters. The PMTs were biased using a circuit similar to that used in the instrument reported by Alcala and coworkers [24] and a dual high voltage supply (Bertan model 362). Data acquisition was accomplished with two IBM data acquisition and control adapters (IBM DACAs, Boca Raton, FL) installed in an IBM-compatible personal computer (Zenith Data Systems, Benton Harbor, MI). The data acquisition software was written in Microsoft (Redmond, WA) QuickBASIC, version 4.0 and Microsoft Macro Assembler, version 5.1. The software is menu driven and provides instantaneous readout of the fluorescence intensity, excited-state lifetime, and the ratio I/τ. It also contains routines for correcting for sample absorption in combination with QuickBASIC for quenching - the subject of the next chapter.

Instrument Calibration

The instrument is calibrated by placing scattering solutions in both the sample and reference cell holders. Instrumental parameters such as PMT bias voltages and monochromator settings are adjusted so that the DC voltages from both detectors are roughly equivalent. Neutral density filters may also be used and are generally needed with excitation in the ultra-violet The DC and AC signals are acquired for both detectors, and these values are used to normalize the modulation measurements.

Calibration
from the T
voltage fro
uses the c
establishes
completed
monochro
presses the
immediate
demodula
modulatio
signal av
averaging
voltage is

B
excited-s
of 10 to
is 370 ps

D
noise in
producin
DC con
RFI at

Calibration of the phase shift is also carried out with scattering solutions. The voltage from the TAC is measured, a known delay is inserted in one of the channels, and the voltage from the TAC is measured again. The software acquires these voltages and uses the delay, entered by the user, to generate a calibration factor. This also establishes the voltage for zero phase shift. Once these calibrations have been completed, the instrument is ready for use. One simply tunes the sample monochromator to the desired emission wavelength, places a sample in the holder, and presses the ENTER key from the appropriate menu option. The user is provided nearly immediately with fluorescence intensity, excited state lifetime from both phase and demodulation, and two values of the ratio I/τ, determined from both phase and modulation. The time required for the measurement is a function of the extent of signal averaging. The measurements are virtually instantaneous with no signal averaging and require about ten seconds when the mean of 100 acquisitions of each voltage is determined.

Because the instrument is limited to a single modulation frequency, the range of excited-state lifetimes one may determine with it is limited. With the phase shift range of 10 to 80 degrees suggested earlier in this chapter, the range of excited-state lifetimes is 370 ps to 11.8 ns.

Performance

Despite a great deal of effort, under "ideal" conditions the dominant source of noise in the instrument is radio frequency interference (RFI). With the PMTs producing only dark current, a signal of about three volts was observed at the V_{peak}-to-DC converter. After extensive testing, it was determined that this noise resulted from RFI at 38.25 MHz being picked up in the cables that carry the signals from the PMTs

and from the freq

mixed with the

correlation freque

interferes with r

operates at 38.25

the mechanism

driver was leaki

cable that carrie

the building A

immediately aft

radiated RFI w

[46]. This cab

38.25 MHz ra

shielded and ac

with semi-rigi

housed preven

once with 1/1

clamped to th

The thus clad

system sits wi

at the output

The "

the available

modulated li

570 nm to

available.

and from the frequency synthesizer. Like the signal from the detectors, this noise is mixed with the output of the frequency synthesizer generating noise at the cross-correlation frequency. Since this noise is at the cross-correlation frequency, it directly interferes with measurements on the signal of interest. Because the mode locker operates at 38.25 MHz, it was logically the source of the RFI. It was determined that the mechanism of the interference was two-fold. RF generated in the mode-locker driver was leaking into the building AC power system, and it was radiating from the cable that carries the mode lock signal to the laser. The propagation of RFI through the building AC power system was greatly reduced by inserting a line filter immediately after the mode locker driver in the mode locker's power cord. The radiated RFI was reduced by adding shielding around the cable as suggested by Ott [46]. This cable is a 60 inch length of RG 58C/U coax that carries ca. four Watts of 38.25 MHz radiation from the mode locker driver to the laser. It is insufficiently shielded and acts as a transmitter at 38.25 MHz. Ideally, one would replace this cable with semi-rigid coax, but other considerations in the laboratory in which the laser is housed prevented this. Instead, the cable was wrapped twice with aluminum foil and once with 1/16th inch low inductance braid. The braid and aluminum foil were clamped to the BNC connectors at each end of the cable with common hose clamps. The thus clad cable was also electrically tied to the optical table upon which the laser system sits with braid. This reduced to the level of RFI to about 100 mV as measured at the output of the V_{peak}-to-DC converter.

The "ideal" conditions alluded to above concern the light source. In terms of the available ranges of wavelengths, the laser system that is used as the intrinsically modulated light source is quite good. From two cavity dumped dye lasers, light from 570 nm to 630 nm (rhodamine 6G dye) and 420 nm to 470 nm (stilbene 3 dye) is available. Excitation in the ultra-violet can be obtained by frequency doubling the

output of
mode loc
infra-red
of the las
of the fre
the Nd:Y
dye laser
doubled
generatio
infra-red
the case
to pump
turbulen
cavity.
the S/N

I
the S/N
excitatio
useful li
are less
this inst
alignme
noise.
perform

output of the rhodamine dye laser and frequency tripling the infra-red output of the mode locked Nd:YAG laser. Light at 532 nm generated by frequency doubling the infra-red output of this laser can also be used. *However*, the signal-to-noise ratio (S/N) of the laser light used depends on several factors. From a fundamental standpoint, all of the frequencies of light available have a S/N less than that of the infra-red output of the Nd:YAG laser from which all of the useful frequencies are obtained. Both of the dye lasers are pumped with light derived from frequency mixing. The noise in the doubled or tripled light from the Nd:YAG laser follows the power of the harmonic generation [47]. Hence the noise in the 532 nm light is the square of the noise in the infra-red and the noise in the 355 nm light is the cube of the noise in the infra-red. In the case of light from the dye lasers, the S/N of the output follows that of the light used to pump the dye laser and is further degraded because the jet of dye is not free of turbulence. The cavity dumper also adds to the noise level as does dust in the laser cavity. Because the fluorescence intensity is directly proportional to the source power, the S/N in the fluorescence measurements follows the S/N in the laser light used.

In practice the S/N of the fluorescence measurements is directly proportional to the S/N of the laser light used, and adequate S/N laser light is rarely obtained. The excitation source for the Nd:YAG laser is a pair of xenon arc lamps. The typical useful life of these is about 400 hours as judged by the needs of other experiments that are less sensitive to the S/N of the laser light (e.g. SPT). Adequate S/N laser light for this instrument is obtained only during the first 50 or so hours of lamp life. Also, the alignment of the Nd:YAG laser and the dye laser must be nearly perfect to minimize noise. Because of these factors that affect the signal-to-noise ratio, satisfactory performance has only rarely been obtained with this instrument.

Th

checked v

earlier. T

TABLE
DETERM

R

R

the liter

from th

uncertai

perform

APP

measure

chemica

phenyla

The accuracy of excited state lifetimes determined with the instrument was checked with a few compounds that have excited state lifetimes in the range determined earlier. The results are shown in Table 4-1 with values determined by SPT and from

TABLE 4-1. EXCITED-STATE LIFETIMES OF STANDARD COMPOUNDS DETERMINED BY SPT AND FDF.

Compound/Solvent	Literature Value	SPT	FDF
Rose Bengal / methanol	549 ps [48]	549 ps	350 $\pm$ 150 ps
Rhodamine B / ethanol	2.85 ns [49]	2.78 ns	4.1 $\pm$ 2 ns

the literature. The concentration of all solutions was 10 μM. The lifetimes calculated from the phase shift and the demodulation factor agree to within experimental uncertainty. The uncertainties in the lifetimes determined by FDF reflect the performance of the laser system at the time the measurements were made.

APPLICATION TO REAL-TIME CORRECTION FOR ERRORS DUE TO QUENCHING

The instrument described in this chapter was used to correct fluorescence measurements for the reduction in intensity caused by collisional quenching. The chemical systems studied were quinine sulfate quenched by chloride ion and dansyl-L-phenylalanine quenched by nitromethane.

Experimental Details

APPARATUS

The instrument described in this chapter was used for all measurements. Excitation was from the frequency doubled output of a cavity dumped dye laser. The laser dye was Rhodamine 6G, and the cavity dumper was set to divide by 10.. The wavelength was 293 nm and the power was ca. five mW (estimated from the dye laser power of 110 mW and SHG efficiency of five percent).

REAGENTS

These chemical systems were also studied in Chapter three, and details concerning reagents and solution preparation can be found there. In addition to those solutions, a scattering solution was prepared by dissolving ca. one gram of non-dairy coffee creamer (Quality Dairy, Lansing, MI) in a few milliliters of distilled water.

PROCEDURES

The instrument was calibrated for both phase and modulation measurements using scattering solutions as described in this chapter. Triplicate measurements were made on each solution, where each measurement is the mean of 100 analog-to-digital conversions.

Results and Discussion

The results for the quinine sulfate - chloride ion system are listed in Table 4-2.

TABLE 4-2. FLUORESCENCE INTENSITIES, LIFETIMES, AND THE RATIO I/τ FOR QUININE SULFATE, 10 μM IN 0.1 M SULFURIC ACID, QUENCHED BY VARYING CONCENTRATIONS OF CHLORIDE ION.

$[Cl^-]$	Intensity	Lifetime (ns)	Intensity/Lifetime
0.0	3695	23	160
0.005	1798	8.3	216
0.01	1304	5.4	241
0.05	510	2.1	243

The lifetimes shown are mean values of the lifetime determined from the phase shift and the demodulation factor. Lifetimes determined from these quantities agreed to within experimental uncertainty. The steady-state intensity and the intensity corrected for quenching by ratioing to the excited-state lifetime are compared graphically on page 115 in Figure 4-13. The fluorescence intensities are normalized to the unquenched value ofI/τ. As was the case with the SPT data in Chapter three, both the intensity and the lifetime decrease as the concentration of chloride ion increases. Note also that values are not given for solutions where the concentration of quencher is greater than 0.05 M. This is because the intensity from these solutions is below the detection limit for an excited-state lifetime. That is, the signal level is on the order of the signal generated from RFI as discussed earlier in this chapter. Unlike the SPT data (Figure 3-10), the ratio of I/τ increases as the concentration of quencher increases. This is because the noise resulting from RFI which is in phase with the exciting light becomes

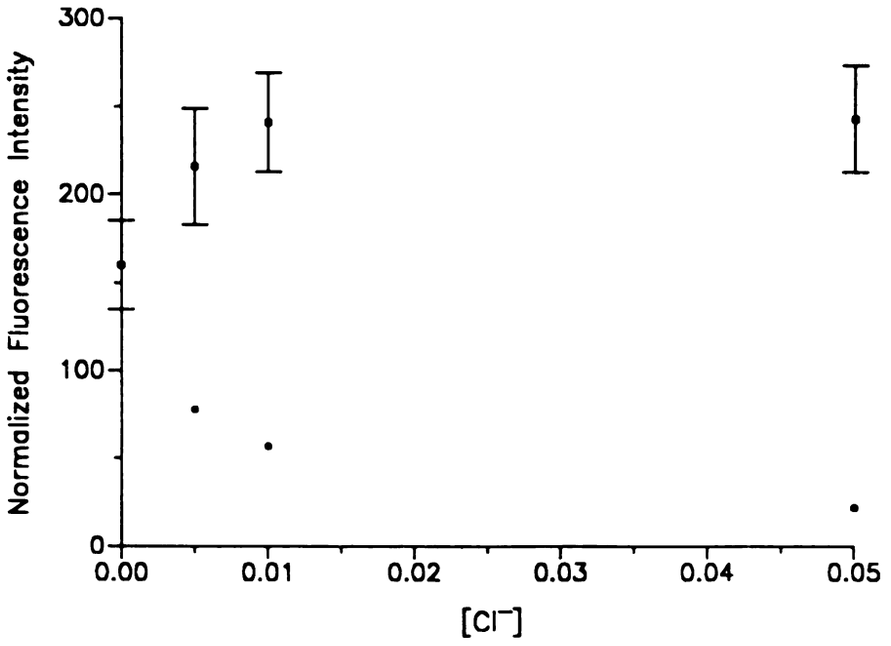

Figure 4-13. Plot of steady-state fluorescence intensity (circles) and fluorescence intensity corrected for quenching by ratioing to the excited state lifetime (squares) for quinine sulfate, 10 μM in 0.1 M sulfuric acid, quenched by chloride ion.

dominant as the cross-correlation signal decreases. This causes the determined excited-state lifetime to be less than the true value. Because the intensity is not affected by the RFI, the determined ratio of I/τ is greater than the true value. This source of error becomes significant as the fluorescence intensity decreases.

The data for the dansyl-L-phenylalanine - nitromethane system is shown on page 116 in Table 4-3. Note that values are not given for solutions where the concentration of quencher is greater than 0.10 M. This is because the intensity from these solutions is below the detection limit for an excited state lifetime. Again, the steady-state intensity and the excited-state lifetime decrease as the concentration of quencher increases. The lifetimes listed here are also mean values of the lifetime determined

TABLE 4-3. FLUORESCENCE INTENSITIES, LIFETIMES, AND THE RATIO I/τ FOR DANSYL-L-PHENYLALANINE, 10 μM IN 2-PROPANOL QUENCHED BY VARIOUS CONCENTRATIONS OF NITROMETHANE.

$[CH_3NO_2]$	Intensity	Lifetime (ns)	Intensity/Lifetime
0.0	3508	12	292
0.005	2816	8.1	347
0.01	2207	6.9	319
0.05	1418	4.6	308
0.10	627	1.9	330

from the phase shift and the demodulation factor, and the lifetimes determined from these quantities agreed to within experimental uncertainty. The steady-state intensity and the intensity corrected for quenching by ratioing to the excited-state lifetime are compared graphically on page 117 in Figure 4-14. The fluorescence intensities are normalized to the unquenched value of I/τ. As mentioned above, the signal level for these solutions is on the order of the signal that results from RFI. These data show an apparent correction for quenching. There is a dominant downward trend in the SPT data for this system (Figure 3-12) that is not evident here. This is a case of one systematic error cancelling the effect of another. The excited-state lifetime is skewed toward lower than true values, and the measured fluorescence intensity appears to be reduced by processes other than collisional quenching as discussed in Chapter three.

In summary, the precision in excited state lifetimes determined with this instrument is strongly dependent on the noise in the output of the laser system. The accuracy of this measurement degrades as the fluorescence intensity is reduced. This is due to a signal that results from RFI which is in phase with the exciting light and

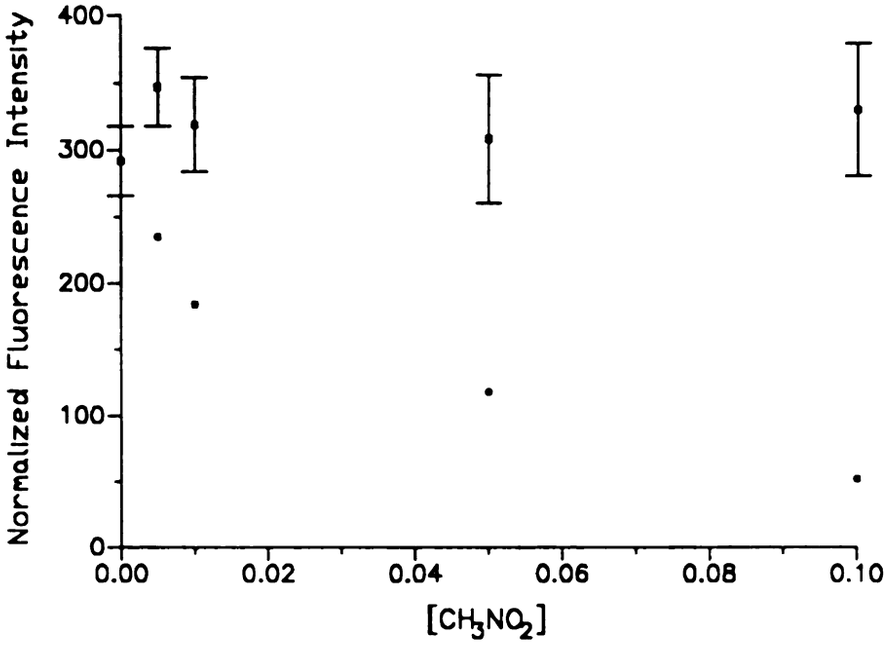

Figure 4-14. Plot of steady-state fluorescence intensity (circles) and fluorescence intensity corrected for quenching by ratioing to the excited state lifetime (squares) of dansyl-L-phenylalanine, 10 μM in 2-propanol, quenched by nitromethane.

causes the lifetime to be reduced relative to the true value. The degree of this distortion increases as the analyte signal level decreases to a point where it is comparable to the RFI-generated signal. These sources of error greatly limit the ability of this instrument to correct for the effects of quenching using the Hieftje-Haugen method [2]. Suggestions for reducing these sources of error are discussed in Chapter six.

CHAPTER 4 REFERENCES

1. Gaviola, E. *Z. Phys.* **1927**, *42*,852.
2. Hieftje, G.M.; Haugen, G.R. *Anal. Chim. Acta.***1981**, *123*, 255.
3. Lakowicz, J.R *Principles of Fluorescence Spectroscopy* Plenum Press: New York, 1983
4. Ware, W.R. in *Creation and Detection of the Excited State,*vol 1A A.A. Lamola, Ed. Marcel Dekker, Inc.:New York 1971.
5. Demas, J.N. *Excited State Lifetime Measurements* Academic Press: New York, 1983.
6. Hecht, E.; Zajac, A. *Optics* Addison-Wesley: Reading MA, 1979
7. Ingle, J.D.; Crouch, S.R. *Spectrochemical Analysis* Prentice Hall: Englewood Cliffs, NJ 1988.
8. Debye, P.; Sears, F.W.; *Proc. Nat. Acad. Sci.* **1932**, *18*, 409.
9. Maydan, D. *IEEE J. Quant. Elec.* **1970**, *QE-6*, 15.
10. Lekavich, J. *Lasers Appl.* **1986**, *4*, 59.
11. Dushinsky, F, *Z. Phys.* **1933**, *81*, 7.
12. Szymanowsky, W. *Z. Phys.* **1936**, *95*, 440.
13. Schmillen, A. *Z. Phys.* **1953**, *135*, 294.
14. Birks, J.B.; Little, W.A. *Proc. Phys. Soc. A*, **1953**, *66*, 921.
15. Bonch-Bruevich, A.M. *Izvest. Akad. Nauk. S.S.S.R.* **1956**, *20*, 591.
16. Birks, J.B.; Dyson, D.J. *J. Sci. Instr.* **1961**, *38*, 282.
17. Spencer, R.D.; Weber, G. *Ann. N.Y. Acad. Sci.* **1969**, *158*, 361.
18. Veselova, T.V.; Cherkasov, A.S.; Shirokov, V.I. *Opt. Spectrosc.* **1970**, *29*, 617.
19. McGown, L.B.; Bright, F.V. *CRC Crit. Rev.* **1987**, *18*, 245.
20. Gratton, E.; Limkeman, M. *Biophys. J.* **1983**, *44*, 315.

21. Gratton, E.; Jameson, D.M.; Hall, R.D.; *Ann. Rev. Biophys. Bioeng.* **1984**, *13*, 105.

22. Gratton, E.; Jameson, D.M.; Rosato, N. Weber, G.; *Rev. Sci. Instrum.* **1984**, *55*, 486.

23. Lakowicz, J.R.; Maliwal, B.P. *Biophys. Chem.* **1985**, *21*, 61.

24. Alcala, J.R.; Gratton, E.; Jameson, D.M. *Anal. Instrum.* **1985**, *14*, 225.

25. Lakowicz, J.R.; Lackzo, G. Gryczynski, I. *Rev. Sci. Instrum.* **1986**, *57*, 2499.

26. Bright, F.V.; Wilson, D.A.; Hieftje, G.M. *Appl. Spec.* **1986**, *40*, 683.

27. Berndt, K. *Opt. Commun.* **1985**, *56*, 30.

28. Bright, F.V. *Appl. Spec.* **1988**, *42*, 1531.

29. Weber, G. J. *Phys. Chem.* **1981**, *85*, 949.

30. Balter, A. *Opt. Commun.* **1982**, *42*, 407.

31. Lakowicz, J.R.; Cherek, H. Maliwal, B. *J. Lumin.* **1984**, *31*, 699.

32. Lakowicz, J.R.; Lackzo, G. Cherek, H.; Gratton, E.; Limkeman, M. *Biophys. J.* **1984**, *46*, 463.

33. Lakowicz, J.R.; Maliwal, B.P. *Anal. Instrum.* **1985**, *14*, 193.

34. Gratton, E.; Limkeman, M.; Lakokwicz, J.R.; Maliwal, B.P.; Cherek, H. Lackzo, G. *Biophys. J.* **1984**, *46*, 479.

35. Lakowicz, J.R.; Gryczynski, I.; Cherek, H.; Lackzo, G.; Joshi, N. *Trend. Anal. Chem.* **1986**, *5*, 257.

36. Keating-Nakamoto, S.M.;Cherek, H. Lakowicz, J.R. *Anal. Chem.* **1987**, *59*, 271.

37. Nithipatikon, K; McGown, L.B. *Appl. Spec.* **1987**, *41*, 395.

38. Lackzo, G.; Gryczynski, I.; Gryczynski, Z.; Wiczk, W.; Malak, H. Lakowicz, J.R. *Rev. Sci. Instrum.* **1990**, *61*, 2331.

39. Malmstadt, H.V.; Enke, C.G.; Crouch, S.R. *Electronics and Instumentation for Scientists*, Benjamin/Cummings: Menlo Park, CA. 1981.

40. Analog Integrated Circuit Data Book, Vol 10. 1990, Precision Monolithics Inc., Santa Clara, CA.

41. Linear Products Databook, 1990-91, Analog Devices, Norwood, MA.

42. Daryanani, G. *Principles of Active Network Synthesis and Design* Wiley: New York. 1976.

43. Micro-CAP II, student edition, release 5. Addison-Wesley and Benjamin Cummings:New York, NY, 1988.

44. Hufault, J.R. *Op Amp Network Design*, Wiley: New York, NY, 1986.

45. Data Acquisition Linear Devices Databook, 1989, National Semiconductor Corporation, Santa Clara, CA.

45. Bowman, L.E.; Victor, M.A.; Crouch, S.R. *Trend. Anal. Chem.* **1990**, *9*, 111.

46. Ott, H.W. *Noise Reduction Techniques in Electronic Systems*, 2nd ed. Wiley: New York, NY, 1988.

47. Fleming, G.R. *Chemical Applications of Ultrafast Spectroscopy*, Oxford University Press: New York, NY, 1986.

48. Ware, W.R.; Pratinidhi, M.; Bauer, R.K. *Rev. Sci. Instrum.* **1983**, *54*, 1148.

49. Comission on Photochemistry, *Pure Appl. Chem.* **1988**, *60*, 1108.

CHAPTER 5: A HIGHLY CORRECTED MOLECULAR FLUORESCENCE SPECTROMETER

When they occur during a fluorescence assay, collisional quenching and sample absorption will cause the measured fluorescence intensity to be less than the value in the absence of these processes. By combining methods that correct fluorescence measurements for the reduction in intensity caused by these processes, one can improve the accuracy of fluorescence measurements. An instrumentation-based approach to realize a fluorescence measurement that is corrected for both collisional quenching and sample absorption is described in this chapter. Because the constructed instrument corrects fluorescence measurements for both of these sources of error, it has been termed a "highly corrected" molecular fluorescence spectrometer.

The method used to correct for collisional quenching is that reported by Hieftje and Haugen [1]. One measures both the steady-state fluorescence intensity, I, and the excited-state lifetime, τ, and determines the ratio I/τ. Because both of these quantities decrease as collisional quenching increases, this ratio is in principle insensitive to collisional quenching and dependent only on the concentration of the fluorophore. The instrument constructed to directly determine the ratio I/τ is described in Chapter four. Correction for sample absorption is accomplished with the cell-shift method as described by Lutz and Luisi [2]. The cell-shift method was chosen because all of the measurements needed for it are fluorescence measurements.

In this chapter, the implementation of the cell shift method and the instrument constructed to accomplish it are described. This is followed by a description of the highly corrected measurement and its application to analytical situations where uncorrected molecular fluorescence would not normally be used.

REVIEW

Although several instruments and methods have been developed at Michigan State University (see Chapter one and references cited therein), the implementation of the cell-shift method reported by Lutz and Luisi [2] was chosen. While intuitive approaches that correct for sample absorption by directly measuring the absorbance of the solution have been developed [3-5], direct knowledge of the solution absorbance is not needed in the method reported by Lutz and Luisi [2]. Their method is one in which the cell is moved [6-8], and measurements of the fluorescence intensity at different locations are recorded. In order to correct for absorption of the emitted fluorescence in addition to absorption of the exciting light, Lutz and Luisi [2] considered the case of a cell shifted along its diagonal as shown in figure 5-1. They derived the following

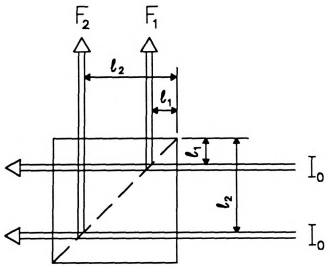

Figure 5-1. Methodology of the cell-shift technique reported by Lutz and Luisi [2]. F_1 and F_2 are fluorescence intensities at cell positions 1 and 2, respectively, where the optical pathlengths are l_1 and l_2.

relation for the corrected fluorescence intensity, F_0, in terms of F_1 and F_2 , the fluorescence intensities at positions 1 and 2, and a geometric term, a:

$$F_0 = F_1 \left[\frac{F_1}{F_2}\right]^a \qquad (5\text{-}1) \qquad\qquad a = \frac{l_1}{l_2 - l_1} \qquad (5\text{-}2)$$

Because the excitation and emission paths change by the same amount when the cell is shifted along its diagonal, the difference in the fluorescence intensity at the two locations reflects the solution absorbance at the excitation and emission wavelengths. Hence, one can correct for both primary and secondary absorption with only two fluorescence measurements. The only assumption made in deriving the above expression that affects the measurement is that the detected fluorescence is collimated. If it were not, the value of the pathlength would not be equal to l_1 (or l_2). Collimation is readily accomplished with appropriate masks in the collection optics of the fluorometer.

A FLUORESCENCE SPECTROMETER THAT CORRECTS FOR QUENCHING AND ABSORPTION

A molecular fluorescence spectrometer was developed to correct for the reduction in fluorescence intensity caused by collisional quenching and sample absorption. A cell holder was designed and fabricated for the cell-shift method and used with the single-photon timing apparatus described in Chapter two and the frequency domain fluorometer described in Chapter four. The cell-shift is accomplished by mounting the cell on two micrometer-driven stages moved by stepper motors. This instrument was used to map the fluorescence response surface of the cell and to make highly corrected fluorescence measurements.

Fluorescence Response Surfaces

EXPERIMENTAL DETAILS

Apparatus

The frequency-doubled output of the Nd:YAG laser used in the SPT system described in Chapter three was used to excite the sample. The laser power was reduced by splitting the beam with a quartz plate and attenuating the reflected beam with neutral density filters such that the power at the sample was about 15 mW.

A holder for positioning the cell was fabricated from two micrometer driven translation stages (Newport, Fountain Valley, CA). The stages were driven by stepper motors connected to the adjustment handles of the micrometer drives with shaft drive assemblies constructed in-house. The stages were mounted orthogonally so that the cell position with respect to the excitation beam and the collection optics could be varied in two directions. The stepper motors were controlled with a stepper motor controller designed and constructed in-house and an IBM-compatible personal computer (Zenith Data Systems) equipped with an IBM Data Acquisition and Control Adapter. Computer control of the stepper motors was accomplished by adding subroutines to the software used in the frequency domain fluorometer described in Chapter four. The combined resolution of the stepper motors and translation stages was 0.0014 mm per step.

The fluorescence measurements were made with the frequency domain fluorometer described in Chapter four. A variable iris was adjusted to an aperture of

approximately one millimeter and placed between the lenses of the collection optics to insure that only collimated fluorescence reached the detector. The imaging resolution of the optical system was about 0.3 mm^2 when the monochromator slits were set to 1000 μm. The waist of the exciting laser beam was reduced with plano-convex lenses to about this value to optimize the fluorescence signal.

A standard 1 cm^2 x 4 cm quartz fluorescence cuvette was used for all measurements.

Reagents

A 0.001 M stock solution of rhodamine B (Aldrich) was prepared in 95% ethanol (Department of Chemistry, Michigan State University). Aliquots of the stock solution were diluted with ethanol to prepare 1.0 μM and 100 μM working solutions.

Procedures

Both solutions were excited at 532 nm and fluorescence was detected at 600 nm. The monochromator slit width was 1000 μm. The voltage applied to the photomultiplier tube was adjusted to yield the maximum signal at the output of the current-to-voltage converter without exceeding the input voltage range of the analog-to-digital converter.

The fluorescence response surface of the cell was mapped using the computer controlled stepper motor driven translation stages and the frequency domain fluorometer described in chapter four. A response surface of 144 points was recorded

for both of the rhodamine B working solutions. The interval between points was one millimeter. Each point was the mean of 100 analog-to-digital conversions.

RESULTS AND DISCUSSION

The concentrations of the rhodamine B solutions were chosen to illustrate minimal and extreme sample absorption. The absorbance of the 1.0 μM solution was 0.007 at the excitation wavelength and not measurable at the emission wavelength. The absorbance of the 100 μM solution was 1.07 at the excitation wavelength and 0.016 at the emission wavelength. Each response surface is illustrated from two different viewpoints so that no part of the surface is obstructed. In these illustrations, the X and Y axes are respectively orthogonal and parallel to the monochromator entrance slit with the distance in the solution increasing with X and Y. Hence, the X axis indicates emission distance, and the Y axis indicates excitation distance. The axes are in units of tenths of millimeters. Position 0,0 was set at approximately the center of the intersection of the cell walls.

The response surface of the 1.0 μM solution is shown on page 127 in Figure 5-2. Because the absorbance of the solution at the excitation and emission wavelengths is small, the response is essentially flat. The slightly higher intensity near the cell walls that are orthogonal to the plane of the entrance slit is due to a slight blurring of the image as the distance in the solution increases. The effective focal length of the collecting lens changes as the cuvette is moved toward the lens due to the difference between the refractive index of the solution and the refractive index of air. The slight texture in the surface reflects noise in the laser.

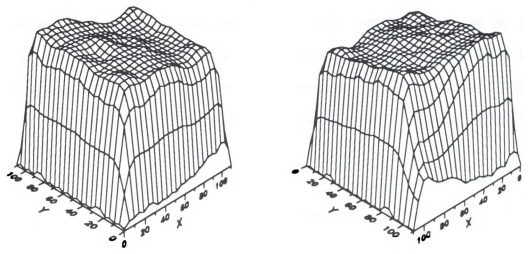

Figure 5-2. Response surface of fluorescence intensity as a function of optical path length in solution for a o1.0 μM solution of rhodamine B in ethanol. The axes units are tenths of millimeters.

The response surface of the 100 μM solution is shown in Figure 5-3. Note that

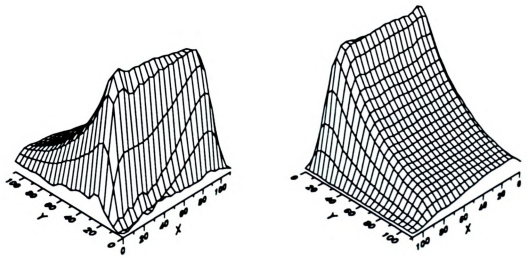

Figure 5-3. Response surface of fluorescence intensity as a function of optical path length in solution for a 100 μM solution of rhodamine B in ethanol. The axes units are tenths of millimeters.

the fluorescence intensity decreases dramatically with increasing distance in the direction of excitation (Y). This is due to the high absorbance of the solution at the excitation wavelength. The absorbance at the emission wavelength causes a slight decrease in the fluorescence intensity as the depth of solution through which the fluorescence is viewed increases (X).

Highly Corrected Fluorescence

Fluorescence measurements corrected for the reduction in intensity caused by sample absorption and collisional quenching were made. The fluorophore chosen for study was quinine sulfate in 0.1 M sulfuric acid. Chloride ion was used to quench fluorescence, and the acid-base indicator bromocresol green was used to increase the absorbance of the solution at both the excitation and emission wavelength.

EXPERIMENTAL DETAILS

Apparatus

The frequency domain fluorometer described in Chapter four, the cell positioning apparatus described earlier in this chapter, and the single-photon timing apparatus described in Chapter three were used to correct for the reduction in fluorescence caused by collisional quenching and sample absorption. For comparison, steady-state fluorescence measurements were made with a Perkin-Elmer model LS-5 fluorometer. A Perkin-Elmer "Lambda3" UV/VIS absorption spectrometer was used for absorbance measurements.

Reagents

A 1.0 m<u>M</u> stock solution of quinine sulfate monohydrate (Aldrich) was prepared in 0.1 <u>M</u> sulfuric acid (prepared by diluting 5.5 ml of concentrated sulfuric acid (Malinckrodt) in one liter of distilled and deionized water (Corning millipure system)). A 1.0 <u>M</u> stock solution of sodium chloride (J.T. Baker) was prepared in 0.1 <u>M</u> sulfuric acid. A 1.0 m<u>M</u> stock solution of bromocresol green (Aldrich) was prepared by dissolving the solid in a minimum amount of 95% ethanol (Department of Chemistry, Michigan State University) and diluting with 0.1 <u>M</u> sulfuric acid. A 100 μ<u>M</u> stock solution of bromocresol green was prepared in 0.1 <u>M</u> sulfuric acid by diluting an aliquot of the previous solution. A total of twelve working solutions were prepared. Each working solution was prepared by diluting to 100 ml a mixture composed of 1.0 ml of the quinine sulfate stock solution, 0.0, 1.0, or 10.0 ml of the sodium chloride stock solution, and 0.0, 10.0, or 50.0 ml of the 1.0 m<u>M</u> bromocresol green stock solution or 0.0, 1.0, or 10.0 ml of the 100 μ<u>M</u> bromocresol green stock solution.

Procedures

The steady-state fluorescence intensity of the working solutions was measured on the Perkin-Elmer fluorometer. The solutions were excited at 350 nm and fluorescence was detected at 450 nm. The bandpass for both excitation and emission was 3 nm.

To obtain the highest accuracy, the excited-state lifetimes were determined with the single-photon timing apparatus. The solutions were excited at 290 nm, and fluorescence was detected at 450 nm with a photomultiplier tube. The fluorescence decay of each sample was acquired over 1024 channels and fit to a single exponential

model. The value of reduced χ^2 was less than 1.2 for all of the curve fits except those for the solutions that were 0.1 M in sodium chloride. A χ^2 of 3 was typical for the curve fits for these solutions.

Fluorescence intensities corrected for sample absorption were measured with the cell-shift method and the frequency domain fluorometer.

RESULTS AND DISCUSSION

Four tables of fluorescence intensity are presented in this section. A table is given for steady-state measurements of fluorescence intensity and for each of the three correction schemes. The data in each table reflects the ability of each measurement strategy to correct for the reduction in intensity caused by collisional quenching and sample absorption.

The steady-state fluorescence intensity measurements are shown in Table 5-1.

TABLE 5-1. STEADY-STATE FLUORESCENCE INTENSITY (ARBITRARY UNITS) FOR QUININE SULFATE SOLUTIONS THAT ARE AFFECTED BY COLLISIONAL QUENCHING AND SAMPLE ABSORPTION.

	ABS @ 450 nm				
	0.0	0.03	0.3	1.0	2.3
[NaCl]					
0.0	9000	7920	3510	900	85
0.01	3835	3510	1600	389	30
0.1	576	522	240	59	6

The columns are labeled with the absorbance of the solution at the emission wavelength. Sample absorption increases across a row and collisional quenching increases down a column. Because the fluorescence intensities shown in this table were obtained with steady-state measurements, the intensity decreases both across a row and down a column. Note that the fluorescence intensity varies over three orders of magnitude even though the concentration of the fluorophore is constant.

The fluorescence intensity corrected for quenching by the Hieftje-Haugen method [1] is shown for these solutions in Table 5-2. Note that the ratios listed in

TABLE 5-2. FLUORESCENCE INTENSITY RATIOED TO EXCITED-STATE LIFETIME FOR QUININE SULFATE SOLUTIONS THAT ARE AFFECTED BY COLLISIONAL QUENCHING AND SAMPLE ABSORPTION.

	ABS @ 450 nm				
	0.0	0.03	0.3	1.0	2.3
[NaCl]					
0.0	523	460	204	52	5
0.01	498	456	207	51	4
0.1	427	387	178	44	5

this table are essentially constant in each column but decrease across each row. The ratio of fluorescence intensity to excited-state lifetime corrects for collisional quenching but not sample absorption.

The results of the cell-shift measurements are shown on page 132 in Table 5-3. Here, the reported quantity is almost constant across a row but decreases down a

TABLE 5-3 FLUORESCENCE INTENSITY (ARBITRARY UNITS) AS MEASURED BY THE CELL-SHIFT METHOD FOR QUININE SULFATE SOLUTIONS THAT ARE AFFECTED BY COLLISIONAL QUENCHING AND SAMPLE ABSORPTION.

	ABS @ 450 nm				
	0.0	0.03	0.3	1.0	2.3
[NaCl]					
0.0	196	227	203	189	105
0.01	91	113	98	123	448
0.1	14	18	15	14	5

column. The cell-shift method corrects for sample absorption but not for collisional quenching.

The fluorescence intensities shown in Table 5-4 are the cell-shift measurements

TABLE 5-4. ABSORPTION CORRECTED FLUORESCENCE INTENSITY RATIOED TO EXCITED-STATE LIFETIME FOR QUININE SULFATE SOLUTIONS THAT ARE AFFECTED BY COLLISIONAL QUENCHING AND SAMPLE ABSORPTION.

	ABS @ 450 nm				
	0.0	0.03	0.3	1.0	2.3
[NaCl]					
0.0	11.4	13.2	11.8	10.0	6.1
0.01	11.8	14.7	11.8	15.9	6.2
0.1	10.0	13.5	10.6	9.9	3.9

from Table 5-3 ratioed to the excited-state lifetime. Here, the reported quantity is almost independent of both collisional quenching and sample absorption. This "highly corrected" fluorescence intensity is nearly constant across a row and down a column.

Consider that the extreme values of this data set vary by a factor of four while the range of observed steady-state fluorescence intensity exceeds three orders of magnitude for the same solutions.

The relative standard deviation of the data obtained using each correction scheme is shown in Table 5-5. The highly corrected measurements are not nearly as

TABLE 5-5. RELATIVE STANDARD DEVIATION OF THE DATA OBTAINED BY EACH MEASUREMENT SCHEME.

	Steady-State	I/τ	Cell-Shift	Highly Corrected
ABS 0 to 1.0	114%	64%	75%	16%
All solutions	135%	87%	95%	31%

widely scattered as the results of the other methods. The correction provided is especially satisfactory if one does not include the solutions that have absorbances greater than 1.0. Although both the ratio of I/τ and the cell-shift schemes are better that the steady-state values, neither comes close to the correction provided by the highly corrected measurement.

Each of the correction schemes provides the best compensation for those solutions that are neither highly quenched nor strongly absorbed. This is primarily due to the very low fluorescence intensity of these solutions. In addition to absorbing the quinine sulfate fluorescence, bromocresol green also absorbs the exciting light. This greatly reduces the fluorescence intensity relative to an absorbing species that would only absorb the emitted fluorescence.

In addition to providing a fluorescence-based measurement that is corrected for both of these sources of uncertainty, the highly corrected measurement concept could allow fluorescence to be more useful in diagnostic work. If changes in the highly corrected fluorescence intensity occur while the concentration of the fluorophore is constant, it could be an indication that other processes such as static quenching or energy transfer are occurring.

CHAPTER 5 REFERENCES

1. Hieftje, G.M.; Haugen, G.R. *Anal. Chim. Acta.* **1981**, *123*, 255.
2. Lutz, H.P.; Luisi, P.L. *Helv. Chim.Acta.* **1983**, *66*, 1929.
3. Parker, C.A.; Barnes, W.J. *Analyst* **1957**, *82*, 606.
4. Holland, J.F.; Teets, R.E.; Timnick, A. *Anal. Chem.* **1973**, *45*, 145.
5. Holland, J.F.; Teets, R.E.; Kelley, P.M.; Timnick, A. *Anal. Chem.* **1977**, *49*, 706.
6. Britten, A.; Archer-Hall, J.; Lockwood, G. *Analyst* **1978**, *103*, 928.
7. Christmann, D.R.; Crouch, S.R.; Holland, J.F.; Timnick, A. Anal. Chem. **1980**, *52*, 291.
8. Christmann, D.R.; Crouch, S.R.; Timnick, A. *Anal. Chem.* **1981**, *53*, 276.

CHAPTER 6: SUGGESTIONS FOR IMPROVEMENTS AND FUTURE WORK

Most of what has been written in this dissertation concerns instrumentation for determining excited state lifetimes. Because the capabilities of modern technology are constantly improving, no developments described in this document can remain state-of-the-art for long. As the Single-Photon Timing (SPT) apparatus described in Chapter three will probably be used by other students, some comments concerning improvements to the constructed instrument are discussed in this chapter. Suggestions for improving the frequency domain fluorometer are also made. If the means could be found to improve the frequency domain fluorometer along the lines described here, it could find more realistic analytical applications. Some of these are also described in this chapter.

SINGLE-PHOTON TIMING

Of the SPT instruments that have been described to date, the apparatus constructed in this work and discussed in Chapter three is probably one of the most versatile. While other instruments have slightly shorter instrument response functions, many of these are not capable of acquiring fluorescence decay data over a continuous temporal window from about two nanoseconds to a microsecond. This capability was made possible with the switched fiber optic delay described in Appendix two. If it is needed, the instrument response can be reduced from its present value of about 45 picoseconds to slightly less than 20 picoseconds. To realize a narrower instrument response, a few of the present components must be replaced.

The first items that should be replaced are obviously those that are presently limiting the instrument. However replacing one component will not make much of a

difference. Four principal items would be needed. These are a subtractive dispersion double monochromator, a six micron MCP-PMT, a 6 GHz amplifier, and a biased TAC. The transit time spread of the present monochromator has been reduced by placing a mask at the diffraction grating. While this reduced the monochromator's contribution to the instrument response to an acceptable level for a 12 micron MCP-PMT, it also reduced the instrument's sensitivity. This is not a problem with efficient fluorophores, but it requires long acquisition times for weakly emitting species. A subractive dispersion double monochromator has no temporal dispersion and would not contribute to the instrument response. If the present monochromator is replaced with a subtractive dispersion double monochromator, the instrument response may be reduced by a few picoseconds. This will be most noticeable in measurements made toward the red end of the visible spectrum. The extent of any improvement will reflect the affect of the masked, Czerny-Turner monochromator that it presently used. Even if there is no discernable reduction in the instrument response, the instrument's sensitivity will certainly be improved. At present, only one subtractive dispersion double monochromator suitable for SPT exists, the model DB-10S, manufactured by American Holographic. It costs slightly under four thousand dollars when ordered with ion milled gratings.

A faster detector or one with a smaller transit time spread would also be needed to reduce the instrument response function. At present the detector that has the smallest transit time spread that is suitable for SPT is the Hamamatsu R2809. This is an MCP-PMT that contains two microchannel plates composed of six micron channels. It has been used in other SPT instruments to yield an instrument response below 20 picoseconds.

If a faster detector such as the one mentioned above is obtained, a higher bandwidth amplifier and attenuator would also be needed. For this six micron MCP-PMT, a amplifier having a bandwidth of at least 6 GHz is recommended. A 10 GHz bandwidth amplifier would be preferred. The semi-rigid coax that is already in place is sufficient for this detector, but the present attenuator would need to be replaced with a higher bandwidth device.

With these faster components, a faster time-to-amplitude converter would be needed to accurately record the instrument response and very fast fluorescence decays. The best device presently available is the Tennelec model 864 TAC, which has a built-in bias amplifier. This allows one to amplify a narrow region of the time base. In this way the normal output voltage range can represent a time range of only a few nanoseconds. While this can improve the temporal resolution of the TAC-MCA measurement system to about 0.2 picoseconds per channel, the bias amplifier can degrade the linearity of the TAC response. This distortion is minor and can be minimized by carefully adjusting the delay so that only the most linear region of the TAC is used.

With a higher bandwidth detector and amplifier and an improved temporal resolution of the measurement system, one small, passive component may be limiting the instrument response. This is the switched coaxial cable delay. The coaxial cable used in it is RG-174 which is not really adequate for the bandwidths mentioned above. An improvement would be a delay constructed with semi-rigid coax and high bandwidth switches, such as those used for microwave signals. Unfortunately such a device is not commercially available, but it could be constructed in-house. The major difficulty would be fitting the semi-rigid coax in a convenient housing such as a NIM. Because semi-rigid coax is manufactured in five foot lengths, it would also be a bit

tedious to splice together pieces of semi-rigid cable to obtain the longer delays needed. Of course one could special-order a given length of semi-rigid coax coiled so as to fit in a NIM.

With these improvements, an instrument response of less than 20 picoseconds should be obtainable. Of course one would have to carefully adjust the discriminator thresholds and change the shaping delay in the CFD to optimize its performance with faster risetime signals.

One of the items that presently limits the ability to resolve fast and complex decays is the sample cell. Reflections from the cell walls are evident in the instrument response. In addition, a distortion caused by them can sometimes be observed in the early part of a fluorescence decay. The best means of removing this source of interference is to use the special cuvettes mentioned in Chapter four. Although they are expensive and must be specially made at present, they are simple to use and are proven to reduce the interference caused by wall reflections to a tolerable level.

Beyond the instrument response considerations, it would be worthwhile to develop the hardware and software needed to acquire time-resolved emission spectra. This is most easily accomplished by operating the MCA as a single channel analyzer (SCA). One sets upper and lower level discriminators and scans the analyzer in time. By simultaneously scanning the monochromator, one collects in each channel the number of photons emitted in the set time window over the wavelength interval corresponding to the width of a channel. One can signal-average spectra by collecting several SCA and averaging over the same temporal window. A complete time resolved emission profile can be obtained by recording SCA scans for several temporal windows.

If there is serious interest in having this capability as a routine research tool, one would need to control the monochromator with the computer. At present this is not possible with the manually controlled SPEX 1681. It would be trivial to drive the American Holographic DB-10S with a stepper motor as was done for the cell-shift measurements described in Chapter five. Also, an MCA that is capable of software control of the discriminator levels would greatly reduce tedium in this experiment. Such an MCA has recently become available. It is the model 5000 MCA manufactured by Viking (Madison, WI).

FREQUENCY-DOMAIN FLUORESCENCE

Changes in instrumentation are certainly needed if the accuracy and precision of the frequency domain fluorometer are to be improved. Two major changes are needed to realize these improvements. These are a more stable light source and a commercial frequency synthesizer. Aside from the RFI problems associated with the laser system used, it is not sufficiently stable for frequency domain fluorescence. This is one of the major advantages of SPT; it is most insensitive to fluctuations in the intensity of the light source. SPT is also more sensitive - one of the reasons that it is more widely used than the various frequency domain techniques. The RFI could be reduced to a more reasonable level by replacing the cables between the mode locker driver and the mode locker crystal with semi-rigid or twinaxial coax. As mentioned in Chapter four, the RFI was reduced slightly by adding shielding to the length of coax between the mode locker driver and the laser. However there is another cable between the end bezel of the laser and the mode-locker crystal. This cable is only partially shielded and is probably the primary source of radiation. Not only would this greatly reduce the RFI in the frequency domain measurements, it would probably remove the 38 MHz noise

that is observed in plots of the autocorrelation of residuals in SPT experiments on long-lived species.

To obtain higher accuracy and precision, it would probably be better to use a cw laser and an external modulator than to continue to use the mode-locked Nd:YAG laser system. By using a He-Cd, Ar^+, or Kr^+ laser, one could obtain much higher power at analytically useful wavelengths, in addition to more stable modulation.

High resolution commercial frequency synthesizers would allow the cross-correlation frequency to be reduced to a more reasonable value. The availability of these and the low noise amplifiers needed to drive a modulator and to modulate the gain of a PMT, would enable not only more effective utilization the capabilities of FDF, but also greatly improve the accuracy of the method. For some time, this author has been interested in studying the signal-to-noise ratio of excited state lifetimes determined by frequency domain techniques as a function of the cross-correlation frequency. It would be straightforward to make such a study in the frequency range of a few Hz to 100 kHz. Rather than designing and constructing active filters for specific frequencies as was required in this work, one could use complete integrated circuit filters such as the National Semiconductor MF5 universal monolithic switched capacitor filter. One only needs to provide an oscillator at the cutoff or bandpass frequency and analog and digital voltages to set the filter's configuration and quality factor. With computer control of the frequency synthesizers and the filter, acquiring the data for this study could be completed in less than one day. The information derived from it could greatly benefit the state-of-the-art of frequency domain fluorescence. The cross-correlation frequency of 30 Hz used in other instruments is almost blindly followed by workers in the field. The attitude of "if it isn't broken, don't fix it" has limited progress in the area. While the time required for an SPT experiment can be as little as

one minute, the best frequency domain fluorometers require about one-half hour to acquire data to determine the same information. The phase shift and demodulation are acquired at each of several modulation frequencies. The time required for this could be greatly reduced by going to a higher cross-correlation frequency, which would minimize the time required for signal averaging. It may also improve the accuracy of the acquired data.

A suitably improved frequency domain fluorometer could be applied to determinations based on flowing streams such as flow injection analysis (FIA) and liquid chromatography (LC). The present apparatus does not possess sufficient precision over the time window needed to profile these systems.

HIGHLY CORRECTED MOLECULAR FLUORESCENCE

The work discussed in Chapter 5 demonstrated the potential of this combined correction strategy. Since the highly corrected measurement scheme requires an accurate determination of the excited-state lifetime, the improvements suggested earlier in this chapter for the frequency domain fluorometer would need to be implemented before much meaningful work in highly corrected fluorescence could be attempted. Moreover, an intense light source is crucial for absorption correction. One must have an intense source so that there is sufficient fluorescence intensity to measure in the presence of strongly absorbing solutions and high concentrations of quenchers. A laser capable of generating one Watt at the excitation wavelength could be very useful in an apparatus similar to the one described in chapter five.

Regardless of whether an intense laser is obtained, the cell-shift scheme could be automated more intelligently than in this work. If the solution absorbance is great,

one could program the controlling computer to use optimum cell positions for the measurements. That is one would use less of a path length difference when the solution is great. One could also make measurements at other locations in the cell to better correct for extreme primary or secondary sample absorption.

The cell-shift method was chosen to provide absorption correction because all of the measurements needed for it are fluorescence measurements. This and the ease with which it could be automated and incorporated with the frequency domain fluorometer and the SPT apparatus made it a logical choice for this work. However, there is no reason that absorption correction could not be accomplished using fiber optics or another approach that would make highly corrected measurements possible in flowing streams.

APPENDIX 1: COMPONENTS OF THE SINGLE PHOTON TIMING APPARATUS

This appendix contains a listing of the components of the SPT instrument, their part numbers, and names and addresses of vendors. Common items such as flexible coaxial cable, mirrors, and ordinary optical mounts are not included.

LIGHT SOURCE AND MONITORING EQUIPMENT

Component	Model Number/Decsription	Vendor/Address
Mode Locked Nd:YAG Laser w/ High Power Second Harmonic Generator	76S	Coherent, Inc. 3210 Porter Dr. Palo Alto, CA 94303
Third Harmonic Generator and Wavelength Separator	7950	
Dye Laser w/ Cavity Dumper Rhodamine 6G dye (570-630 nm)	702	
Dye Laser w/ Cavity Dumper Stilbene 3 dye (420-470 nm)	702	
Cavity Dumper Drivers (Two)	7220	
Ultra-fast PIN Photodiode	S-2	Antel Optronics, Inc. 3225B Mainway Burlington, ON L7M 1A6 Canada

LIGHT SOURCE AND MONITORING EQUIPMENT, CONTINUED

Component	Model Number/Decsription	Vendor/Address
Sampling Oscilloscope	7904A Mainframe 7T11A Sampling time base 7S11 Sampling Unit S-4 Sampling Head	Tektronix, Inc. P.O. Box 500 Beaverton, OR 97077
Conventional Oscilloscopes (Two)	2225	
Autocorrelators (Two)	514-A w/KDP crystal #530-080 for Rhodamine 6G dye 514-B w/BBO crystal #530-040 for Stilbene 3 dye	INRAD, Inc. 161 LeGrand Ave. Northvale, NJ 07647

OPTICS

Component	Model Number/Decsription	Vendor/Address
Pellicle Beamsplitter	0501000	ESCO Products, Inc. 171 Oak Ridge Rd. Oak Ridge, NJ 07438
Plano-convex lenses (25.4 mm dia. and fused silica unless indicated otherwise)	01LQF028, 50 mm f.l. 01LQF136 150 mm f.l.	Melles Griot 1770 Kettering St. Irvine, CA 92714
	SPX016, 50.2 mm f.l. SPX022, 100.0 mm f.l.	Oriel Corporation 250 Longbeach Blvd. Stratford, CT 06497
Connectorized Fiber Optic	2m, 100/140 G.I. fiber w/SMA on one end and an ST connector on the other	Boston Electronics 72 Kent St. Brookline, MA 02146

OPTICS, CONTINUED

Component	Model Number/Decsription	Vendor/Address
Fiber optic positioner with chuck	FPR-C1 FPH-CA3	Newport Corporation 18235 Mt Baldy Circle Fountain Valley, CA 92728

ELECTRONICS

Component	Model Number/Decsription	Vendor/Address
NIM Bin and Power Supply	TB3/TC911-6	Tennelec, Inc. 601 Oak Ridge Tpke. Oak Ridge, TN 37831
Quad Constant Fraction Discriminator	TC 455	
Switched Delay	TC 412A	
Time to Amplitude Converter	TC 862	
Multichannel Analyzer	PCA/AT (8K)	The Nucleus Inc. P.O. Box 2561 Oak Ridge, TN 37830
High Voltage Power Supply (0 to 5KV)	305	Bertan Associates, Inc. 121 New South Rd. Hicksville, NY 11801
2 GHz Amplifier	ZFL 2000	Mini-Circuits P.O. Box 350166 Brooklyn, NY 11235
1 dB Attenuator	SAT-1	
Microwave cable assembly (mounted inside chilled housing for MCP-PMT)	G2ZEKR52007.0	W.L. Gore and Associates, Inc. 1901 Barksdale Rd. Newark, DE 19711

ELECTRONICS, CONTINUED

Component	Model Number/Decsription	Vendor/Address
0.085" semi-rigid coaxial cable		Omni-Spectra 21 Continental Blvd. Merrimack, NH 03054
SMA connectors for semi-rigid coax	2001-7885-00	
SMA Connectors for RG 174 coax	554-90/010	Amphenol Corp. RF/Microwave Div. 3237 Rt. 112 Suite 2 Medford, NY 11763
LEMO Conectors	FFA.00.250.CTAC22 (for 0.085" semi-rigid coax) FFA.00.250.CTAC27 (for RG 174 coax)	LEMO USA, Inc. 335 Tesconi Circle Santa Rosa, CA 95406

OTHER COMPONENTS

Component	Model Number/Decsription	Vendor/Address
Second Harmonic Generator in Gimbal Mount	KDP-R6G	INRAD, Inc. 161 LeGrand Ave. Northvale, NJ 07647
w/ Plano-Convex Lenses, (25.4 mm dia)	40390, 250 mm f.l. fused silica 41360, 100 mm f.l. borosilicate glass	Oriel
Czerny-Turner Monochromator	1681	Spex Industries 3880 Park Ave. Edison, NJ 08820 McPherson 530 Main St. Acton, MA 01720

OTHER COMPONENTS, CONTINUED

Component	Model Number/Decsription	Vendor/Address
Photomultiplier Tube	R928	Hamamatsu Corp. 350 Foothill Rd.
Microchannel Plate Photomultiplier Tube	R1564U/11 serial # PD553	Bridgewater, NJ 08807
Cooled Housing for MCP-PMT	TE-321/RF	Products for Research 88 Holten St. Danvers, MA 01923
Switched Fiber Optic Delay w/ Detector		See Appendix 2

APPENDIX 2: AN ELECTRONICALLY SWITCHED FIBER OPTIC DELAY

The use of a high repetition rate light source in a Single Photon Timing (SPT) instrument imposes a restriction on the time over which data can be acquired. This restriction is due to the requirement that the data channel that contains the temporal reference signal be connected to the STOP input of the time-to-amplitude converter (TAC). This, coupled with the fact that signals in the two data channels must be separated by at least 40 ns when they pass through the constant fraction discriminator (CFD), necessitates the insertion of delays in each of the data channels. Because the only reasonable means to delay the fluorescence channel is to insert an electronic delay (i.e., a coaxial cable) between the CFD and the TAC, one must insert a delay in the temporal reference channel before the CFD. Placement of a coaxial cable delay between the detector and the CFD is not desirable as the risetime of the waveform would not be preserved after passing through the needed length of coaxial cable. The best solution is to optically delay the temporal reference pulse between the point at which the pulse train is sampled and the detector. This is most easily accomplished with an optical fiber. However, a fixed length of optical fiber imposes a restriction on the time over which data can be acquired. Consequently most TCSPC instruments that use a high repetition rate laser source are limited to recording very fast fluorescence decays. This appendix discusses in detail the design and fabrication of a switched fiber optic delay that allows the user of a TCSPC instrument to easily change the time over which data is acquired. The finished device is housed in a triple-width NIM module.

As the name implies, the switched fiber optic delay consists of different lengths of fiber optics connected with fiber optic switches. The delay depends on the total length of fiber optic between the input and the detector. Different delay times are obtained by directing the pulses of light via fiber optic switches through different

lengths of fiber optic. A schematic drawing of the device is shown below in Figure A2-1.

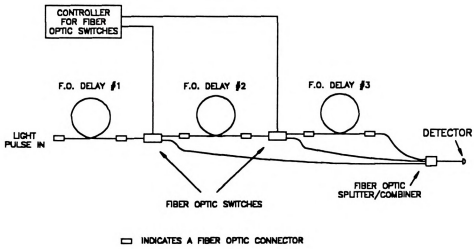

FIGURE A2-1. Schematic diagram of a switched fiber optic delay.

The length of the shortest delay to be inserted in the temporal reference channel must be chosen such that the instrument's ability to record very fast decays is not limited by the length of the fiber. If this fiber is too long, time zero will lie outside the temporal window of the TAC. An optical fiber that is too short will not provide sufficient temporal separation of the two data channels at the CFD. In order to determine the correct length of this fiber optic, one must carefully consider the transit time of photons and electrons in both data channels beginning at the point at which the laser pulse train is sampled. One should choose the length of this fiber such that the propagation time through the temporal reference channel equals the minimum propagation time for the fluorescence channel less the narrowest temporal window of the TAC. As the maximum scan rate of the TAC combined with the input voltage range of the multichannel analyzer (MCA) used in our instrument yields a window that is approximately 20 ns wide, one must accurately account for every portion of each data channel's propagation time. Of course one must consider the velocity of

propagation through the coaxial cables used in the instrument as well as the refractive index of the fiber optic when calculating the propagation time for each data channel.

A length of 14 m was chosen for the first fiber optic. This length of optical fiber delays the temporal reference signal just enough such that time zero lies near the upper limit of the TAC-MCA window, thus providing optimum conditions for recording very fast decays. In addition, this length of fiber optic provides adequate separation of the two data channels at the CFD. The second fiber optic is 20 m in length, which when added to the 14 m fiber optic allows data to be recorded over a 100 ns window. To acquire data over a longer time period, an external fiber optic can be inserted in the optical path (by means of two connectors on the rear panel of the NIM module). At present, this may be a 50 m and/or a 100 m fiber optic. These allow the user to easily configure the instrument to acquire data for up to a microsecond.

COMPONENTS

This section contains a description of the major components of the switched fiber optic delay. Where appropriate, the rationale behind the choices made is discussed. A complete description of vendors, part numbers, and other information necessary for the purchase of the components is also given.

Optical Fibers, Connectors, and Switches

Aside from the length of the optical fibers used, several choices must be made with respect to the type of optical fibers, the style of connectors, and the mechanism and type of the fiber optic switches used.

Optical fibers have been in widespread use, especially in the communications industry, for several years. Many types of optical fibers are available offering a broad range of bandwidths, spectral characteristics, package ruggedization, and ease of handling. General information on optical fibers can be found in catalogs from manufacturers [1] or resellers [2] of optical fibers.

For this application, high bandwidth, low attenuation from 400 to 700 nm, and ease of handling are the desired attributes for the fiber optics used. Of the commercially available fiber optics, single mode fibers possess the greatest bandwidth. However they are difficult to work with and special equipment is required to mate two fiber optics. Multi-mode fiber optics, on the other hand, are very easy to handle and mate, and their bandwidth is sufficient for this application. Of the family of multimode fiber optics, the least expensive and most common is the so called "100/140 GI" fiber. This fiber optic has a core diameter of 100 μm and a cladding thickness of 20 μm. Its construction is slightly different than the step index model that is commonly used for explaining the total internal reflection mechanism by which light propagates through the fiber optic. The refractive index of the cladding increases with distance from the core. This gradient in the refractive index increases the bandwidth of these "graded index" fibers relative to step index fibers.

Although the transmission of the 100/140 GI fiber is optimized at 1300 nm, losses in the visible region of the spectrum are tolerable over the lengths needed for a switched fiber optic delay for TCSPC. This fiber would not be suitable for conducting light below 400 nm or for conducting visible light over several kilometers. However, in any fiber optic application one should recognize that the bulk of the loss of the overall system will probably occur where light is coupled to the fiber. Consider that over ten percent of the light will be lost as it is coupled to the fiber when a simple lens

is used to focus collimated light onto the end of a fiber (approximately four percent loss for each surface of the lens and four percent for the air-fiber interface).

Since the 100/140 GI fiber is widely used commercially, the least expensive and most readily available package for it is more rugged than is needed in a typical laboratory. The most common package for 100/140 GI fiber consists of the fiber proper and an additional millimeter or two of strength members enclosed in a PVC jacket. Fibers covered only with a thin PVC jacket are also available, but they are not as widely used and hence more expensive than the more rugged version. However, the near-bare fibers require less storage volume for an equal length of fiber. Jacketed fiber cables were used in the constructed device because of their lower cost.

Many types of connectors are available for fiber optics. The more advanced designs enable an ease of interconnection of fiber optics similar to that for coaxial cables fitted with BNC connectors. In fact one of the better connectors for fiber optics, the "ST" connector, uses a bayonet mating mechanism similar to the BNC connector. Double female ST connectors analogous to the BNC "barrel" provide convenient interconnection of two fibers. Chassis mount connectors designed to mate an ST connectorized fiber with a TO-18 "can" package also exist. This provides a very convenient means of coupling detectors or sources mounted in this popular package to a fiber optic.

The heart of the switched fiber optic delay is of course a fiber optic switch. Although the principle is quite simple, this author had a great deal of difficulty in locating a manufacturer of such a device. Essentially two manufacturers exist: DiCon Fiberoptics (Berkeley, CA) and JDS Optics (Nepean, ON, Canada). DiCon manufactures electronically actuated switches, and JDS manufactures both

electronically actuated and manually actuated switches. Both types of fiber optic switch operate by a moving fiber mechanism. They differ primarily in the method of actuation. One by two (1x2) and one by four (1x4) switches are available from both vendors. For the design shown in Figure A1-1, electronically actuated 1x2 switches from DiCon were chosen. Cost was the primary criterion in the choice of vendor.

The last component prior to the detector is listed in Figure A1-1 as a "fiber optic splitter/combiner". The actual component used in the switched fiber optic delay is perhaps more correctly termed a "multi-leg fiber optic assembly". Commercially available, bidirectional splitter/combiners are either 1x2 or 1x4 devices, and cost in excess of $250 for a 1x2 device and $400 for a 1x4 device. Rather than using an off-the-shelf device, a less expensive, custom made three fiber optic to one ST connector combiner was purchased. This device, termed by the manufacturer (Boston Electronics, Brookline, MA) as a multi-leg assembly, is simply three short fiberoptics with ST connectors on one end that are brought together at the other end in a single, drilled out ST connector. Since this connector is intended to mate with what is a comparatively broad area detector, this means of construction accomplishes the task at hand while costing less than half the price of a conventional fiber optic splitter/combiner needed for this application.

Detection

The last component in the optical path of the switched fiber optic delay is the detector. Of the relatively inexpensive, fast detectors used for TCPSC, silicon avalanche photodiodes are the most widely used. The risetime of these devices is less than 500 ps, and is only surpassed by the fastest PIN type photodiodes which are about 25 times more expensive. Of the commercially available silicon avalanche

photodiodes, those manufactured by RCA (RCA Inc, Electro Optics Division, Vaudreuil, QU, Canada) have the fastest risetime and the greatest gain. The photodiode used in the switched fiber optic delay was RCA part # C30902E (TO-18 package).

Since the moderately high DC voltage needed to bias the photodiode is not directly available from the NIM bin power supply, the circuit shown in Figure A2-2 was developed to provide the necessary bias voltage.

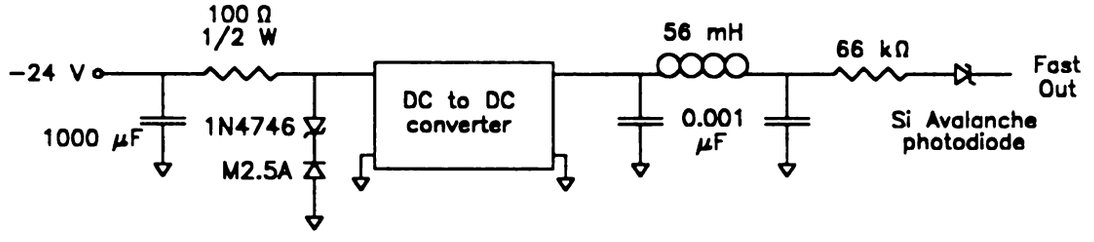

Figure A2-2. Diagram of circuit employed to bias the silicon avalanche photodiode.

The circuit is designed around a DC-to-DC converter (Endicott Research Group, Endicott, NY) that is rated to provide an unregulated 225 volt output when supplied with a 24 volt input. Two modifications were needed beyond a simple insertion of this device between the NIM power supply and the photodiode. The first was a requirement to reduce the output voltage to less than -195 volts, the breakdown voltage of the photodiode. According to the manufacturer, the output voltage of the converter is proportional to the input voltage from the specified input to about 20 percent of that value. Hence a simple Zener shunt regulator [3] was inserted to regulate the DC-to-DC converter's input voltage to a value that would produce the required output voltage. The fabrication of the needed regulator was accomplished with a Zener diode having a breakdown voltage of 18.4 volts and a one Watt power diode. The second modification was the incorporation of a "pi" filter [4] at the output

of the DC-to-DC converter. The unfiltered output of the DC-to-DC converter contained an unacceptable level of switching noise at about 25 kHz. The constructed pi filter did not eliminate the switching noise, but did reduce it to an acceptable level.

The output voltage of the DC-to-DC converter after the pi filter is -187 volts. It contains 400 mV_{p-p} of 25 kHz switching noise, as measured with a conventional 1 MΩ oscilloscope. This does not appear to affect the performance of the photodiode as used in a SPT experiment, but the dark response of the device contains about 150 mV_{p-p} of switching noise as measured with a 1 MΩ oscilloscope. This noise level is not observable in a 50 Ω system.

CONSTRUCTION

A description of the construction and layout of the switched fiber optic delay is in order should it require repair or modification. As previously mentioned, the device is housed in a triple-width NIM module. All of the components related to the fiber optic switches and the photodiode bias supply are mounted on a large piece of perf board which is mounted on the right hand side of the NIM module. Removal of the right-hand panel of the NIM module will reveal this board. The only components mounted on the bottom are the diodes used in the Zener shunt regulator. These components are the most likely suspects should a problem develop in the photodiode signal.

The first two fiber optics in the optical delay path are coiled and mounted between pieces of perf board (and double sided pc board) which are firmly connected and mounted in "layer cake" fashion with standoffs and long bolts. The fiber optic assembly can be removed by removing the left hand panel of the NIM module, and

removing the four brass nuts visible on the bottom of the board exposed when the right hand panel was removed.

The delay fiber optics are orange and can be readily identified as the length of each fiber optic is written on the sheath of the connector on either end of the fiber. The input and output fibers of the switches are also color coded, and the manner of connection of the fiber optics is shown in Figure A2-3. The figure also shows the position of each fiber optic switch when power is applied to it.

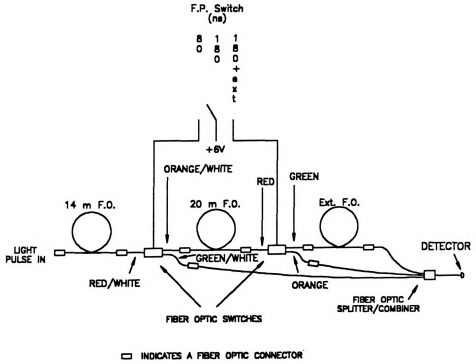

Figure A2-3. Color-coding of optical fibers used in the switched fiber optic delay.

The switches are identical with respect to color coding of the attached fibers. To aid in identifying the fibers from the fiber optic switches, the fiber optics for the first switch were lightly painted with "white out" near the fiber's connector. These fibers are indicated by a color/white label (e.g., red/white) in Figure A2-3.

The power lines to both of the fiber optic switches are bypassed at the solder contact for the switch with a 1,000 μF capacitor.

The silicon avalanche photodiode and current limiting resistor are contained in a small "black box" (Pomona Electronics, Pomona, CA) mounted inside the front panel of the NIM module. The photodiode is mounted in a panel receptacle for an ST connectorized fiber optic designed to mate the fiber optic with a TO-18 package. The output from the photodiode is accessed via an SMA connector on the front of the NIM module labeled "Fast Out". The output attenuated by a factor of five (200Ω series resistor), is also available on the front panel via an SMA connector labeled "Monitor", following a suggestion by Steiner, Holtom, and Kubota [5].

CONTROLS AND SPECIFICATIONS

Detailed information concerning the connectors and controls on the front and rear panels of the NIM module and other pertinent items are presented in this section.

Front and Rear Panel Connections and Controls

FRONT PANEL

Input	ST fiber optic connector, located near the bottom of the front panel.
Optical Delay	Three-position switch, allows the user to select different delay times via selecting different optical paths. Values of 80 and 180 ns are available with the fiber optics mounted inside the NIM module. Additional delay times are possible if an external fiber optic is connected at the rear panel. At present two fiber optics are available; 50m and 100m. These provide delay times of 430 ns (50m) and 680 ns (100m). A delay of 930 ns is possible if these fiber optics are connected in series.
Outputs	Two male SMA connectors, labeled "Fast Out" and "Monitor" provide a very fast signal N ns after a picosecond pulse of light is applied at the input, where N is the setting of the switch labeled "Optical Delay". The signal is a negative, Lorentzian-like pulse having risetime of less than 500 ps and a total width of approximately one ns. The signal is the output of a fast, silicon avalanche photodiode, RCA part # C30902E. The full photodiode signal is available at the connector labeled "Fast Out", whereas the signal at the connector labeled "Monitor" is the photodiode signal attenuated by a factor of five.

REAR PANEL

Fuses — Two switched fuse holders, labeled F.O switches, 0.5 Amp (for the Fiber Optic Switches) and Detector, 0.1 Amp. Both are slow blow fuses.

External Delay — Two fiber optic ST connectors for the insertion of an additional fiber optic to increase the length of the longest available delay time. These connectors should be capped while not in use to prevent the accidental emission of laser light and contamination of the connectors. At present, two fiber optics are available for this purpose. These fiber optics are 50 m and 100 m in length, and provide total delays of 430 ns and 680 ns respectively. A delay of 930 ns is possible by connecting these two fiber optics in series before connecting them to the NIM module.

+12 V output — BNC connector providing +12 volt power. This is intended to provide power for the amplifier in the data channel of the TCSPC instrument (Minicircuits model ZFL 2000). WARNING - This power source is not fused.

ADDITIONAL INFORMATION

Power Requirements

360 mA, +6 volts

50 mA, -24 volts

Vendors, Part Numbers, and Miscellaneous Information

A complete listing of vendors and part numbers for the components in the electronic switched fiber optic delay is given below. Suggestions for alternate sources are included for some of the components.

Company/Address	Item/Part Number	Approximate Cost
	NIM modules	
EG&G Ortec 100 Midland Rd. Oak Ridge, TN 37831 (615) 482-4411 (800) 251-9750	Triple-width NIM module	$90
Tennelec, Inc. 601 Oak Ridge Turnpike Oak Ridge, TN 37831 (615) 483-8405 (800) 255-1978	Triple width NIM module (alternate source)	$80

Fiber Optic Switches

DiCon Fiberoptics 950-C Gilman St. Berkeley, CA 94710 (415) 528-0427	1x2 fiber optic switch part # S12-N-100-ST-S	$400
JDS Optics P.O. Box 5245 Nepean, ON K2C 3H5 Canada (613) 727-1303	alternate source for fiber optic switches	

Fiber Optics and Connectors

Boston Electronics 72 Kent St. Brookline, MA 02146 (617) 566-3821 (800) 347-5445	100/140 GI fiber optics with stainless steel ST connectors Multileg assembly	$1.30 per m plus $25 per connector $125
Light Control Systems 2 Bridgeview Circle Tyngsboro, MA 01879 (508) 649-9870	alternate source for fiber optics	
OFTI 5 Fortune Dr. Billerica, MA 01821 (508) 663-6629	double female ST fiber optic connector part # 300-4STC-1002 ST/TO-18 receptacle part # 300-4STC-0001 also a source for fibers and connectors	

DC-to-DC converters

Endicott Research Group, Inc. 2601 Wayne St. Endicott, NY 13760 (607) 754-9187	DC-to-DC converter E512 series, part # varies according to availablity	$25

Silicon Avalanche Photodiodes

RCA , Inc. Electo-Optics P.O. Box 900 Vaudreuil, QU J7V 7X3 Canada	Silicon avalanche photodiode part # C30902E	$80
AEG Corporation P.O. Box 3800 Somerville, NJ 08876 (201) 722-9800	alternate source for silicon avalanche photodiodes part # BPW28B	$300

APPENDIX 2 REFERENCES

1. Technical Literature, Corning Glass Corporation, Corning NY

2. Newport Corporation, Fountain Valley, CA, 1990 Catalog

3. Malmstat, H.V; Enke, C.G.; Crouch, S.R. *Electronics and Instrumentation for Scientists* Benjamin/Cummings: Menlo Park, CA, 1981, p.62.

4. *The ARRL Handbook for the Radio Amateur*, 64th ed., American Radio Relay League: Newington, CT , 1987, p. 11-8.

5. Steiner, R.F.; Holtom, G.; Kubota, Y. in *"Laser Spectroscopy of Nucleic Acid Complexes" in Lasers in Polymer Science and Technology: Applications"* vol IV, CRC Press: Boca Raton, FL, 1989, J.P. Fouassier and J.F. Rabex Eds.

APPENDIX 3: A USER'S MANUAL FOR SINGLE PHOTON TIMING EXPERIMENTS

In this Appendix, instructions are given for acquiring a fluorescence decay with the single-photon timing (SPT) instrument described in Chapter 3. Cautions concerning some of the more delicate components are also raised. And as they are non-trivial from the standpoint of curve fitting, suggestions are made for the determination of multi-exponential decays and the decay of anisotropy. Specific acquisition parameters are given for acquiring the excited-state decay of a "standard compound", rose bengal, in methanol. It is assumed that the reader is thoroughly familiar with the SPT technique, the operation of the laser, and the acquisition and analysis software. It is also assumed that the reader has previously read the manuals for the major components.

This Appendix is not intended to serve as a step-by-step set of instructions for obtaining a fluorescence decay with the SPT instrument described in Chapter 3; that would be extraordinarily lengthy. To aid novice users, a flow chart is given, but it is not intended to serve as a recipe. In this author's opinion, SPT is a *technique:* a methodology for recording the decay of excited-states. An SPT apparatus is a tool for recording this information, not a "black box" in which a sample is inserted and a "magic" number is printed out. The importance of a thorough understanding of the technique, and the components from which the instrument is assembled, cannot be stressed too much.

Because some of the acquisition parameters must be optimized for the excited-state decay under study, one essentially adjusts these parameters to suit the decay under investigation. Since the user obviously does not have *a priori* knowledge of the

particular excited-state lifetime, the adjustments are made on-the-fly. Making these adjustments properly and efficiently is the key to the efficient use of one's time and the resource that is the SPT instrument. Once the instrument is fully prepared, one simply collects data until the desired signal-to-noise ratio is obtained.

GENERAL CONSIDERATIONS

In this Appendix, and elsewhere in this dissertation, the desireability of a narrow, symmetric, and smooth instrument response function (IRF) is stressed. As some readers may not fully appreciate the value of these characteristics, a few words concerning their importance is in order. Although the effects may not be significant, a measurement scheme in which the system under study is perturbed distorts the quantity that is determined. This is certainly true for the acquisition of a fluorescence decay. An understanding of exactly the extent to which the instrument, be it an SPT apparatus or one based on another technique, distorts the true fluorescence decay is crucial to correcting the determined excited-state lifetime. An accurate record of the IRF is needed for the numerical techniques by which the lifetime is extracted from the experimentalk data. The quality of the IRF affects the ability of these algorithms to provide an accurate correction. Consider also that an instrument having a short but skewed IRF will produce less accurate and reliable data than an instrument with a slightly longer but perfectly symmetric IRF. This is true regardless of the difference between the excited-state lifetime and the IRF.

The Laser System

Unlike the other experiments that use the output of one of the synchronously pumped, mode-locked, cavity-dumped dye lasers, SPT is relatively insensitive to

fluctuations in intensity. However, obtaining a reproducible and narrow instrument response function (IRF) is strongly dependent on proper adjustment of the dye laser cavity length and the phase and delay adjustments on the cavity dumper driver. If satellite pulses are present in the dye laser pulse train, the IRF will not only be needlessly broadened, it also may not be smooth because the IRF can be fast enough to record the individual satellites. Such an IRF will reduce the accuracy of reconvolution analysis. It will also cause additional distortion in the acquired fluorescence decay.

The proper adjustment of the cavity dumper driver can result in contamination of the pulse train. If the RF pulse to the Bragg cell is not temporally centered with respect to a pulse in the dye laser, part of an adjacent pulse can be ejected from the dye laser cavity in addition to the main pulse. If this is the case, a small afterpulse may be evident 13 ns following the IRF. This corresponds to the interpulse spacing of the mode-locked pulse train.

Aside from proper alignment and adjustment, one should be aware of another characteristic of dye lasers. Similar to the plasma background of ion lasers, the spectral output of the dye laser is contaminated with broad-band fluorescence from the laser dye. This can cause a distortion if the laser dye fluorescence is significant at the sample's emission wavelength. This is generally not a problem if one is frequency doubling the dye laser's output, because only the sharp laser pulse is frequency doubled.

Cables and Connectors

The fast signals in an SPT instrument require high bandwidth coaxial cable, such as semi-rigid coax and high bandwidth connectors, e.g. SMAs. Although semi-rigid coax appears rugged, it should be treated with care. Because its shield is a solid copper tube, semi-rigid coax is formed to the desired shape before the connectors are attached. If the finished cable is distorted, the connection to the center contact of the SMA connector can be broken. At the very least, the 50 Ω impedance connection will be altered, which causes a reduction in the cable assembly's bandwidth.

Detectors

There are three detectors in the SPT instrument. They are a silicon avalanche photodiode, a conventional side-on PMT, and a 12 μm MCP-PMT. The photodiode is housed and biased such that the user need not do anything other than turn on the power to the switched fiber optic delay. As PMTs are widely used, no cautions will be given beyond those normally associated with these devices. However, MCP-PMTs are not as widely used and are more fragile than conventional PMTs. One should handle them with a great deal of care as they are especially sensitive to physical shocks. Apply and remove the bias voltage slowly. The instrument response has been optimized for operation at 3,100 volts. Do not exceed the maximum rated voltage of 3,400 volts. The chiller in which the MCP-PMT is installed need not be operating unless dark counts are a significant. But since the MCP-PMT can be warmed through ohmic heating, it is a good practice to circulate water through the housing whenever the MCP-PMT is biased.

THE TEMPORAL REFERENCE CHANNEL

A diagram of the instrument that emphasizes the two data channels is shown in Figure A3-1. The temporal reference channel begins with laser light reflected by the

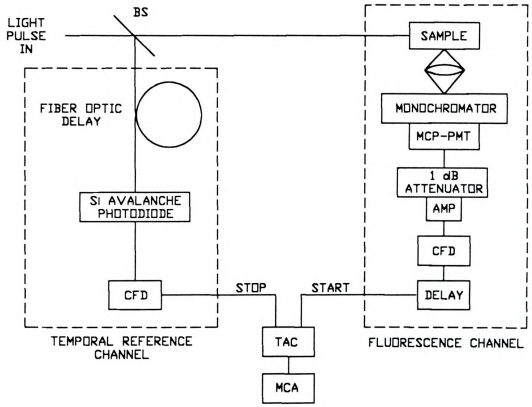

Figure A3-1. Diagram of tthe SPT apparatus emphasizing the two data channels.

pellicle beamsplitter. This light is conducted to the switched fiber optic delay with a two meter fiber optic. A fiber optic positioner has been modified to facilitate coupling the laser light into the fiber optic. It has been modified by mounting a small plano-convex lens its focal length from the tip of the fiber optic. The f-number of the lens was chosen to match the numerical aperture of the fiber optic. The fiber optic positioner allows the user to translate the fiber in the X, Y, and Z directions relative to

the point of focus of the laser light. A good method for the alignment of the positioner involves removal the other end of the fiber optic from the switched fiber optic delay. This allows one to directly view the intensity of the light conducted through the fiber optic and more readily optimize the adjustments for the fiber optic positioner. Once the other end of the fiber optic has been reconnected to the switched fiber optic delay, the preparation of the temporal reference channel is nearly complete.

The SMA connector labeled "fast out" on the switched fiber optic delay is connected to one of the channels of the CFD with a semi-rigid coaxial cable that is about six inches long. This cable has an SMA connector at one end (to mate to the switched fiber optic delay) and a LEMO connector on the other end (to mate with the CFD). The SMA connector which mates to the other SMA connector on the switched fiber optic delay is labeled "monitor" and is terminated at the connector with a 50 Ω terminator. This termination ensures that the signal presented to the CFD is the same as the signal that was viewed on the oscilloscope when the CFD was adjusted. A delay cable for this channel of the CFD was constructed from a very short (ca. 2 cm) length of semi-rigid coax. Optimum values for the walk and threshold adjustments were 0.501 volts and 0.028 volts, respectively.

The output of the CFD is connected to the STOP input of the TAC with RG174/U coax. The cable is ca. eight inches long and is connectorized to mate with both the CFD and the TAC.

THE FLUORESCENCE CHANNEL

The fluorescence channel also begins at the pellicle beamsplitter. Light not reflected by the beamsplitter continues to the sample. Proper alignment with respect to

the collection optics is achieved by adjusting the mirrors prior to the sample so that the laser light is centered on the two alignment irises. As discussed in Chapter 3, the collection optics were chosen to minimize the volume of the sample viewed. This reduces the effect of the transit time of laser light through the cuvette. If filters are needed to improve stray light rejection, they should be inserted in the collection optics between the two lenses. A polarization analyzer can also be placed here. At present, the LASER lab has two polarization analyzers for the SPT instrument: one for the near infrared and one for ca. 400 to 700 nm. These are mounted in appropriate holders and stored in the sample compartment of the SPT instrument.

Either of the two available monochromators may be employed. The SPEX monochromator is used with the MCP-PMT, and has a mask at the grating as discussed in Chapter 3. Two gratings are available for this monochromator. The one presently installed is blazed at 500 nm and the other is blazed at 700 nm. The grating blazed for the near IR has not yet been used, but may be needed if one is working with a weak, near-IR emitting fluorophore. Both gratings have 1,200 grooves per mm. Two PMTs are available for the McPherson monochromator. They are both manufactured by Hamamatsu, and are model numbers R928 and R406. They have maximum efficiencies at 400 nm and 730 nm, respectively. Each is installed in a shuttered housing, and one can easily exchange them as they are mounted with four socket-head machine screws.

The MCP-PMT is installed in a refrigerated housing. If this detector is chilled, the user should make certain that the cooling water is flowing before the Peltier cooler is powered. About two hours are required for the temperature of the detector to stabilize. The equilibrium temperature inside the housing is about 40 degrees Celsius below the temperature of the cooling water.

The signal from either detector is conducted through a short length of coaxial cable to a 1 dB feedthrough attenuator. This attenuator is connected to the input side of a 2GHz amplifier. The amplified signal is fed directly to a CFD. Again, semi-rigid coax is used to conduct the signal from the MCP-PMT, and RG174/U flexible, coaxial cable is used for the PMT. The CFD channels for these detectors have been optimized for the respective signals. A short length of RG174/U is used for the delay for the PMT, and, as discussed in Chapter 3, the CFD for the MCP-PMT was modified to accommodate the very fast risetime of the MCP-PMT signal. The output of the CFD is passed through the switched coaxial cable delay before being fed to the START input of the TAC. As discussed in Chapter 3, the switched coaxial cable delay is needed to eliminate cross-talk between channels of the CFD, and is set so that "time zero" is near the end of the TAC's timebase. The delay setting is most easily optimized while recording an IRF.

THE TAC AND MCA

The two data channels converge at the TAC. The time base of the TAC can be continuously varied from 25 ns to 3 ms. The MCA response is sharpest when the TAC output width is ca. 3 μs. At maximum temporal resolution (TAC set to its maximum sweep rate and the MCA set to maximum gain) setting the switched coaxial cable delay to 53 ns will locate the IRF near the middle of the 15th 16th MCA memory group.

Data acquisition over just a few nanoseconds is accomplished with a non-zero MCA offset and selection of the appropriate memory group. The MCA input voltage range is resolved into a number of channels equal to the set MCA gain. The offset inserts a pedestal voltage equal to the selected number of channels of offset. The

memory group is the fraction of the selected gain that is displayed on the screen. Hence, to acquire only the 512 channels of the memory group mentioned above, one would set the offset to 7,684 and select the 15th 16th memory group. A smaller offset and larger memory group will, of course, increase the time window over which data are acquired while keeping the temporal resolution constant.

MORE ON THE LIGHT SOURCE

Light from the lasers is vertically polarized. Two half-wave plates are available for polarization rotation. They are Newport "zero-order" half-wave plates for 300 and 585 nm. Each is mounted in an appropriate holder.

Excitation in the UV can be realized with the second harmonic generator (SHG). It consists of two lenses, a KDP crystal, and a bandpass filter for the UV (see Appendix 1). It is useful for doubling the output of the rhodamine 6G dye laser. If it is utilized, it should be inserted between the two alignment irises. One should keep in mind that the polarization of the frequency doubled light is rotated 90 degrees relative to the visible laser light. Hence the UV is horizontally polarized.

The period of the dump frequency of the cavity dumper driver should be set to at least five times the anticipated lifetime. Although it can be set to 4, the minimum working value of the divide by N setting is 10. The stability of the dye laser generally increases with the value of this setting, and 10 is a good compromise between laser stability and tuning range, and acquisition time. Obviously the divide by N setting must be increased if one is recording the decay of a long-lived molecule. A special trigger box has been constructed to allow the repetition rate to be reduced further than the minimum rate of the cavity dumper driver (148 kHz for N = 259). It is fed by the

38.25 MHz signal from the mode-locker driver and its output is connected to the cavity dumper driver's "EXT PLS IN" input. The appropriate front panel control can be set to allow the repetition rate to be selected by the frequency of the external signal. However, the 38.25 MHz signal from the mode-locker driver should not be connected to the cavity dumper driver's 38 MHz input.

DATA ACQUISITION

Once all of the components are powered and ready, acquisition can commence. It is generally best to start with the IRF. This ensures that all of the components are functioning properly, and it takes just a few minutes. One of the best means of acquiring an IRF is to monitor Raman scattering from cyclohexane. The strongest Raman band occurs ca. 2850 cm^{-1} from the laser line. Unless the cyclohexane has been purified (see Chapter 3), fluorescence from impurities will be observed. One should use constant and narrow monochromator slits (i.e. 0.5 mm) to restrict the volume of the sample that is viewed. One should narrow the alignment irises If one needs to reduce the TAC valid convert rate. This attenuates the fluorescence intensity without changing the IRF.

After checking the IRF, one can begin acquiring the fluorescence decay. In order to maintain the integrity of the IRF, one should keep as many of the acquisition parameters constant as possible. This includes such seemingly trivial items as the number and type of filters used in the collection optics. Clearly, the IRF measurement must be repeated if parameters such as the TAC time base are changed. Remember that the decay should be acquired such that it is bracketed by dark counts. It should be immediately evident if the time over which the decay is recorded should be increased or decreased. The first step to increase the temporal window over which the fluorescence

decay is acquired is to decrease the TAC sweep rate. Because the TAC has a 0.5 to 1.5 X multiplier in addition to a step-wise time base setting, one can "fine tune" the timebase for the fluorophore at hand. This will work to a point, but a limit willquickly be reached.

This limit is due to the reversed timing configuration. Because the STOP signal must reach the TAC after the decay is complete, one must increase the delay in the temporal reference channel to acquire more of the fluorescence decay. (This is not possible in some SPT instruments, but it is easily accomplished with the one constructed in this work.) The delay for the temporal reference channel can be increased with the switched fiber optic delay (see Appendix 2). Unlike the TAC timebase setting, the switched fiber optic delay cannot be varied in a continuous fashion. However, by optimizing the TAC time base, the MCA offset, and the two delays, one can acquire the fluorescence decay over a time window that is reasonably close to a time corresponding to 5τ. Also consider that the region of data for curve fitting can be specified with the analysis software. Hence, one can acquire the decay over a longer than needed time window. The only disadvantage to this procedure is that the resolution suffers slightly.

If any of the TAC or MCA parameters have been changed, another IRF with the same settings as those used for the sample must be acquired. However, if the decay time is long in comparison to the IRF, one does not need to include reconvolution in the data analysis.

Complex Decays

The complexity of the decay can be estimated by viewing the data as log counts versus channel number. This is easily accomplished with the MCA software. If a complex decay is evident, one should acquire data until the peak channel contains on the order of 10,000 counts. Although 1,000 counts in the peak channel is sufficient for simple decays, a higher signal-to-noise ratio is needed to confidently curve fit with a more complex model. Even though more counts are preferred for complex decays, it is good practice to save the data at 1,000 counts in the peak channel.

This is more important for the decay of anisotropy. Because the quantity of interest is dependent on the *difference* between multiple decay curves, a high signal-to-noise ratio is absolutely necessary. In fact, the number of dark counts should be roughly equal in each of the polarization-dependent decays to achieve the greatest confidence in the determined quantities.

For complex decays, the challenge is not in acquiring the data, rather it is in obtaining a good fit. This is generally achieved only after expending some effort. However, keep in mind what makes kinetic sense for the compound under study. Consider that the acquired decay may be contaminated with fluorescence from an impurity. The single-photon sensitivity of the technique requires that the sample be as pure as reasonably possible. This includes the solvent and the sample proper.

Time Calibration

The procedure for a time-calibration was discussed in Chapter 3. The only point that will be reinforced here is that the TAC valid convert rate should not exceed 1 kHz.

FILES AND NAMING CONVENTIONS

One generates several files over the course of an excited-state lifetime determination. Because their identity can easily be forgotten, it is good practice to follow simple conventions for the file names. While the file name itself should be chosen to reflect the sample under investigation, the extension should be chosen to indicate the type of file. Consider these suggestions:

Name.EXT	Identity
SAMPLE.DAT	MCA data file
SAMPLE.199	data file in 199 format
INS@710.DAT	IRF @ wavelength (MCA)
SAMPLE.FIT	single exp fit
SAMPLE.2FT	double exp fit
SAMPLE.RES	residuals file
SAMPLE.AUT	autocorrelation file
2NSTAC.DAT	time calibration w/ 2 ns steps
SAMPLE.IMP	impulse response functions (when global analysis is used)
SAM-HH.199	
SAM-HV.199	to indicate excitation and
SAM-VH.199	emission polarizations for
SAM-VV.199	anisotropy measurements

A REFERENCE FLUOROPHORE

For future reference, the parameters for acquiring the decay of rose bengal in methanol are described in detail. The compound was from Aldrich and the solution was 10 μM in B&J Brand methanol. The sample was excited at ca. 570 nm with 5 ps FWHM pulses of light. The laser power at the sample was too low to be measurable with the Coherent model 210 power meter. The repetition rate of the laser was 3.8 MHz (cavity dumper divide by 10). Fluorescence was detected at 600 nm, and the entrance and exit slits were 0.5 mm. No filters were included in the collection optics. The MCP-PMT was biased at 3,100 volts. The coaxial cable delay was set to 53 ns. The switched fiber optic delay was set to 80 ns. The TAC timebase was 25 ns. The MCA parameters were: gain = 8192, offset = 6144, and the memory group was the fourth quarter. The time calibration was 2.77 ps/ch with these parameters. The TAC valid convert rate was adjusted to ca. 1,200 by narrowing the two alignment irises. The TAC valid convert rate for dark counts was about 25 counts per second. The acquisition was stopped when ca. 1,000 counts were acquired in the peak channel (channel 250). This occurred after 4.58 minutes of data collection. The fluorescence decay was indistinguishable from the background by channel 1,400.

An IRF was also acquired. This was accomplished by monitoring Raman scattering from cyclohexane. Except for the scattering wavelength of 682 nm and the TAC valid convert rate of ca. 500, all of the other acquisition parameters were the same as those for the fluorescence decay of rose bengal. The peak channel of the IRF was channel 234. Acquisition of the IRF was complete after 0.4 minutes.

The fluorescence decay of rose bengal in methanol and the IRF are listed in a log book of standard fluorescence decays.

A FLOW DIAGRAM FOR SPT

To facilitate the training of novice users, a flow diagram of the basic sequence of an SPT experiment is given in Figure A3-2. It is assumed that the laser is on and has been properly adjusted for SPT. If the LED in the temporal reference CFD is on and has a constant intensity, the temporal reference signal is probably functioning

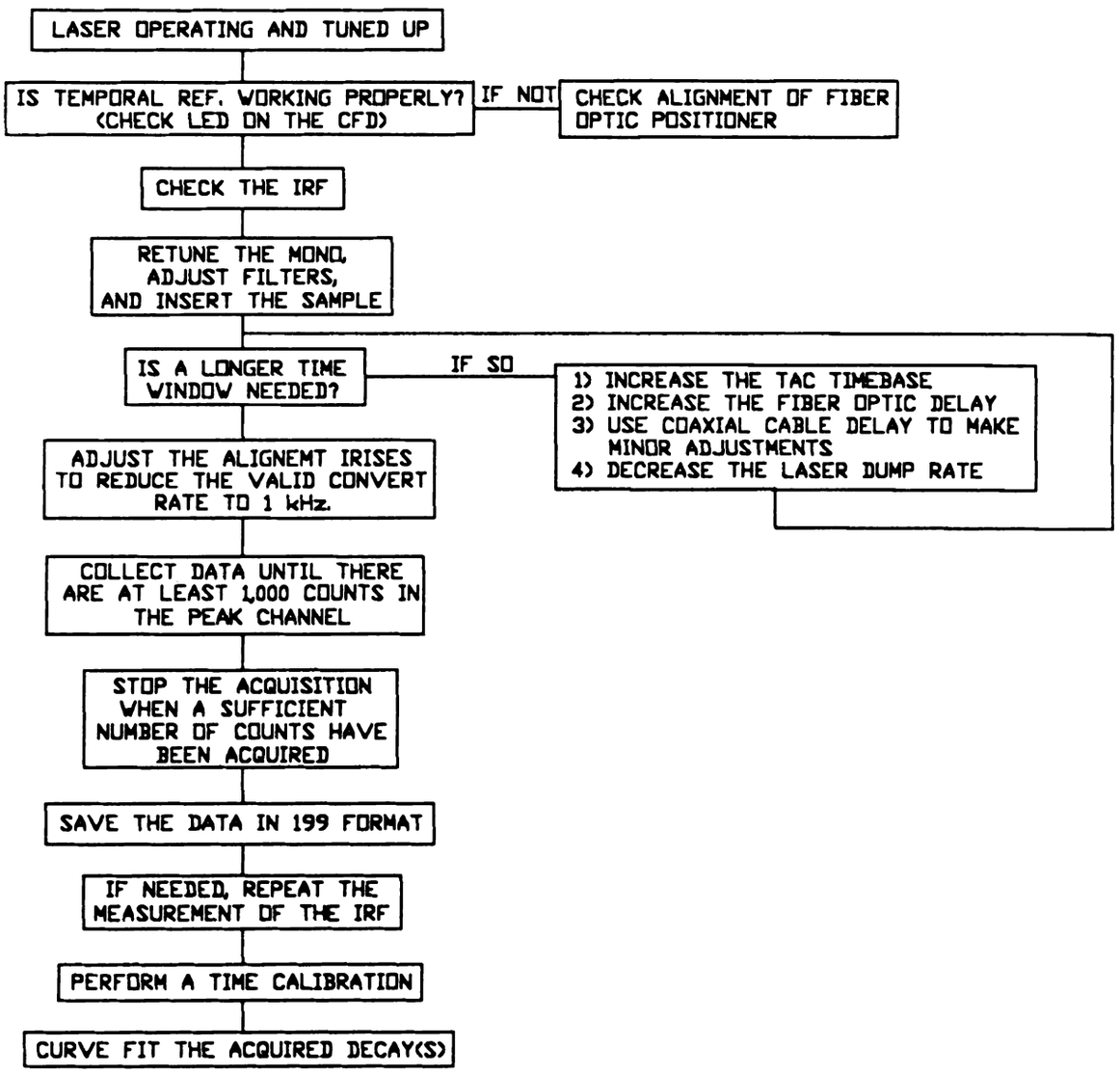

Figure A3-2. Flow diagram for SPT Experiments.

properly. If it is off or flickering, the fiber optic positioner probably needs realignment. It is best to begin with an IRF - a good choice is to use Raman scattering from cyclohexane. The first-time user should set the MCA gain to 8192, use no offset, and examine the full MCA memory (memory group F). The TAC should be set to its maximum sweep rate of 0 to 10 volts in 25 ns. The switched fiber optic delay should be set to the minimum delay (80 ns) and the coaxial cable delay should be set to 53 ns. Excitation can be from either of the dye lasers or the frequency doubled output of the rhodamine 6G dye laser. The wavelength of the dye laser can be estimated to within a nm with the calibration plots that are kept near the dye lasers. The laser power at the sample should be reduced to ca. 10 mW by reducing the aperture of the alignment irises. The strongest Raman signal is 2850 cm^{-1} from the exciting laser line. The monochromator slits should be set to 0.5 mm. The user may or may not place appropriate filters in the collection optics. If the MCP-PMT is used, it should be biased at 3,100 volts. The high voltage should be added in small steps with the shutter closed. One should start to see dark counts at ca. 2,600 volts. These are manifested by brief flashes from the LED in the CFD for the MCP-PMT. The number of dark counts that are generated during the selected time window can be monitored at the TAC valid conv. out BNC. After the MCA has been set to ACQUIRE mode and the shutter has been opened, one should see an increase in the number of valid TAC conversions per second, and the emergence of a sharp peak should be observed on the MCA display. The alignment irises should be adjusted to yield a TAC valid convert rate of ca. 1 kHz. Because the Raman signal is concentrated over a very narrow time window, only a few seconds of acquisition are needed to obtain 1,000 counts in the peak channel when the TAC valid convert rate is 1,000 Hz. At this point, the user may wish to move the temporal location of the IRF slightly by toggling the 1ns or the 2ns delay switch on the coaxial cable delay. After the delay has been set such that the IRF is

located near the highest MCA channel and a good IRF has been acquired, the MCA should be paused and the data should be saved. It is generally good practice to save the data as both an MCA *.DAT file and an IBH *.199 file. After the cyclohexane has been replaced with the sample (a novice may want to start with a reference compound such as rose bengal or rhodamine B) and the monochromator has been retuned to the sample's emission wavlength, one can start to acquire a fluorescence decay. For the case of rose bengal, the excited-state lifetime is very short, and one should not have a problem acquiring the complete decay. Such a molecule is also helpful for acquainting the user with the MCA acquisition parameters of gain, offset, and memory group. Blindly adjusting these parameters can be very frustrating, so READ THE MCA MANUAL FIRST ! A new user should have no problem reproducing the decay of rose bengal in methanol as shown in the log book of reference fluorescence decays.

If a longer-lived compound is being studied, one will probably have to increase the width of the temporal window over which a decay is recorded. The first step is to increase the TAC timebase. But as mentioned earlier, one may also have to increase the delay in the temporal reference channel. It may also be necessary to decrease the cavity dumper repetition rate. Again the coaxial cable delay can be used to shift "time zero". By adjusting these parameters and those of the MCA, one can acquire fluorescence decay data from an upper limit of ca. 1 μs down to the limit imposed by the IRF.

APPENDIX 4: A SIMPLE FREQUENCY SYNTHESIZER

As funds to purchase a commercial frequency synthesizer could not be obtained, a simple, single-frequency device was constructed. The basic design behind this device is rather simple. The RF frequency which is used to step down the frequency of measurement to the cross-correlation frequency is generated by heterodyning. The cross-correlation frequency is mixed in a double-balanced mixer with a radio frequency (RF) that matches the modulation frequency of the laser. The output of the mixer contains frequency components of RF $\pm$ nδ where RF is the radio frequency, δ is the cross-correlation frequency, and n = 1,2,3 .... The desired frequency is RF + δ (n=1), and it is isolated from the comb of frequencies generated by the mixer with a crystal filter. This frequency, 76.8243 MHz, is then amplified and fed to the mixers used to heterodyne the signal from the photomultiplier tube.

Relatively low gain, high bandwidth RF amplifiers are needed to amplify the signals in the frequency synthesizer and the output of the crystal filter. These amplifiers were built in-house using commercially available RF amplifiers constructed from two RF transistors. The amplifiers used were from the MAR series manufactured by Minicircuits (Brooklyn, NY). Each amplifier is built on a small (5 cm by 7 cm) piece of 50 Ω epoxy glass "G10" printed circuit (PC) board. The circuit is shown in the PC board layout illustrated on page 183 in Figure A4-1. Facilities to properly fabricate PC boards were not available, so an alternate method was developed. It was discovered that by carefully cutting and lifting the copper foil off of one side of new, double sided PC board, the unwanted copper could be removed. Although far from perfect, this technique sufficed to prepare PC boards with nearly 50 Ω traces. A trace that is 0.108 inch wide on G10 PC board will have an impedance of 50

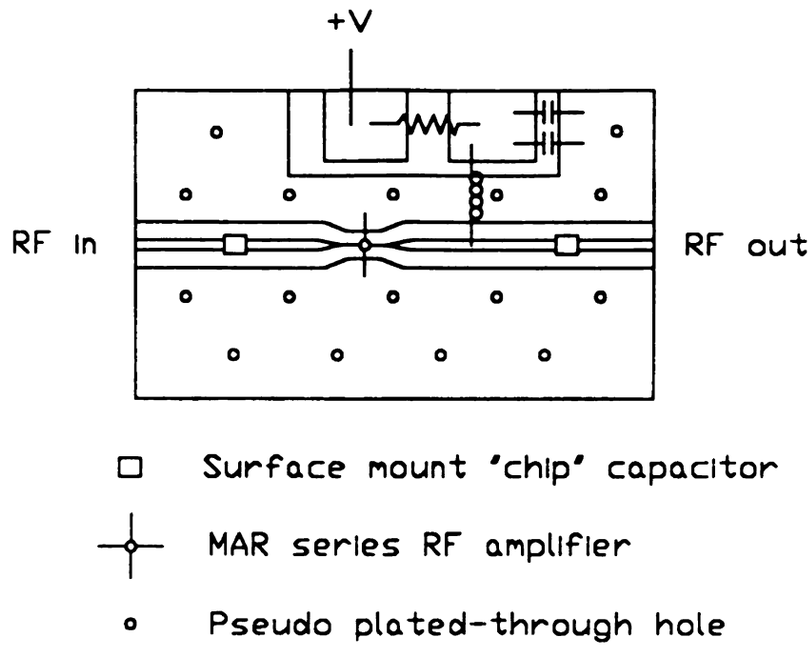

Figure A4-1. Printed circuit board layout for MAR series amplifiers

Ω. The traces made in this manner were close enough to 50 Ω for the low gain amplifiers in the MAR series, but not the high gain amplifiers. Plated-through holes were simulated by drilling a small hole in the PC board and inserting a small piece of 22 gauge wire. The wire was folded over and soldered to both sides of the PC board. The power supply scheme suggested by the manufacturer was followed. Power is supplied through a current limiting resistor to a small pad on the PC board. The current path is from this pad to the output side of the amplifier in the 50 Ω line through an inductor (100 μH to 1 mH, Dale IL-2). This arrangement supplies power to the amplifier while keeping the RF from leaving the 50 Ω line. Two bypass capacitors (0.1 μF tantalum and 0.01 μF ceramic) are placed between the pad and ground to provide a low impedance path to ground for any RF that does leak through the inductor. The RF at the input side of amplifier travels through a surface mount "chip" capacitor (0.1 or 0.01 μF) before reaching the amplifier proper. This acts as a DC block to prevent the DC power from traveling down the 50 Ω line. A chip capacitor is also inserted in the output 50 Ω line for the same purpose. The traces are brought to a point at the legs of

the amplifier to minimize step discontinuities which can cause reflections at high frequency. The PC board is mounted in an RF shielded enclosure (Pomona "black box"), and the input and output signals are conducted through BNC connectors. The shield of each BNC connector is soldered to the ground plane of the PC board on both sides of the 50 Ω line. These provide the only path to ground in the circuit. Amplifiers constructed in this fashion provided gains within a few percent of the manufacturer's specification.

A diagram of the completed synthesizer is shown in Figure A4-2.

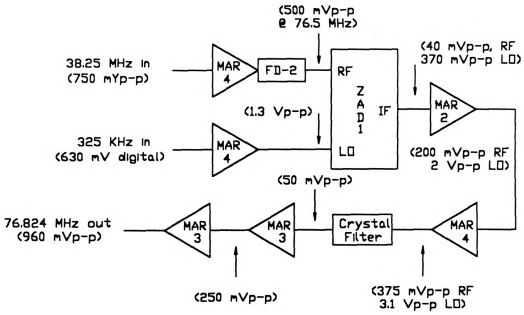

Figure A4-2. Diagram of the completed synthesizer showing voltage levels at each point in the circuit.

There are two inputs to the synthesizer. These are a digital signal at the cross-correlation frequency and an RF signal at exactly half of the fundamental modulation frequency of the laser. Both signals are derived from a cavity dumper driver which is synchronized to the mode locker driver. The former is obtained by setting the divide by N setting on the cavity dumper driver to 117. This provides a digital signal at the

sync output equal to the RF frequency (38.25 MHz) divided by 117. This is the cross-correlation frequency (325 KHz). The RF signal originates in the ovenized crystal oscillator in the mode locker driver, and it is accessed at the 38 MHz out connector on the cavity dumper driver. The RF is exactly half of the mode locked frequency. This is because there are two nodes, and hence two loss points, along one wavelength. The RF is doubled in a frequency doubler (Minicircuits FD-2) and amplified before being fed into the RF port of a double balanced mixer (Mincircuits ZAD-1). The 325 KHz signal is also amplified before the mixer, and this signal is connected to the LO port. The frequency comb generated in the mixer and accessed at the IF port is amplified twice prior to the crystal filter (Four pole bandpass filter, K&L Microwave, Phoenix, AZ). The output of the crystal filter is amplified twice such that the power level is sufficient to drive the two mixers that follow the two PMTs.

The components of the frequency synthesizer are mounted on a 12" by 32" piece of double sided PC board to which several pseudo plated-though holes have been added. Fifteen-volt power is supplied from a single supply (Power One) from the underside of the large PC board. A line filter was placed at the connection to the 110 VAC system to further reduce the chance that residual RF would leak into the AC power system. The large PC board and the power supply are mounted in a wooden box for stability.